Energy Management and Demand Response of Industrial Systems

by

Omar Alarfaj

A thesis
presented to the University of Waterloo
in fulfillment of the
thesis requirement for the degree of
Doctor of Philosophy
in
Electrical and Computer Engineering

Waterloo, Ontario, Canada, 2018

Examining Committee Membership

The following served on the Examining Committee for this thesis. The decision of the Examining Committee is by majority vote.

External Examiner:	Athula Rajapakse Professor Dept. of Electrical and Computer Engineering, University of Manitoba
Supervisor:	Kankar Bhattacharya Professor Dept. of Electrical and Computer Engineering, University of Waterloo
Internal Member:	Ramadan El-Shatshat Lecturer Dept. of Electrical and Computer Engineering, University of Waterloo
Internal Member:	Claudio Canizares Professor Dept. of Electrical and Computer Engineering, University of Waterloo
Internal-External Member:	Gordon Savage Professor Dept. of Systems Design Engineering, University of Waterloo

Author's Declaration

I hereby declare that I am the sole author of this thesis. This is a true copy of the thesis, including any required final revisions, as accepted by my examiners.

I understand that my thesis may be made electronically available to the public.

Abstract

Energy management is an important concept that has come to the forefront in recent years under the smart grid paradigm. Energy conservation and management can help defer some capacity addition requirements in the long-term, which is very significant in the context of continuously growing demand for energy. It can also alleviate the adverse environmental impacts of commissioning new generation plants. Therefore, there is a continuous need for the development of appropriate tools to ensure efficient energy usage by existing and new loads and the efficient integration of distributed energy resources (DER).

There is a need for energy conservation in the industrial sector as it accounts for the largest share of energy consumption among all customer sectors. Also considering their high energy density, industrial facilities have significant potential for participating in demand side management (DSM) programs and help in reducing the system peak demand by reducing or shifting their load in response to energy price signals. However industrial demand response (DR) is typically constrained by the operational requirements such as process interdependencies and material flow management.

An EMS framework is proposed in this thesis for optimal load management of industrial loads which includes improved load estimation technique and uncertainty mitigation using MPC. The framework has been applied to a water pumping system (WPS) where an equipment level load modeling is implemented using a NN-based model. Another EMS framework is proposed for an oil refinery process. The refinery EMS is developed based on power demand modeling of the oil refinery process, considering an on-site cogeneration facility. A joint electrical-thermal model is proposed for the cogeneration units to account for the electricity and steam production costs.

In addition to load management, DR for industrial loads is investigated as another energy management application. However since DR requires interaction between the energy supplier and the customer, this thesis considers DR from both the local distribution company's (LDC) and industrial customer's perspectives. From the LDC's perspective,

the objective is to reduce the network operational costs by minimizing peak demand and flattening the load profile for better utilization of system resources. From the industrial customer's perspective, the objective is to minimize the energy cost using both load management decisions and DR signals sent by the LDC. While the developed EMS models are used to represent the industrial customer's operations, a distribution optimal power flow (DOPF) model is developed to represent distribution system operations.

The DR strategy proposed in this thesis is based on effective communication between the customer's EMS and the LDC's operations using a day-ahead contractual mechanism between the two parties, and a real-time operational scheme to mitigate the uncertainties through improved forecasts for energy prices and power demand. Two types of DR signals are proposed; a desired demand profile signal and a retail price signal, which are developed by the LDC and sent to the customer to achieve the desired DR in a collaborative manner. In the retail price based control approach, the signal is produced by a retail pricing model which is designed based on customer's historical data collected by the LDC.

Acknowledgements

All praise is due to Allah, the most beneficent, the most merciful, for guidance and help in all aspects of my life.

I would like to express my sincere appreciation and thanks to my supervisor Prof. Kankar Bhattacharya for his guidance, encouragement, and tremendous support throughout this work. Prof. Kankar's commitment for high quality research is an inspiration for pursuing excellence and success not only in academic endeavors but in every other aspect of life.

I extend my thanks to Dr. Ramadan El-Shatshat, Prof. Claudio Canizares, and Prof. Gordon Savage for serving in my examination committee and for their valuable feedback. Their careful reading and comments have significantly improved the quality of this thesis. I am also very thankful to Prof. Athula Rajapakse, from University of Manitoba, for serving as the external thesis examiner and for his insightful comments and observations. I would like also to thank Prof. Maren Oelbermann for chairing my thesis examination committee.

From the bottom of my heart, I would like to thank my parents for their passion and continuous support. Their good wishes and prayers have accompanied me at every turn of my life.

I am also deeply grateful to my wife Asma for her overwhelming love and care. I owe Asma my deepest gratitude for her patience along this long journey to fulfill my goals. My children Jenan, Abdulrahman, and Nadia always brought the most joyful moments in my life, even during the most stressful times.

My appreciation goes to my colleagues Omar Alrumayh, Talal Alharbi, Hisham Alharbi, Abdullah Bin Humayd, Walied Alharbi, and Badr Lami for their support to overcome difficulties during my study. Special thanks to my best friends Ali Albishi, Saud Wasli, and Ayman Alharbi for the wonderful friendship and for their great contributions to my intellectual and personal skill development.

Dedication

To my parents for their unconditional love and support,

To my family who gave color to my life.

Table of Contents

List of Tables

List of Figures

Chapter 1

Introduction

1.1 Motivation

Energy management is an important concept that has come to the forefront in recent years, with the advent of the smart grid. Energy conservation and management can help defer some capacity addition requirements in the long-term, which is very significant in the context of continuously growing demand for energy. It can also alleviate the adverse environmental impacts of commissioning new generation plants. Therefore, there is a continuous need for the development of appropriate tools to ensure efficient energy usage by existing and new loads and the efficient integration of distributed energy resources (DER).

There is a high need for energy conservation in the industrial sector as it accounts for the largest share of energy consumption among all customer sectors. In 2015, industrial systems accounted for 51% of the total energy usage in Canada [1], and such large energy consumption calls for energy management by the industrial facilities to improve their energy efficiency. When these facilities are equipped with DERs, higher efficiency can be achieved through the effective management of energy production and storage. Also, the large industrial loads have significant potential for participating in demand side manage-

ment (DSM) programs and help in reducing the system peak demand. Industrial customers can play an important role in DSM by reducing or shifting their load in response to energy price signals [2]. In addition to the aforementioned benefits to the power system, there are economic benefits to industrial customers for implementing demand response (DR) controls under dynamic pricing schemes [3]. However, industrial DR is often constrained by the operational requirements of these systems such as process interdependencies and material flow management.

The growing deployment of smart grid technologies, such as smart metering and process automation, in industrial systems, is encouraging the development of advanced algorithms for optimum load control. Compared to residential loads where controls are applied on aggregated or selected loads, it is possible to control individual industrial loads through existing process controls [3]. Therefore, there is a higher degree of load controllability in the case of industrial loads, which provides wider space for energy management system (EMS) applications, and provides the industrial facility with tools for system monitoring and analysis.

As EMS is introduced in industrial facilities, the diversity of load types would require good load modeling techniques to capture the characteristics of these loads and how their operations and conditions affect energy consumption. The monitoring capability of EMS, capturing real-time measurements of power system quantities, encourages the application of measurement based load fitting techniques with different load model structures; such as polynomial and neural network (NN) models [3, 4]. These models represent the relationship between power system quantities and industrial process control variables under different operating conditions. As the models improve in precision and accuracy, further operational and economic efficiency can be achieved by the optimization model within the EMS.

Another factor affecting the performance of the EMS is the uncertainty in forecasted variables. Since the optimization horizon of an EMS is for a future time period, inputs are obtained using forecasting algorithms which vary in accuracy, which renders the expected benefits of EMS decisions to be uncertain. To this effect, uncertainty management

techniques such as model predictive control (MPC) can be applied in EMS to reduce the impact of uncertainty in optimization results.

The aforementioned developments have motivated the present research to propose and develop an EMS and DR frameworks for industrial facilities for optimal load management in the smart grid environment.

1.2 Literature Review

This section presents an overview of previous research works reported in the literature on the topics related to this research, including; industrial load management, and DR of industrial customers.

1.2.1 Industrial Load Management

The purpose of industrial load management (ILM) is to improve the energy consumption behavior of the industrial facility and hence reduce its energy costs. The reduction in energy costs can be attributed to reduction in demand charges, decreased power losses, efficient utilization of equipment [5], and optimized operational schedules. An ILM model was proposed in [6] with the objective of minimizing the energy cost while satisfying the operational and material flow constraints for a flour mill facility. Process constraints were modeled to ensure proper sequence of equipment operation. The facility's peak power demand was not considered for minimization but it was limited below a certain value using a constraint.

An optimal ILM model was proposed in [7] for an electrolytic process. A mixed-integer non-linear programming (MINLP) optimization problem was formulated with the objectives of minimizing the energy costs and peak demand charge. The industrial load models developed in [6] and [7] were implemented at the processing unit level with the assumption of a linear relationship between process energy consumption and production rate. To this

effect, the production rate of each process, as a percentage of rated production capacity, was used to determine the percentage loading of all processing devices at each operating time interval in the optimization horizon. The integration of DER within industrial facilities premises was not considered in these works.

An optimal ILM model was proposed in [3] for optimizing the processes schedule of a flour mill and a water pumping system (WPS). The optimization was formulated as an MINLP problem with the objective of minimizing the energy cost and peak demand charge under process operation and material storage constraints. Different types of process interdependencies were modeled such as sequential, interlocked, and parallel processes and the model combined industrial load control and distribution feeder voltage optimization. First and second-order polynomials were used to model the active and reactive power consumption of industrial equipment as a function of terminal voltage and process control variables. Historical measurements were used to estimate the polynomial model parameters using the least square error method. However, the work did not consider the integration of DER such as renewable energy sources (RES) and energy storage systems (ESS) within the industrial facility's premises.

An optimal ILM was formulated in [8] as a mixed integer linear programming (MILP) model with the objective of maximizing the profit for a steel mill facility. The work considered energy and material flow management simultaneously since there is a trade-off between material production revenues and the facility's energy cost. The steel mill processes were classified into batch or continuous process; the batch process received the input material at the beginning of each processing cycle and output the products at the end of the cycle, while a continuous process received the input material and outputs the products continuously. The energy consumption by batch processes was considered controllable while continuous processes were considered as uncontrollable loads. The energy consumption by controllable loads was modeled as a function of the amount of processed material using polynomial load models. It was noted that it is better to increase the optimization horizon to multiple days due to industrial process interdependencies, which will however result in higher computational complexity.

A generic framework was developed in [4] for optimal energy management of an industrial customer using voltage varying approach. The proposed framework comprised an NN-based load model developed using historical data relating the active power demand with process output and voltage. This load model was incorporated in the optimal energy management model to determine the optimal voltage profile for minimizing the energy consumption and load tap changer (LTC) operations while meeting the process constraints. The performance of the proposed framework was compared with two non-optimized strategies namely, fixed voltage operation and controlled voltage reduction (CVR). The results showed potential reduction in energy consumption by applying the voltage optimization decisions. Monte Carlo simulation approach was used to validate the expected savings from the proposed framework under different process profiles. However, the work did not consider process schedule optimization since the focus was on voltage optimization, and a simple forecast was used instead. Considering process scheduling would allow for load shifting and improve the voltage optimization capability. However, it would require more detailed modeling of the industrial process power demand as a function of the process control variables.

An optimization model was proposed in [9] for scheduling of water-cooled chillers in an automotive manufacturing plant in Ontario, Canada, with the objective to minimize energy and peak demand costs. Polynomial load models were developed using the regression technique for the chillers to estimate the active power demand as a function of inlet temperature, outlet temperature, and water flow rate where actual measurement data was used to estimate the load model parameters. In addition to operational scheduling, a planning problem was also considered for the optimal sizing of chiller tank storage. However, this work did not consider the uncertainties in process cooling demand and in energy price, in the proposed energy management model.

The equipment level load modeling considered in the reviewed papers for ILM were based on polynomial models which have limited capability in estimating higher-order load models, making the parameter identification problem challenging. Therefore, an improved load estimation approach need be considered to enhance the ILM optimization perfor-

mance. The reviewed papers, furthermore, did not consider the forecasting uncertainties associated with the ILM model inputs such as energy price, demand, and RES generation. Although good forecasting algorithms reduce the margin of errors significantly, they are still prone to deviations from actual values. Considering these deviations, as the ILM optimization decisions are implemented, which are based on forecasted inputs, the expected benefits may not be achieved as the industrial facility's actual operation will be subjected to actual values. Therefore uncertainty management techniques need to be considered in order to reduce the impact of uncertain inputs on the ILM optimization decisions. These techniques include stochastic programming, Monte Carlo simulations, and MPC.

1.2.1.1 Water Pumping System Load Management

Multi-objective optimization of the operation of a WPS was proposed in [10] which considered four objectives namely; minimizing electric energy costs, minimizing peak demand charges, minimizing the number of on/off operations of the pumps, and minimizing the difference between the initial and final water levels in the storage reservoir. The pumps were equipped with fixed speed drives so they could only be switched on or off in the optimization problem. While, rotational speed variation was considered in the modeling of WPS pumping load in [3], the mechanism for varying the pumps speed in the load simulations was not explained. In practice, variable speed drives (VSD) are commonly used for controlling the rotational speed of motor driven pumps in order to control the water flow rate.

VSD based pumps allow a wider window for speed variability and hence a greater flexibility for WPS water flow optimization by the EMS. A comparative study presented in [11] with three speed control options- fixed speed, variable speed with VSD shared by multiple pumps, and variable speed with dedicated VSD per pump, showed that, dedicated VSD per pump is the best option from the perspective of efficiency, reliability, and life cycle assessments. In addition to energy savings, VSDs improve the controllability of the process and enhances their reliability [12]. The reliability enhancement is achieved via minimizing

the number of pump on/off switching operations which improves the pumps life cycle and reduces maintenance costs [13].

1.2.1.2 Oil Refinery Load Management

Only a few works reported in the literature have focused on electrical load management of petrochemical industries. Most of the energy management research for oil refineries do not consider the electrical demand management of the facility. Production scheduling optimization studies were reported in [14, 15, 16, 17] with the objective of maximizing refinery production; however, none of them considered electrical energy costs in the analysis. In [18], an optimal strategy for ILM was proposed based on the integration of a cogeneration system into a petrochemical facility. A joint electrical-thermal model was developed for the cogeneration system where electric power output was modeled as a function of input fuel flow rate using a second-order polynomial. The strategy considered the exchange of power between the cogeneration equipped petrochemical facility and the power utility, with the petrochemical facility having a pre-defined load profile. Since the industrial load was not modeled as a function of process control variables, load control could not be implemented in the process optimization.

An optimization model for ILM of an oil refinery was proposed in [19] with the objective of minimizing electrical energy costs. The model considered process interdependencies, process interruptibility, processing times, and operational sequences. A fixed electricity consumption per time interval was assumed for the processing units, therefore the model did not consider the relationship between the amount of processed material and energy consumption. It was assumed that several processing units, such as liquefied petroleum gas (LPG) recovery and vacuum distillation units, can have a delayed start after being fed from preceding processing units. It was also assumed that some units, such as hydrofiners, are interruptible. Both of these assumptions are not practical, considering that a refinery need to maintain a continuous-flow operation [20], which means that all processing units must operate simultaneously to arrive at a steady-state operation where every unit pro-

cesses its incoming feed continuously. Processing can only be delayed or interrupted during emergencies where limited capacity storage tanks are utilized for storing unprocessed intermediate flow temporarily. These tanks cannot be used for ILM as process contingency practices require keeping them half-full all the time in preparation for interruptions in upstream or downstream processing units.

From a review of the literature it is noted that the electrical energy management of oil refinery was not considered in a comprehensive manner. None of the works considered mass flow based modeling of the refinery electricity demand. Also cogeneration facility operation optimization in conjunction with refinery load management was not examined. Furthermore, the potential of refinery participation in DR provisions was not studied. Therefore, there is a need to examine the above issues under dynamic electricity pricing scheme.

1.2.2 Industrial Load Demand Response

Researchers have examined DR provisions from industrial facilities from the local distribution company's (LDC's) perspective where the objective is to minimize the peak demand, and from the customers' perspective where the objective is to minimize their energy costs [21]. A battery energy storage system (BESS) aided DR strategy was proposed in [22] from an industrial facility's perspective, seeking to minimize its energy cost and hence optimize the energy exchange with the utility in the presence of RES. Assuming a fixed-load facility equipped with BESS, the strategy optimized the charging and discharging schedule of the BESS taking into account the non-linear behaviour of rechargeable batteries.

Another DR scheme from an industrial customer's perspective, with the objective of minimizing its energy cost, was proposed in [2] to shift the facility's demand from peak to off-peak periods under day-ahead hourly prices. The DR problem included constraints for process limits and in-facility distributed energy resource (DER) operation. The case study carried out on an oxygen generation facility demonstrated the effectiveness of the scheme in shifting the load and reducing the energy costs.

A DR scheme for industrial facilities was proposed in [23] from the utility's perspective, based on a strategy that generated different pricing signals for different classes of industrial customers to prevent excessive load shifting as a result of their simultaneous responses. Customer behavior was modeled based on deep communication with the utility which was used for price optimization. However, these prices did not incorporate customer feedback of potential demand changes at the day-ahead stage. A cooperative scheme for industrial DR was proposed in [24] which minimized two conflicting objectives, the customer's electricity cost and the discomfort cost; the solution so obtained was a trade-off between the two objectives. The cooperative DR problem was solved using game theory to maximize the customers' payoffs while applying a *punishment mechanism* to render the problem stable in the presence of non-cooperative customers.

A DR scheme was proposed in [25] based on virtual power plant (VPP) structure comprising customers and RES, wherein the customers sent their proposed load curves, ranked by their preference, to a centralized DR aggregator which determined the optimal combination of load curves for customers' operation based on system cost minimization and customers' benefit maximization objectives. The DR aggregator participated in the wholesale market for DR and energy transactions and managed an internal market for VPP participants. The scheme was applied to residential, commercial, and industrial load profiles, submitted day-ahead, by customers.

A demand response (DR) scheme was proposed in [26] which considered the perspectives of both the local distribution company (LDC) and residential customers. The proposed scheme was based on a new modeling framework considering price-responsive and LDC controlled loads in a three-phase unbalanced distribution network. In the case of price-responsive loads, the customers were assumed to be equipped with home energy management systems (HEMS) which responded to price changes by changing the power demand of the customer. The price-demand relationship was modeled using linear and exponential functions whose parameters could be estimated using historical data sets. The optimization objectives considered were minimizing the energy drawn by LDC and minimizing feeder losses. However, this case did not consider any active communication between the

customer's HEMS and the LDC; the LDC only collects load data using smart meters to estimate the price-demand relationship. In the case of LDC controlled loads, it was assumed that the customers provided the LDC with information on the amount of shiftable loads based on a peak demand cap for the system that is communicated by the LDC to the customers. In addition to minimizing the LDC energy drawn and feeder losses, minimizing the customers' energy costs was also considered as a third optimization objective in this case. However no retail pricing was considered in calculating customers' energy costs which was calculated using the market prices instead.

From a review of the literature it is noted that very few works have considered all the issues of DR for industrial facilities in a comprehensive manner. Several of them have not considered peak demand minimization, or uncertainties in RES, or have examined the problem from one perspective only. Furthermore, most works have considered a dynamic pricing signal to activate the DR actions of the loads, which act independently, without taking into account the operational characteristics of the load facility processes. There is a need to develop a framework which addresses the above issues, and formulate a real-time price signal to activate the DR actions, which is based on two-way communication between the LDC and the industrial facility. Moreover, there is also a need to examine the operational time-frames of such DR mechanisms for actual implementation.

1.3 Research Objectives

The main goal of this research is optimal energy management of industrial loads which accounts for the largest portion of total electricity consumption in Canada. Specifically in this research, the focus will be on two major industrial load types; a utility sector load represented by a municipal WPS, and an energy sector load represented by an oil refining process. Accordingly, the main objectives of this research are outlined as follows:

- Propose EMS frameworks for optimal load management of different types of industrial loads. The frameworks will consider facilities equipped with DER such as RES and ESS. Also, as the industrial facility's daily operation is subject to variations in demand, energy price, and RES generation, the proposed framework will consider the uncertainty associated with forecasting these variables in order to reduce their impact on EMS decisions by applying the MPC technique.

- Develop load estimation models for industrial loads which can be incorporated into the EMS framework. The load estimation of a WPS facility will be carried out at the equipment level using the NN-based load modeling approach, which has the capability to model high order nonlinear load characteristics with reasonable computational complexity. The load estimation of the oil refining facility will be carried out at processing unit level because of the large scale and complexity of the refining processes.

- Develop a distribution optimal power flow (DOPF) model for distribution feeders representing the power utility feeding the industrial facilities. The DOPF model will consider unbalanced three-phase representation of the distribution feeder comprising three-phase and single-phase loads. It will also include the load models of the industrial facilities developed earlier. The DOPF model will be used to investigate the impact of industrial EMS decisions and load management on distribution feeders.

- Propose a DR strategy considering both the utility's and customer's perspectives for reducing the system peak demand and minimizing the customers energy costs. The strategy will consider two types of DR signals; desired demand profile signal and retail pricing signal. It will also consider the uncertainties in RES and non-industrial loads connected to the distribution feeder.

1.4 Outline of the Thesis

The rest of this proposal is structured as follows: Chapter 2 presents a brief background to the topics related to this research including; EMS, load modeling, MPC, WPS process, oil refinery process, and DSM. Chapter 3 describes the developed EMS and load estimation models for the WPS facility. Chapter 4 presents the proposed DR framework for the industrial loads. Chapter 5 presents the proposed EMS model for the oil refinery based on power demand modeling of the process. Finally, chapter 6 presents the main conclusions and contributions of this thesis, and identifies some directions for future research work.

Chapter 2

Background

2.1 Nomenclature

Indices

b	Bus, b = *1, 2, ..., B*
c	Capacitor, c = *1, 2, ..., C*
l	Line, l = *1, 2,..., N.*
p	Phase, p = *a, b, c*
t	Time interval, hours, t = *1, 2, ..., T*
tc	Load tap changer (LTC), tc = *1, 2, ..., TC*

Parameters

$\overline{Cap}$	Maximum switched capacitor's setting
$\underline{Cap}$	Minimum switched capacitor's setting
I_L^{sp}	Load current at specified power, $[A]$
$\overline{Tap}$	Maximum setting of LTC
$\underline{Tap}$	Minimum setting of LTC
U_3	Identity matrix of dimension 3x3

V^{sp}	Specified nominal phase voltage, $[V]$
$\overline{V}$	Maximum limit on phase voltage, $[V]$
$\underline{V}$	Minimum limit on phase voltage, $[V]$
ΔQ_c	Step change in reactive power from switched capacitor, $[kVAR]$
ΔS	LTC voltage regulation step change, [%]

Variables

Cap	Switched capacitor's setting
I	Phase current, $[A]$
I_L	Load's phase current, $[A]$
I_r	Receiving-end phase current, $[A]$
I_s	Sending-end phase current, $[A]$
P_L	Load's active power, $[kW]$
P_{Loss}	Feeder power losses, $[kW]$
Q_L	Load's reactive power, $[kVAR]$
Tap	LTC tap setting
V	Bus phase voltage, $[V]$
V_r	Receiving-end phase voltage, $[V]$
V_s	Sending-end phase voltage, $[V]$
X_c	Capacitor's reactive impedance, $[\Omega]$
Z_L	Load's impedance, $[\Omega]$
θ_L	Load's phase angle, $[rad]$

2.2 Energy Management Systems

EMSs were introduced in the power system to provide the utility with the tools to manage the system efficiently. With advances in software development during the 1990s, standardized EMSs started emerging, which could be applied to various customers with little customization, and reduced the initial cost of integrating them [27]. As software advance-

ments continued, present day EMSs are loaded with many decision support and control modules with user friendly interfaces.

2.2.1 EMS Functions and Architecture

The basic functions of an EMS are [27]:

- System monitoring
- Decision support
- System control

Supervisory control and data acquisition (SCADA) monitoring system is an essential element in EMS which collects measurement data periodically and sends it to the system control center. These data include power flows, breaker status, and voltage levels which are important for safe and reliable operations. Further analysis of power system data is carried out by decision support tools to enable the system operator to take efficient and reliable control actions. These tools include; power flow, contingency analysis, transient stability, unit commitment, generation dispatch, voltage control, load forecasting, and system reporting.

EMS decisions are used to control the power system operations in three different ways [27]:

1. Closed-loop control: the EMS control actions are implemented automatically on power system equipment, such as in automatic generation control (AGC) which adjusts the generation output for frequency regulation.
2. Supervised control: the control action is implemented by the operator through the EMS as in remote breaker switching.

3. Manual control: the control action recommended by EMS is implemented manually in case the means of automatic control are not available.

The most important measure for assessing EMS performance is system availability. This is considered from two aspects; first, the control actions of the EMS should prevent prolonged outages, and second the EMS should be designed in a reliable manner to prevent loss of communication with monitoring and control devices. Figure 2.1 [27] shows the EMS architecture with high level of device and communication redundancy between the control center and the remote terminal units (RTUs) used for collecting and transmitting data at different power network locations. The redundant hardware and communication links takes over in case of failures, to ensure EMS availability.

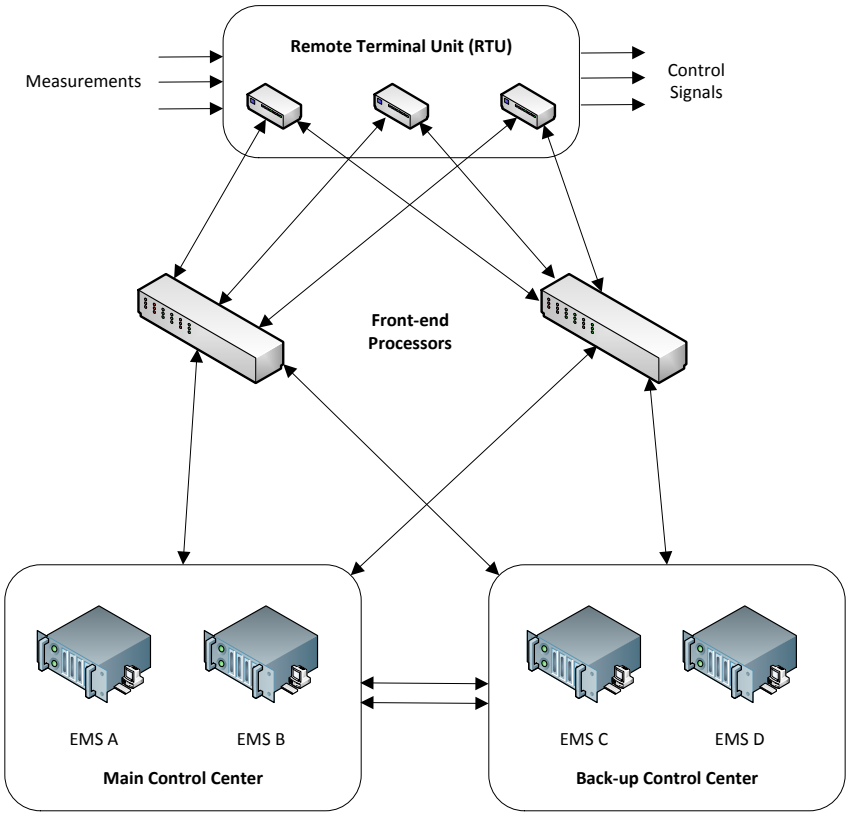

Figure 2.1: EMS Architecture [27].

2.2.2 Power System Operations

The efficiency of grid operations is improved through EMS applications, such as the optimal power flow (OPF), to find the optimal operation decisions. The OPF problem is a generalized formulation of the economic load dispatch (ELD) problem which involves adjusting the available controls to minimize an objective function subject to specified operating and security requirements. The general formulation of the OPF problem is given below where u represents the control variables and x represents the state variables of the power system [27]:

$$\begin{aligned} Minimize \quad & f(x,u) && (2.1)\\ Subject\ to \quad & h(x,u) = 0 && (2.2)\\ and \quad & g(x,u) \leq 0 && (2.3) \end{aligned}$$

Various objective functions can be considered for minimization in the OPF formulation, such as:

- Cost of operation
- Real power losses
- Equipment installation cost
- Reactive power supply cost
- Total carbon emissions

Equality constraints represent the demand-supply balance considering both real and reactive power flow equations. Inequality constraints include the system operational and security requirements such as limits on power generation and bus voltage levels.

2.2.3 Distribution Optimal Power Flow

The DOPF model determines the optimal operation decisions for the LDC distribution network. An unbalanced three-phase representation of the distribution network is considered for the development of the DOPF model; which comprises equations for loads, switched capacitors, transformer load tap changers (LTCs), network equations, operating limits, and feeder power loss equations. The models of the network components are developed based on the work presented in [28].

2.2.4 Load Models

The loads are of constant impedance type, as given below.

$$V_{b,p,t} = \quad Z_{L_{b,p,t}} I_{L_{b,p,t}} \qquad \forall b, \forall p, \forall t \tag{2.4}$$

$$Z_{L_{b,p,t}} = \quad \frac{V_{b,p}^{sp^2}}{P_{L_{b,p,t}} + jQ_{L_{b,p,t}}} \qquad \forall b, \forall p, \forall t \tag{2.5}$$

2.2.5 Load Tap Changer Model

The LTC is modeled as a three-phase regulator connected in series with the distribution transformers.

$$V_{s_{tc,p,t}} = \quad A_t V_{r_{tc,p,t}} \qquad \forall tc, \forall p, \forall t \tag{2.6}$$

$$I_{s_{tc,p,t}} = \quad A_t^{-1} I_{r_{tc,p,t}} \qquad \forall tc, \forall p, \forall t \tag{2.7}$$

where

$$A_t = (1 + \Delta S_{tc} Tap_{tc,p,t}) U_3 \tag{2.8}$$

2.2.6 Switched Capacitor Model

This is modeled as a variable capacitive impedance with multiple settings at different fractions of the total capacitance.

$$V_{b,p,t} = X_{c,p,t} I_{c,p,t} \qquad \forall c, \forall p, \forall t \tag{2.9}$$

$$X_{c,p,t} = \frac{-jV_{b,p}^{sp^2}}{Cap_{c,p,t} \Delta Q_c} \qquad \forall c, \forall p, \forall t \tag{2.10}$$

2.2.7 Network Equations

These include voltage and current relationships between all components of the distribution feeder.

$$\sum_{l} I_{r_{l,p,t}} = \sum_{l} I_{s_{l,p,t}} + \sum_{L} I_{L,p,t} \qquad \forall b, \forall p, \forall t \tag{2.11}$$

$$V_{r_{l,p,t}} = V_{s_{l,p,t}} = V_{b,p,t} \qquad \forall b, \forall p, \forall t \tag{2.12}$$

2.2.8 Operating Limits

These include allowable bus voltage deviations from the nominal values, and possible switching positions for LTCs and switched capacitors.

$$\underline{V_{b,p}} \leq V_{b,p,t} \leq \overline{V_{b,p}} \qquad \forall b, \forall p, \forall t \tag{2.13}$$

$$\underline{Tap_{tc}} \leq Tap_{tc,p,t} \leq \overline{Tap_{tc}} \qquad \forall tc, \forall p, \forall t \tag{2.14}$$

$$\underline{Cap_c} \leq Cap_{c,p,t} \leq \overline{Cap_c} \qquad \forall c, \forall p, \forall t \tag{2.15}$$

2.2.9 Distribution Feeder Losses

Hourly power losses of the distribution feeder are calculated as follows:

$$P_{Loss_t} = \sum_{l,p} |Re(V_{s_{l,p,t}} I^*_{s_{l,p,t}} - V_{r_{l,p,t}} I^*_{r_{l,p,t}})| \quad \forall t \tag{2.16}$$

2.3 Load Modeling

There are two main methods for load model estimation, component-based and measurement-based [29]. In the component-based methods, models of individual components making up the load are aggregated, this approach requires identifying the physical properties and dynamic behaviors of the load components. In the measurement-based methods, power demand data is collected using measurement devices and a suitable technique is used to determine a closed-form relationship between the power demand and the control variables, hence this method can be considered as an identification problem. Polynomial models and NN-based models have been used widely as a load model structure in the measurement-based approach, applying a regression or NN training for identification of model parameters.

2.3.1 Polynomial Models

Polynomial models are commonly used for single/multiple input, single-output data modeling since interpolation polynomial is a basic mathematical technique. The general expression for a polynomial model of degree m with n number of inputs is given as:

$$y = a_0 + \sum_{i=1}^{n} a_i x_i + \sum_{i_1=1}^{n} \sum_{i_2=i_1}^{n} a_{i_1,i_2} x_{i_1} x_{i_2} + \sum_{i_1=1}^{n} \dots \sum_{i_2=i_{m-1}}^{n} a_{i_1,\dots,i_m} x_{i_1} \dots x_{i_m} + e \tag{2.17}$$

Nonlinear regression is used to identify the parameters of the polynomial model in (2.4), a_0, a_i, a_{i_1,i_2}, and $a_{i_1,\dots,i_m}$ while e denotes the error which represents the deviation between the regression model estimates and actual measured values. The parameter identification problem is solved by least squares technique after converting the nonlinear regression into the following multiple linear regression model:

$$y = a_0 + \sum_{i=1}^{n} a_i x_i + \sum_{i_1=1}^{n} \sum_{i_2=i_1}^{n} a_{i_1,i_2} x_{i_1,i_2} + \sum_{i_1=1}^{n} \dots \sum_{i_2=i_{m-1}}^{n} a_{i_1,\dots,i_m} x_{i_1,i_m} + e \tag{2.18}$$

where

$$x_{i_1,i_2} = x_{i_1} x_{i_2} \tag{2.19}$$

$$x_{i_1,i_m} = x_{i_1} x_{i_2} \ldots x_{i_m} \tag{2.20}$$

The polynomial model gives higher approximation accuracy as the polynomial degree m increases. However, the model complexity increases significantly with increase in m or with increase in the number of inputs n. This increase in complexity makes the parameter identification problem practically infeasible for typical size problems due to the high computational burden. Therefore polynomial models are usually used in conjunction with a structure selection technique which reduces the degree of complexity by reducing the number of terms and polynomial degree, which however reduces the modeling accuracy [30].

2.3.2 Neural Network Model

The most important features of an NN are that it comprises large number of basic units (neurons) that are highly parallel and strongly connected and can be trained using data [30]. The universal approximation capability of NN makes it a commonly used tool for data modeling. The universal approximation capability on NN means that it can approximate any smooth function to a certain degree of accuracy [26]. Compared to polynomial models, NN based models have better approximation capability for high-order load models [31]. The neuron is the building block of the NN and its structure with n inputs is shown in Figure 2.2. The neuron inputs are multiplied by weights (w_1,w_2,...w_n) and then the weighted inputs are summed with a bias (b). The neuron activation function (f_N) is applied to the sum which results in the neuron output. There are two saturation type functions commonly used as activation functions, the log-sigmoid (logistic) function given by:

$$f_N(x) = logistic(x) = \frac{1}{1 + e^{-x}} \tag{2.21}$$

and the tan-sigmoid (hyperbolic tangent) function given by:

$$f_N(x) = tanh(x) = \frac{e^x + e^{-x}}{e^x - e^{-x}} \tag{2.22}$$

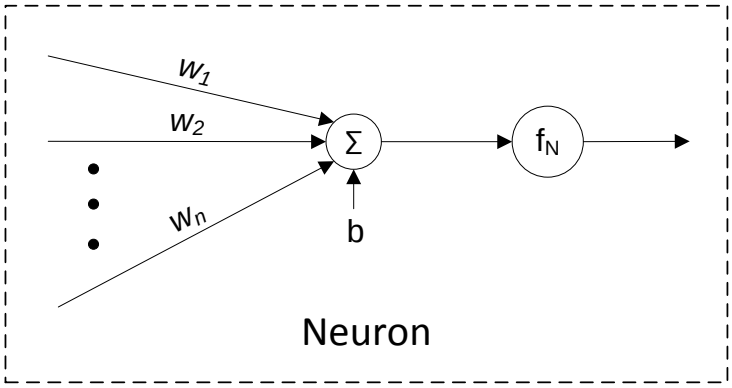

Figure 2.2: Single neuron structure.

The structure of a single hidden layer NN with n inputs and m outputs and k neurons in the hidden layer is shown in Figure 2.3. The relationship between the NN inputs and outputs, in terms of network weights and biases, is given below:

$$y_m = \sum_{i=1}^{k} [\, f_i(w_{1i}^{in} x_1 + ... + w_{ni}^{in} x_n + b_i^{in})\ w_{im}^{out}\,] + b_m^{out} \tag{2.23}$$

The input and output data used for NN training are divided into three sets; training set, validation set, and testing set. The NN training is carried out by varying the weights (w) and biases (b) in order to reduce the error between the estimates and the actual values by minimizing a performance index such as the mean squared error (MSE), the mean absolute error (MAE), the sum of squared error (SSE), or the sum of absolute error (SAE) [32]. The back propagation algorithm is commonly used to calculate the gradients of the network output with respect to network parameters in order to identify the contribution of each parameter to the error in output [30]. The network parameters are updated continuously based on the gradients identified in the back propagation algorithm until the performance index value applied to the validation set stops improving [32].

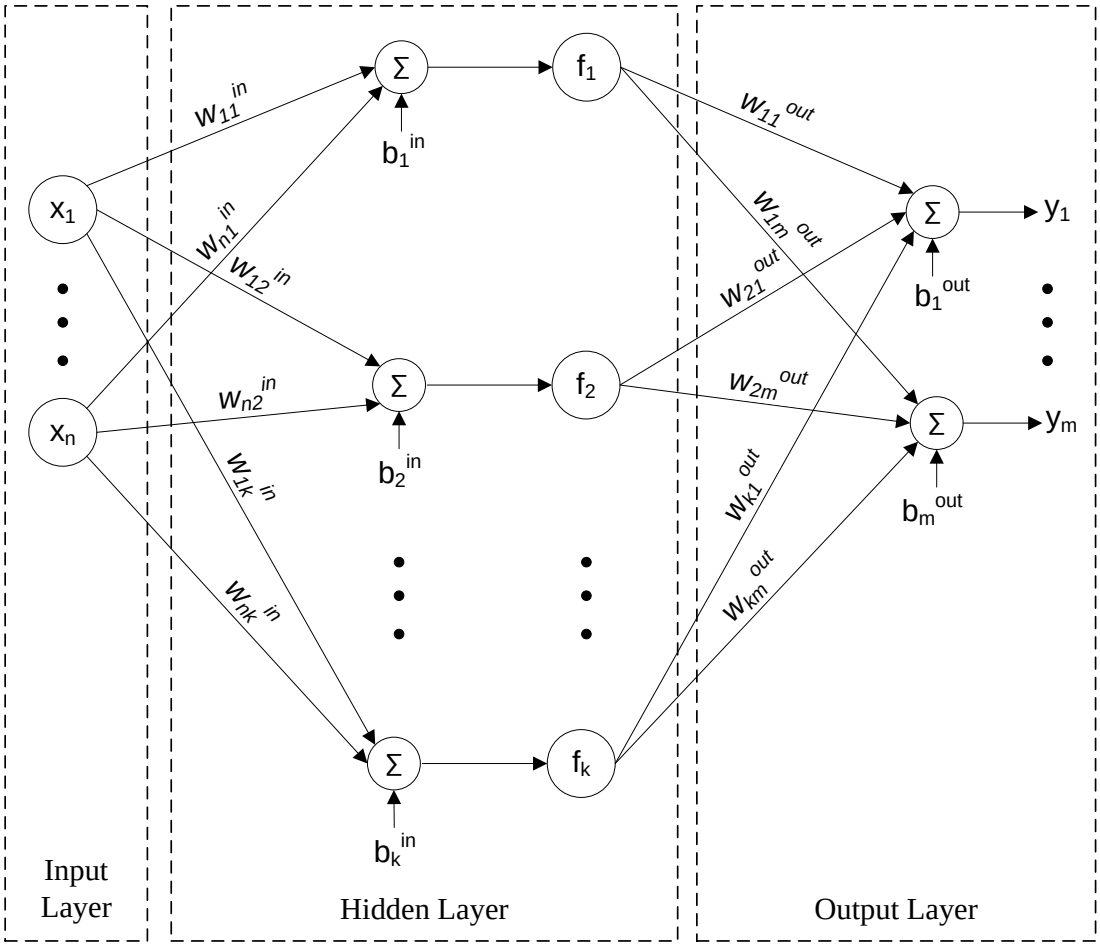

Figure 2.3: NN structure with a single hidden layer.

2.4 Mathematical Programming

Mathematical programming refers to the formulation of an optimization problem and solving it using a suitable optimization method. Solving an optimization problem is achieved by finding the set of values for decisions variables that will result in minimizing or maximizing a certain objective function subject to equality and inequality constraints. Depending on the nature of the objective function and constraints, the problem can be classified as

linear program (LP) or non-linear program (NLP). Also based on the type of decision variables, an optimization problem can be classified as continuous, integer, or mixed-integer program (MIP). In this work, General Algebraic Modeling Systems (GAMS), which is a commercial mathematical modeling platform, is used to formulate and solve the optimization problems. GAMS is a high-level modeling system for mathematical optimization, that utilizes various solvers to handle the different types of optimization problems.

LP problem consists of linear objective function and constraints. LP problem is classified as mixed integer linear program (MILP) when at least one decision variable is an integer variable. The constraints of an LP problem forms a polyhedron of feasible solutions where the optimal solution lies at one of its vertices. LP problems are typically solved using the Simplex and Interior-point methods. The Simplex method is a systematic procedure for evaluating the objective function value at the polyhedron vertices to find the optimal solution [33]. While the interior point method the candidate solution traverses through the interior of the polyhedron to arrive at the optimal solution [34]. Solving MILP problem is more challenging due to the presence of integer decision variables. The Complete Enumeration method can be used to solve MILP problems but it becomes computationally expensive in the presence of large number of integer variables [35]. More computationally efficient methods are the Cutting Plane and and the Branch and Bound methods [36]. In the Cutting Plane method, constraints are added to the problem until all the vertices of the feasible space corresponds to integer solutions. While the Branch and Bound method involves an intelligent enumeration of candidate solutions while discarding a large set of useless candidates using upper and lower bounds that are determined though solving subproblems with smaller feasibility space [35].

An optimization problem is classified as NLP when the objective function or one of the constraints is a non-linear function of the decision variables. In the presence of at least one integer decision variable, the problem is classified as mixed integer non-linear program (MINLP) problem. The most common NLP optimization methods are the Gradient methods, and Interior-point methods [35]. In the Gradient methods, the slope of the function is used to determine the direction of the search direction for optimal solution.

The Interior-point methods traverse through the interior of the feasible space while using barrier functions to arrive at the optimal solution [33]. The solver used in this work to solve NLP problems is the IPOPT [37] solver which is an NLP optimizer which implements the interior point method to solve large-scale models whose functions can be nonconvex. The robustness of IPOPT solver relies on the used solver for linear barrier function. The default linear solver used by IPOPT in GAMS is MUMPS which is a sparse symmetric large-scale linear solver.

MINLP problems are generally solved using decomposition algorithm which involves solving a series of NLP and MIP problems. The solution methods discussed earlier are then used to solve the NLP and MIP problems. Decomposition-based solvers are computationally efficient in terms of solution time and required memory space. Also, Heuristic methods are widely used for large MINLP problems that enormous amount of computational time [34]. These methods include Genetic Algorithm, Particle Swarm Optimization, Ant Colony Optimization, Tabu Search, and Simulated Annealing methods [33]. the solver used to solve MINLP problems is the DICOPT [38] solver which is an decomposition algorithm that involves solving a series of NLP and MIP problems using selected NLP and MIP solvers. The algorithm starts by solving the relaxed MINLP problem using the NLP solver and if the resulting solution is an integer solution, then the search stops. Otherwise the algorithm continues by searching for an integer point though solving an MIP master problem. The integer variables are fixed for the next NLP solve and the algorithm continues alternating between NLP and MIP solves until the solution of the NLP subproblems starts worsening. In this work, the selected NLP and MIP solvers for DICOPT are SNOPT and CPLEX, respectively.

2.5 Model Predictive Control

MPC is an optimization-based strategy to deal with uncertainties in forecasted variables. In MPC, the optimization problem is solved for a given horizon but the solution is im-

plemented for the first time step only [39]. Then in the second iteration the optimization horizon is moved forward and the problem is solved again and implemented at the second time step, and so forth. Despite the computational burden, MPC is expected to yield better optimization solutions since the uncertainty in variables is expected to reduce as the solution horizon is shifted forward.

There are two types of MPC; rolling horizon MPC and receding horizon MPC. In the rolling horizon MPC the length of the optimization horizon is fixed, as shown in Figure 2.4(a), while the optimization problem is shifted forward by one time step every iteration. In the receding horizon MPC, the last time step of the optimization horizon is fixed as shown in Figure 2.4(b) while the length of the horizon shrinks with every iteration. Receding horizon MPC is more suitable when a certain variable is required to be at a certain level by the end of the optimization horizon in preparation for the next optimization cycle; however, as the optimization window shrinks its capability to improve the solution may be impacted [40].

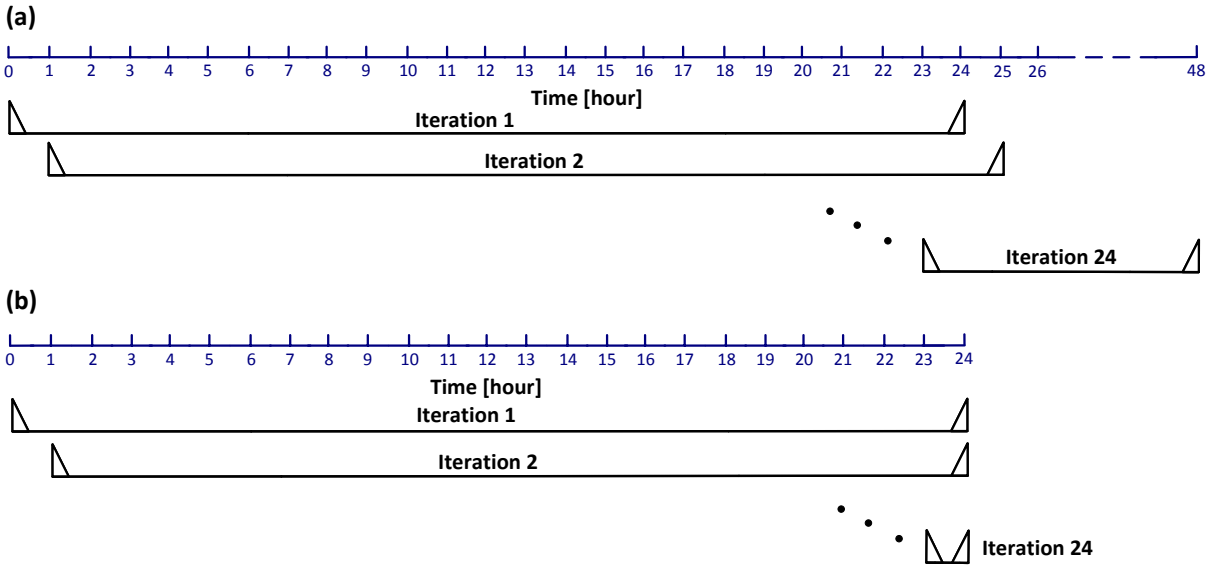

Figure 2.4: (a) Rolling-horizon MPC (b) Receding-horizon MPC.

2.6 Water Pumping System

Water pumping stations account for the largest share of the energy consumed in a water distribution system, and they typically comprise multiple pumps driven by induction motors [11]. The pumps uplift the water to a number of elevated reservoirs. Water then flows by gravity from the reservoirs to the municipal demand centers. Figure 2.5 [10] shows a typical WPS comprising five centrifugal pumps supplying water to an elevated storage reservoir.

The WPS is faced with continuously varying water demand and hence needs to have very flexible water flow characteristics. Also the WPS operator has to ensure adequate water level in the reservoir, meeting the capacity limits, under variable municipal water demand. This necessitates variable water flow from the pumping station to the storage, which can be achieved by controlling the operational status (ON/OFF) of pumps based on an optimized schedule. Wider range of variability can be achieved by controlling both the operational status of pumps and the water flow rate out of each pump. The water flow rate of pumps can be varied using pressure control valves or by changing their rotational speed. Varying the rotational speed is the energy efficient option since it reduces energy consumption significantly [12]. For centrifugal pumps, the flow rate (q) is directly proportional to the rotational speed (N) while the power demand (P) is proportional to N^3, according to the affinity laws given below [41]. Therefore, large energy savings can be achieved by changing N.

$$q \propto N \tag{2.24}$$

$$P \propto N^3 \tag{2.25}$$

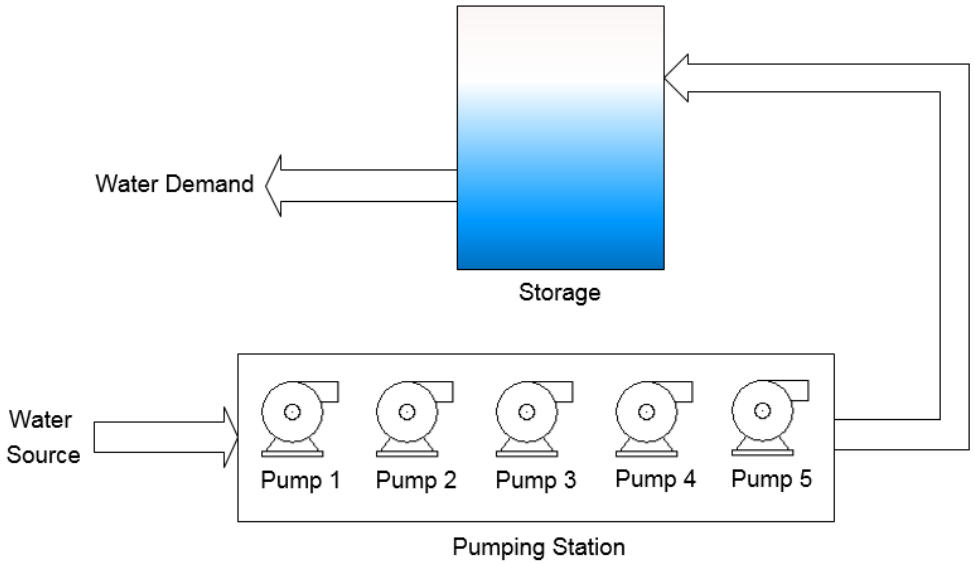

Figure 2.5: Layout of a WPS facility [10].

2.7 Oil Refinery Process

An oil refinery is a complex processing facility for transforming crude oil to marketable refined products by fractionating the crude stream through distillation and then improving the fractions quality using physical and chemical treatment processes. Various refined products are produced by refineries around the world including; gasoline, kerosene, diesel, lubricating oils, waxes, fuel oil, asphalt, and LPG. These products are used in transportation, lighting, heating, power generation, and paving of roads.

Figure 2.6 [42] shows the process flow of a general oil refinery. The first step in oil refining is distillation of crude oil into boiling range fractions in the Crude Distillation Unit (CDU). These fractions include wet gas, naphtha, distillates such as diesel and kerosene, gas oil, and residue. As the CDU processes all crude oil input stream to the refinery, the refinery capacity is usually expressed in terms of CDU processing capacity [20]. The CDU output streams are further processed by different refinery processes. The wet gas is processed in the gas recovery unit where LPG is recovered. The kerosene and naphtha

are hydrotreated in the hydrogen treatment units which carry out chemical reactions for removing the heteroatoms including sulfur, nitrogen, and heavy metals in order to meet the clean fuel regulations. Another purpose of hydrotreating is to prevent catalyst deactivation in some refining processes caused by heteroatoms [20].

The crude residue of the CDU is processed in vacuum distillation unit (VDU) for further fractionation, producing vacuum oil, lube distillates, residual oil and asphalt stock. The residual oil, the heaviest residue of distillation, is processed in delayed coking unit and visbreaking unit. The coking process cracks the residual oil into light products including fuel gases, gasoline, petroleum coke, and large volumes of coker gas oil [20]. The visbreaking unit produces reduced viscosity gas oil through thermal cracking of residual oil. Lube distillates are processed in the lube oil processing unit to produce lubricants and waxes while the asphalt unit produces asphalt using the stock resulting from the VDU process.

Fluid catalyst cracking (FCC) is one of the most important processes in refining as it accounts for up to 40% of total refinery products [20]. The FCC process uses catalytic reaction at high temperature and low pressure to convert gas and vacuum oils from distillation to light gases, gasoline blendstock, and diesel blendstock. The distillate hydroforming unit is used to reduce the sulfur content of kerosene and diesel which results in the formation of hydrogen sulfide (H_2S) gas.

Another very important process in refining is the catalytic reforming unit. This unit processes naphtha stream, mainly from CDU, using catalytic reactions to produce reformate which is a high-octane gasoline blendstock. Large volumes of hydrogen gas (H_2) are produced as by-product of the reforming process which supplies the refinerys needs of hydrogen [20]. The isomerization unit enriches the naphtha with saturated hydrocarbons resulting in high-octane isomerate fuel [43]. The alkylation unit further processes the isomerate fuel from isomerization unit to produce high-octane gasoline blendstock (Alkylate).

The share of electrical energy for various processing units of the refinery, described in Figure 2.6, is given in Table 2.2 [42]. Electricity demand of the refinery is typically supplied either from the power grid or from on-site generation which accounted for about 27% of the

electrical energy supply to the petrochemical industry in USA, in 2002. The vast majority of on-site generation was from cogeneration facilities as they produce both electricity and heat for refining processes yielding a very high energy efficiency of 60-80% [44].

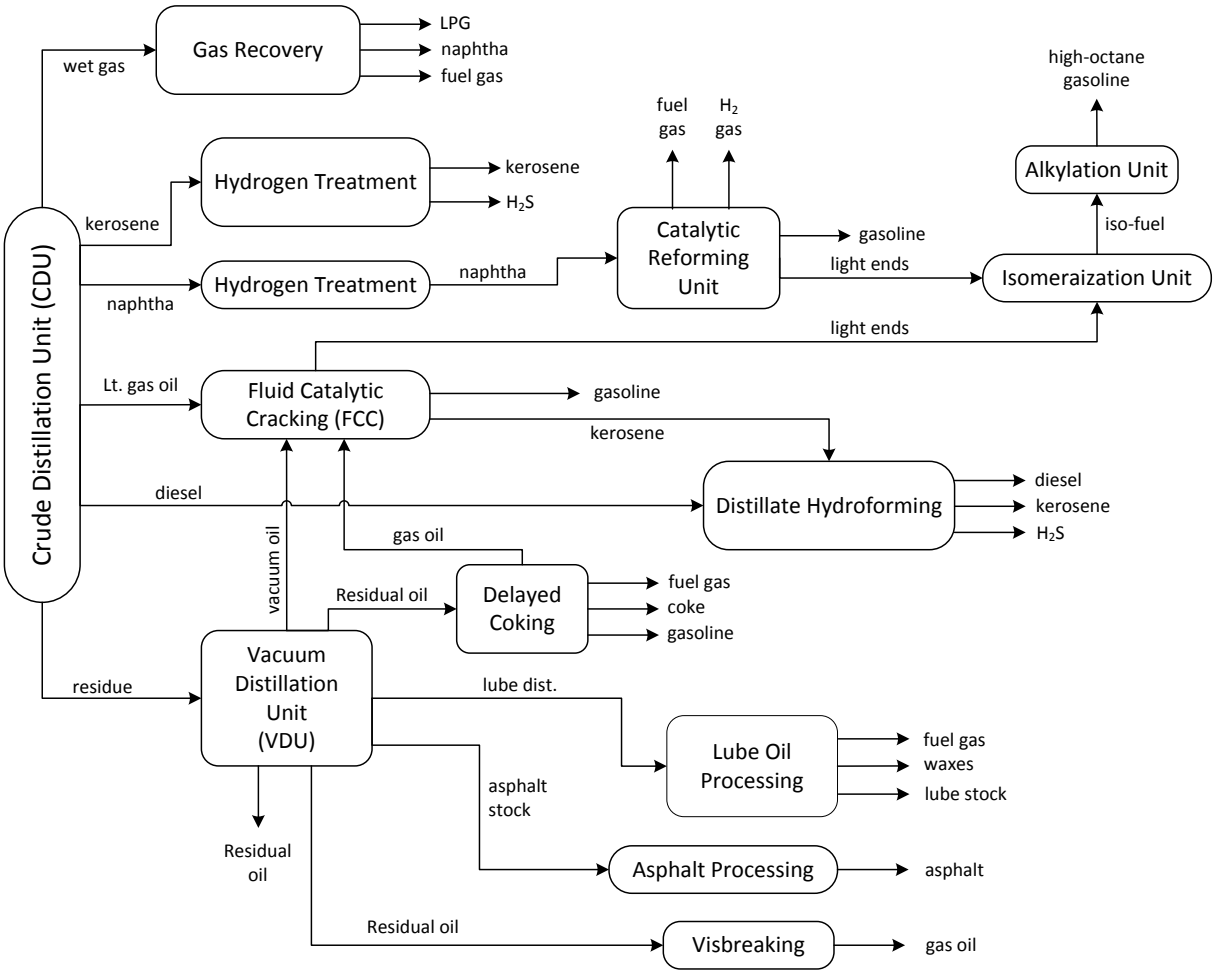

Figure 2.6: Process flow of oil refinery [42].

Table 2.2: Share of Electrical Energy Demand of Various Processing Units of the Refinery

Processing Unit	*Share Electrical Energy Demand (%)*
Crude Distilation	13.8
Vacuum Distilation	2.3
Delayed Coking	1.2
Catalytic Cracking	26.5
Distillate Hydroforming	9.4
Lube Oil Processsing	4.6
Asphalt Processing	1.2
Visbreaking	2.1
Naptha Hydrogen Treatment	5.8
Catalyst Reforming	17.1
Isomerization	1.2
Alkylation	5.5
Gas Recovery	7.1
Kerosine Hydrogen Treatment	2.3

2.8 Demand Side Management

DSM refers to the set of programs used by the power utility to encourage the customers to change their power usage in terms of time of use, instantaneous power demand, and total energy consumption. DSM programs can be classified into two main categories; economic-based and stability-based programs [45]. Economic-based programs are designed to minimize the price spikes during high demand periods by providing customers with incentives to change their energy usage patterns. Stability-based programs are designed to stretch the generation and transmission limits of power grids without investing in additional infrastructure [45]. DSM programs promote power system efficiency and sustainability by maximizing the utilization of existing infrastructure and reducing the carbon emission levels, using smart pricing, monetary incentives, and government policies. However, it requires sophisticated coordination between the power system operator and customers to reduce the overall operational cost of the system [46].

There are three general approaches for customers' DR; reducing energy consumption during critical periods of peak demand on grid, continuous response to market energy price changes, and utilizing on-site power generation or storage systems to reduce the demand from power grid [47]. DR results in one of the following three outcomes [48]:

- Peak clipping- reducing peak energy consumption to prevent the load from exceeding generation capacity or equipment thermal limits.
- Valley filling- encouraging off-peak energy consumption by customers and other entities such as energy storage devices and plug-in electric vehicles.
- Load shifting- combination of the previous two outcomes where energy consumption is shifted from on-peak period to off-peak period.

Based on the type of DSM signal, DR can be classified as physical DR and market DR, which are used jointly to achieve efficient and safe operation of the power grid [49].

In physical DR, the power utility sends a mandatory request to customers to participate in DSM in case of events where grid limits are reached such as line congestions and out-of-service equipment. Market based DR uses dynamic pricing and incentives to encourage the customers to participate in DSM, and is classified into price-based DR programs and incentive-based DR programs, respectively.

2.8.1 Price-based DR Programs

Price-based DR programs use dynamic pricing instead of the classical flat pricing to encourage customers to change their energy usage behavior. Traditionally, utilities have provided highly reliable service with fixed energy rates that were determined well in advance. However, given the high level of uncertainty in present power systems, actual conditions can become considerably different from those predicted at the time of energy price determination, which could result in extreme stresses on the power grid. As the cost of providing electricity varies with time, location, system, and weather conditions, closer tracking of these changes is needed by flexible pricing where energy prices are calculated and posted close to the time of consumption, and are applied for shorter time horizon [50].

Dynamic pricing includes TOU, critical peak pricing (CPP), IBR, and real-time pricing (RTP). TOU tariff applies different energy prices at different time intervals during the day, where on-peak interval usage is charged a much higher price than off-peak interval usage [48]. Figure 2.7 [51] shows Ontario TOU tariffs during weekdays for summer and winter pricing schemes. In CPP, TOU pricing is generally implemented but a higher price is applicable for a limited number of hours or days in the year when the system peak load is very high and reliability is at risk [48]. IBR pricing is designed such that customers with higher energy usage are charged a higher energy price, if they exceed a certain threshold defined for each energy usage block [48]. In RTP, energy price varies at different time intervals of the day, typically every hour of even shorter interval [48]. Applying dynamic pricing is effective in shifting a significant portion of loads from on-peak to off-peak period, thus reducing the overall system peak. However, it does not necessarily result in a reduction

in overall energy consumption [49].

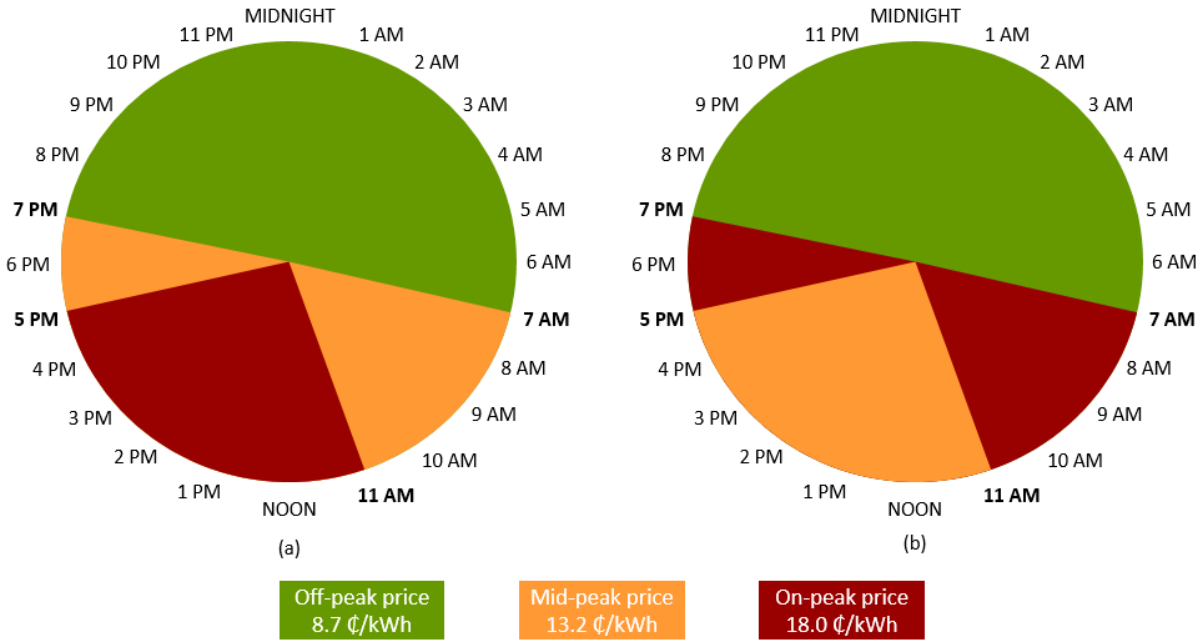

Figure 2.7: Ontario weekdays TOU tariff (a) summer pricing (b) winter pricing [51].

2.8.2 Incentive-based DR Programs

Incentive-based DR uses monetary incentives to encourage the customer to participate in the following programs [48]:

- Direct load control: power utility has a direct control of customers equipment.
- Interruptible/curtailable load: power utility provides customers with incentive discounts if they participate in load shedding programs.
- Demand bidding and buyback: large customers can respond to system contingencies by load curtailment at specific bid price offered by the power utility in the capacity market.

- Emergency demand response: incentive payments for customers who voluntarily respond to emergency DSM signals sent by power utility with short notice.

2.9 Summary

This chapter presented a brief background to the topics related to this research including; EMS, load modeling, Mathematical Programming, MPC, WPS and oil refinery processes, and DSM. EMS functions and architecture was discussed in the first section with emphasis on power system optimization and OPF as one of the most important functions of the EMS, in addition to DOPF mathematical models. The second section discussed polynomial and NN-based load modeling techniques which are used to determine the relationship between energy consumption and load control variables. A background about mathematical programming was presented in the third section with emphasis on the optimization tools and solvers used in this work. MPC was discussed in the forth section as an uncertainty management technique. A description of the WPS and the oil refinery processes was presented in the fifth and sixth sections. The last section discussed DSM and DR schemes in practice.

Chapter 3

A Controlled Load Estimator Based Energy Management System for Water Pumping Systems[‡*]

3.1 Nomenclature

Indices

i	Iteration, i = *1,2,...,I.*
j	WPS pump, j = *1,2,...,J*
k	NN hidden layer neuron, k = *1,2,...,K*
t	Time interval, hours, $t = 1, 2, ..., T$

[‡]Parts of this chapter have been published in: O. Alarfaj and K. Bhattacharya, "A controlled load estimator-based energy management system for water pumping systems," IEEE Transactions on Smart Grid, vol. 9, no. 6, pp. 6307-6317, 2018.

[*]An earlier version of this work was presented in: O. Alarfaj and K. Bhattacharya, "Power consumption modeling of water pumping system for optimal energy management," in Power and Energy Society General Meeting (PESGM), 2016. IEEE, 2016, pp. 15.

Parameters

b_k	Bias of NN hidden layer neuron
b^{out}	Bias of NN output layer neuron
D_t	Municipal water demand, $[m^3/h]$
DoD	BESS depth of discharge, $[p.u.]$
E_R	BESS energy storage capacity, $[kWh]$
L_{min}	Minimum water storage volume, $[m^3]$
L_{max}	Maximum water storage volume, $[m^3]$
L_0	Initial water storage volume, $[m^3]$
M	Large number
P_R	BESS charging/discharging power rating, $[kWh]$
P_{RE_t}	Power from renewable energy source (RES), $[kW]$
q_{min}	Minimum water flow rate out of WPS pump, $[m^3/h]$
q_{max}	Maximum water flow rate out of WPS pump, $[m^3/h]$
SOC_0	Battery energy storage system (BESS) initial state of charge (SOC), $[kWh]$
w_k	Weight of the connection between NN input layer and hidden layer neurons
w_k^{out}	Weight of the connection between NN hidden layer and output layer neurons
x, y	NN input, output
λ_p	Peak demand coefficient, $[\$/kW]$
λ_{dch}	BESS discharging efficiency, [%]
λ_{ch}	BESS charging efficiency, [%]
ρ_t	Energy price, $[\$/kWh]$

Variables

ir_t	Storage water inflow rate, $[m^3/h]$
or_t	Storage water outflow rate, $[m^3/h]$
$P_{t,j}$	Power demand of WPS pump, $[kW]$
P_{max}	Peak power drawn by the WPS from LDC, $[kW]$

Pb_t	Active power discharge (+ve) or charge (-ve) from/to BESS, $[kW]$
P_{LDC_t}	Active power exchanged by the WPS with the local distribution company (LDC), $[kW]$
$q_{t,j}$	Water flow rate out of WPS pump, $[m^3/h]$
sl_t	Storage water volume, $[m^3]$
SOC_t	SOC of BESS, $[kWh]$
$st_{t,j}$	Binary decision variable for operation status of a pump (1:ON, 0:OFF)
T_m	Mechanical torque of a pump, $[N.m]$
ω	Angular speed of a pump, $[rad/s]$
$Zdch_t$	Binary decision variable for discharging BESS (1: discharge, 0: do nothing)
Zch_t	Binary decision variable for charging BESS (1: charge, 0: do nothing)

3.2 Introduction

Water distribution systems are one of the most important industrial loads with significant energy consumption, a major part being pumping stations typically comprising multiple pumps driven by induction motors [11]. Optimizing the energy consumption of water pumping systems (WPS) by investing in EMSs can result in large savings in energy costs, in addition to alleviating the environmental impact of energy usage.

Load modeling is an essential part of EMS as it relates the power demand with the process variables and operating conditions. As load models improve in precision and accuracy, further operational and economic efficiency can be achieved by integrating them in the optimization model within the EMS. Polynomial models and neural network (NN) based models have been used in the literature as a load model structure. First and second-order polynomials were used in [3] to model the active and reactive power consumption as a function of the voltage and process control variables of a flour mill and a water pumping facility. A polynomial model was used in [8] to estimate the energy consumption as a function of the amount of processed material. NN-based load models are reported in

[31, 52, 53, 54] utilizing the universal approximation capability of NN [31].

The EMS model for WPS implemented in this work is based on the optimal load management model proposed in [3] for minimizing energy cost and demand charge for the WPS facility. However, in order to improve the load modeling accuracy of the WPS load, a novel Controlled Load Estimator (CLE) based EMS, shown in Figure 3.1, is proposed in this work which comprises, a) a simulation of the WPS load, b) NN training, and c) the EMS. The load simulation is used to construct the load data set under various operational conditions. This data set is input to the NN to arrive at the functional representation of the WPS load model, which is then integrated within the EMS to determine the optimal control variables. Finally, these optimal variables are fed back to the load simulation to arrive at updated simulations of power demand data. This process continues and an efficient and smart control of the EMS is arrived at.

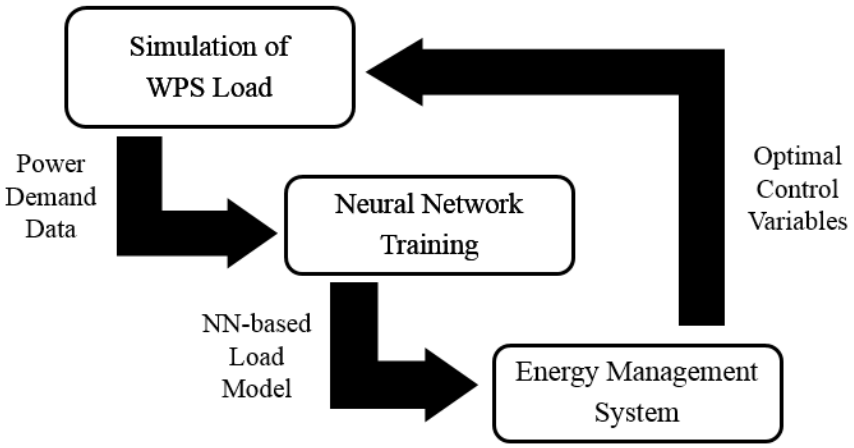

Figure 3.1: Architecture of the proposed CLE based EMS for WPS.

Another challenge facing the development of EMS is dealing with forecasting uncertainties. Since the optimization horizon of an EMS is for a future time period, typically 24 hours ahead, inputs are obtained through forecasting algorithms which vary in accuracy. Therefore, expected benefits from EMS decisions may not be attained as the system is

subjected to actual inputs rather than forecasted inputs used in the EMS. Although good forecasting algorithms reduce the uncertainty in inputs, they are still prone to deviations from actual values.

For further uncertainty minimization, model predictive control (MPC) techniques are being adopted into EMS formulations. The theoretical aspects of MPC are well established and has proven its practicality in many control applications [39]. MPC is used in [39, 39, 54, 55] for EMS applications of residential buildings and microgrids considering uncertainties in energy price, power demand, and weather forecasts. This work applies receding horizon MPC algorithm in order to reduce the impact of forecasting uncertainties on the performance of EMS optimization. Three sources of uncertainty are handled using MPC technique which are; water demand, energy price, and generation from RES.

With increasing awareness of environmental impacts, several industrial facilities are considering investing in RES within their premises to supplement or substitute their energy needs from conventional sources. In this work it is assumed that the WPS is equipped with wind based generation. Moreover, because of the intermittent nature of the wind based RES, a battery energy storage system (BESS) is used in conjunction in order to maximize renewable energy utilization.

In view of the above discussions, the main contributions of this work are:

- A comprehensive EMS framework is proposed for a WPS considering various operational aspects including load management, water flow management, process control technology, equipment operational limits, uncertainty mitigation, and carbon footprint alleviation. The proposed framework comprises a module for simulation of the WPS load, a module for estimation of the WPS load using NN, and an EMS model for determining the optimal schedules.

- A load simulation model is developed in PSCAD to compute the power demand of the WPS under different operating conditions; the load dataset thus created, is used to estimate the WPS load model using a NN-based approach.

- An iterative CLE approach is proposed which comprises a feedback of the EMS optimal decisions to the WPS load simulation module, followed by NN re-training, and re-solving the EMS model. This approach improves the accuracy of load estimation at optimal operating points, and enables the EMS model to re-examine the optimality of the reached solution considering other potential schedules. Eventual convergence of the CLE leads to a smart and efficient control of the WPS.

- The uncertainties associated with forecasting of WPS load, energy price, and RES generation are considered by reformulating the EMS problem using MPC technique in order to reduce the impact of uncertainties on the model performance.

- The proposed CLE based EMS framework is extended to consider WPS equipped with RES and BESS. To this effect the EMS model is appropriately extended to include BESS constraints, and RES inputs.

The rest of the chapter is structured as follows: Section 3.3 describes the developed load estimation model for the WPS considering modeling uncertainty. The EMS model for WPS is described in Section 3.4. Case study results are reported and discussed in Section 3.5. Finally, Section 3.6 presents the conclusions of this chapter.

3.3 Water Pumping System Load Modeling

To the best of the authors' knowledge, there are no reported works in the literature that relate the electricity consumption of the variable speed pumps with their water output flow rate. Instead pump manufacturers usually provide performance curves which are constructed from field tests. However, these curves are not useful for the present application as they don't present a direct functional relationship between the power demand of the pump and the water flow rate at various rotational speeds. Therefore measurement based function fitting models are used in this work to estimate the relationship between the WPS input power and output water flow quantities.

Variable speed pumping is considered in this work through the development of a simulation model for the WPS considering VSD driven pumps. The power demand model of the WPS is developed in two main steps. The first step is to develop a simulation model for the WPS electrical load in PSCAD. The second step is to use the data generated from the PSCAD simulations to train a NN in order to arrive at a closed-form relationship between the WPS control variables and the associated power demand. The NN-based model is selected since it provides a better approximation for high-order load models as compared to other measurement based models reported in the literature. The advantage of using a measurement based model for load estimation is the provision of training using actual measurement data that can be collected during the operation of an actual WPS facility. A simple feedforward NN with single hidden layer was sufficient in the present work to arrive at a well fitted function model with reasonable accuracy and fast convergence.

Another approach which has been widely used for model estimation is the polynomial curve fitting by regression. However, it has been reported in the literature that NN has better capability of function fitting than the polynomial models, specially for higher order functions [31]. A new analysis is carried out to compare the NN based function approximation versus the polynomial curve fitting approach for a single pump data set of the WPS, in terms of the resulting mean squared error (MSE) for the two models, as shown in Table 3.1. It is noted that the NN model results in significantly higher estimation accuracy, or lower value of MSE, without increasing the complexity of the optimization problem, since both models result in nonlinear programming (NLP) optimization models.

The centrifugal pumps are modeled in PSCAD as a three-phase induction machine supplied from the grid through a VSD, as shown in Figure 3.2. The machine is started initially in speed control mode and then after it reaches its rated speed of $0.97\,pu$ and the transients die out, the machine is switched over to torque control mode to model the mechanical loading imposed by water pumping. In the torque control mode, the output mechanical torque is assumed to be equal to the square of the rotational speed according to centrifugal pumps torque characteristics given by:

$$T_m = \omega^2 \tag{3.1}$$

In the PSCAD simulation model, Figure 3.2, The VSD rectifies the grid ac voltage using a bridge rectifier and then inverts it to ac supply with controllable frequency and voltage using a PWM inverter. The control strategy used for varying the machine speed is based on V-f control in which the ratio of the supplied voltage magnitude to its frequency is kept constant when operating at less than the rated frequency. This control strategy ensures a constant torque characteristic for the machine at speeds lower than its rated speed.

The NN toolbox in MATLAB is used for fitting the data with the network topology shown in Figure 3.3. The relationship between the NN inputs and outputs in terms of network weights (w) and biases (b) is given below, where set k represents the index for hidden layer neurons in the NN model and f_k is the activation function used in the hidden layer of the network, which is a tan-sigmoid function.

$$y = \left[\sum_{k=1}^{K}(f_k(w_k x + b_k)w_k^{out})\right] + b^{out} \tag{3.2}$$

where

$$f_k(n) = tanh(n) = \frac{e^n + e^{-n}}{e^n - e^{-n}} \tag{3.3}$$

Uncertainty in the load model may arise from data acquisition and NN modeling errors. Data acquisition errors are not considered in this work since the data set is developed through PSCAD simulations, and are immune to noise and measurement errors. The modeling errors are handled by the novel CLE proposed in Figure 3.1 and described in the flowchart in Figure 3.4. In the proposed CLE, the power demand model of the WPS is estimated using the load simulation module and the NN module, and included in the EMS to find the optimal WPS schedules. These are then feedback to re-train the load simulation and NN to improve the accuracy of the estimated WPS load model. This process is repeated until a certain stopping criterion is achieved.

Table 3.1: Comparison of Estimation Performance of Function Approximation Models

Model	MSE
2^{nd} order polynomial	2.57E-04
3^{rd} order polynomial	1.35E-05
4^{th} order polynomial	1.32E-05
NN	2.06E-07

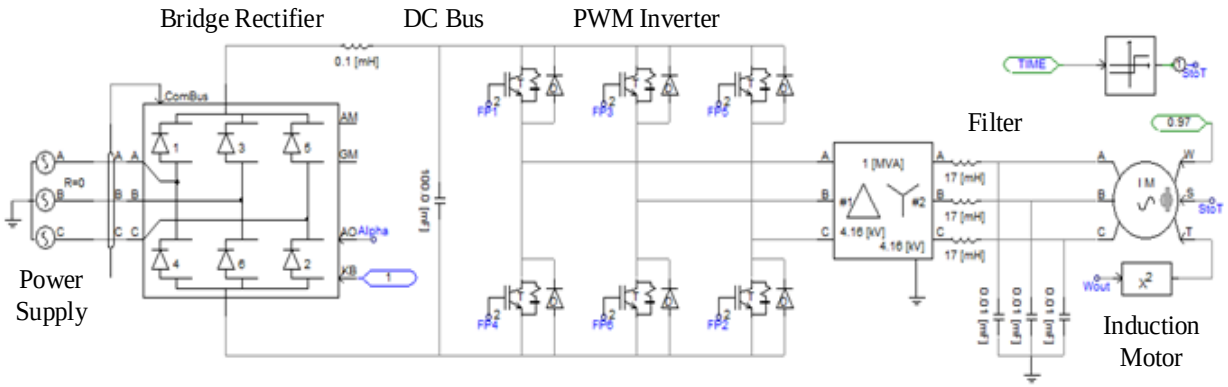

Figure 3.2: Simulation model for VSD driven pumps.

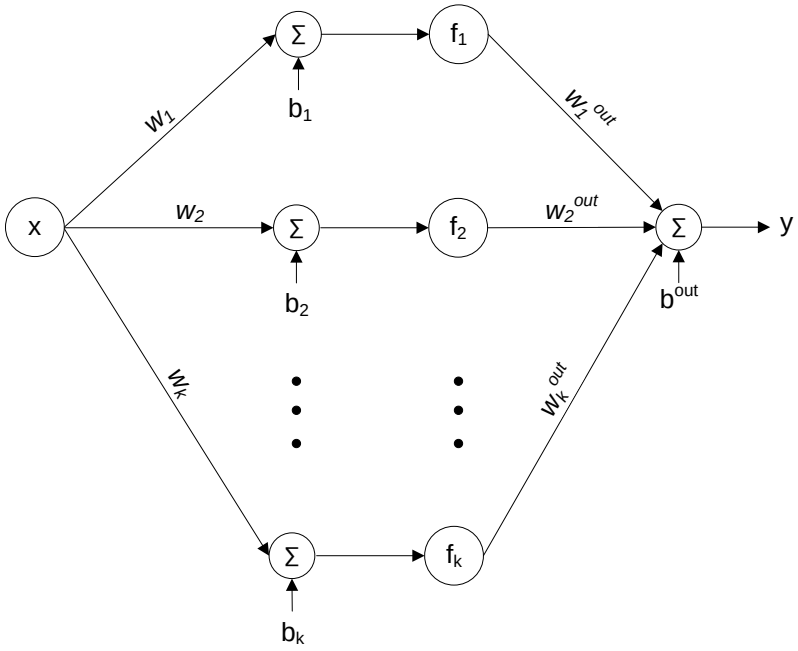

Figure 3.3: Neural network topology.

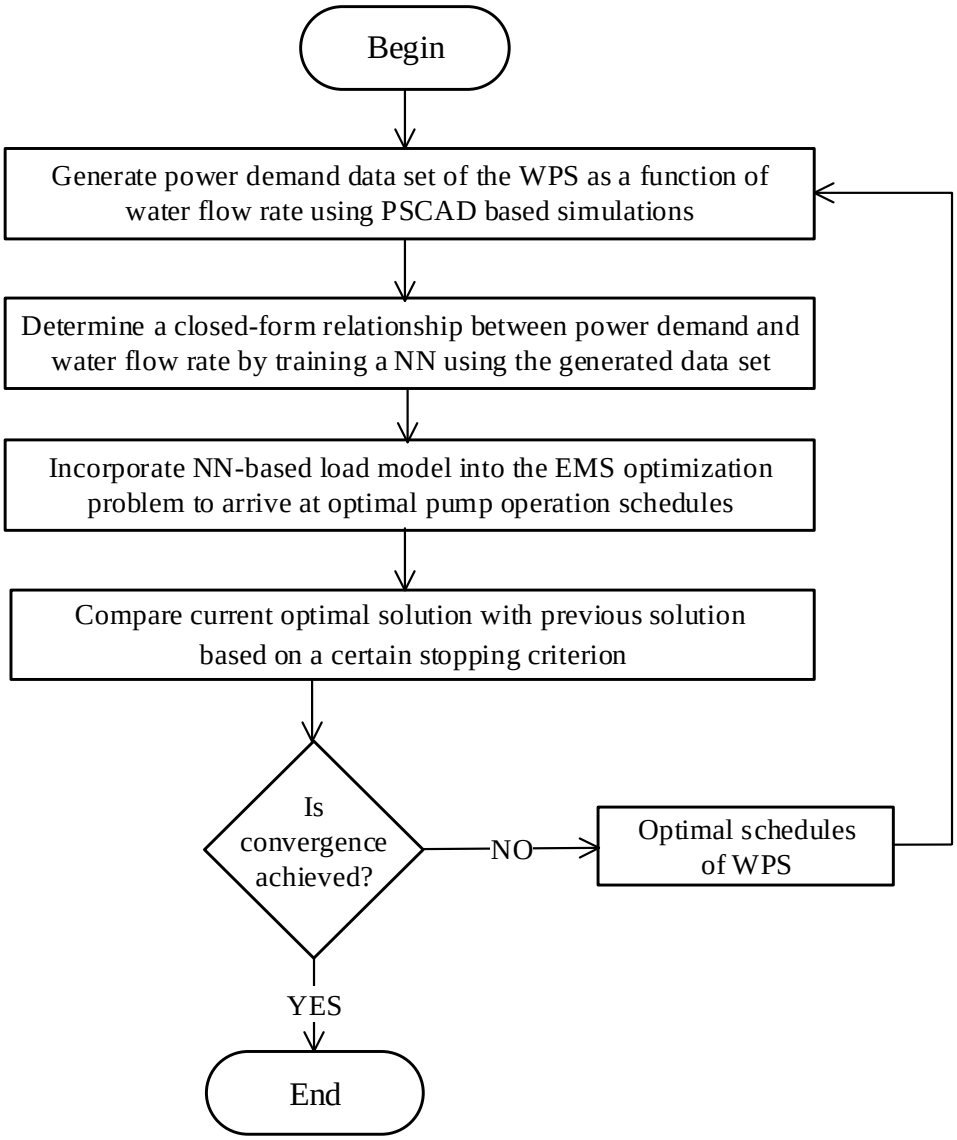

Figure 3.4: CLE based EMS flowchart for the WPS

3.4 Energy Management System of WPS

The proposed EMS model carries out a load scheduling optimization in order to minimize the energy consumption cost and demand charge for the WPS facility.

3.4.1 Objective Function

The objective function minimizes the energy cost and demand charge of the WPS, over a period of time, and is given as follows:

$$Min. \qquad Z = \sum_{t} \rho_t \, P_{LDC_t} \, \Delta t + \lambda_p \, P_{max} \tag{3.4}$$

The first term in (3.4) represents the total energy cost based on hourly energy prices. The second term in (3.4) represents the demand charge to the WPS facility where the peak demand cap (P_{max}) is used to constrain the hourly power drawn from the local distribution company (LDC), as given below:

$$P_{LDC_t} \leq P_{max} \qquad \forall t \tag{3.5}$$

3.4.2 Load Model

The WPS load is modeled as a relationship between the water flow rate out of a pump ($q_{t,j}$) and its power demand ($P_{t,j}$), based on the NN model obtained in (3.2).

$$P_{t,j} = \sum_{k} [f_{k,j}(q_{t,j} w_{k,j} + b_{k,j}) \, w_{k,j}^{out}] + b_j^{out} \qquad \forall t, \forall j \tag{3.6}$$

3.4.3 Power Balance

The power balance relationship for the WPS load and generation is given below, where P_{LDC_t} is positive when the WPS purchases power and negative when selling. BESS power

is also bidirectional where Pb_t is positive during BESS discharging and negative during charging.

$$\sum_j P_{t,j} = P_{LDC_t} + P_{RE_t} + Pb_t \qquad \forall t \tag{3.7}$$

3.4.4 Water Flow Constraints

The water flow management for the WPS is modeled using the following equations:

$$sl_t = L_0 + \sum_{x \le t} ir_x \Delta t - \sum_{x \le t} or_x \Delta t \qquad \forall t, x \epsilon t \tag{3.8}$$

$$ir_t = \sum_j q_{t,j} \qquad \forall t \tag{3.9}$$

$$or_t = D_t \qquad \forall t \tag{3.10}$$

$$q_{min}\, st_{t,j} \le q_{t,j} \le q_{max}\, st_{t,j} \qquad \forall t, \forall j \tag{3.11}$$

$$L_{min} \le sl_t \le L_{max} \qquad \forall t \tag{3.12}$$

$$sl_t = L_0 \qquad t = T \tag{3.13}$$

The water storage volume (sl_t) is calculated in (3.8) in terms of water inflow rate (ir_t), water outflow rate (or_t), and initial water storage volume (L_0). The water inflow rate, in (3.9) is the sum of water flow rates out of all pumps, where the water outflow rate is determined from the forecasted demand in (3.10). Limits on pump water flow rate and storage water volume are imposed by (3.11) and (3.12), respectively. A recovery of the initial storage volume L_0 by the end of the optimization period is enforced by (3.13).

3.4.5 Distributed Energy Resources

The DER considered in the EMS formulation are RES and BESS. The RES output power (P_{RE_t}) is modeled as a negative load using forecasted data for a typical day. The BESS is modeled by the following equations:

$$\frac{Pb_t \Delta t}{\lambda_{dch}} Zdch_t + Pb_t \Delta t \lambda_{ch} Zch_t = SOC_{t-1} - SOC_t \qquad \forall t, t \neq 1 \qquad (3.14)$$

$$\frac{Pb_t \Delta t}{\lambda_{dch}} Zdch_t + Pb_t \Delta t \lambda_{ch} Zch_t = SOC_0 - SOC_t \qquad t = 1 \qquad (3.15)$$

$$SOC_t = SOC_0 \qquad t = T \qquad (3.16)$$

$$-P_R \leq Pb_t \leq P_R \qquad \forall t \qquad (3.17)$$

$$(1 - DoD)E_R \leq SOC_t \leq E_R \qquad \forall t \qquad (3.18)$$

$$-MZch_t \leq Pb_t \qquad \forall t \qquad (3.19)$$

$$MZdch_t \geq Pb_t \qquad \forall t \qquad (3.20)$$

$$Zch_t + Zdch_t \leq 1 \qquad \forall t \qquad (3.21)$$

Equations (3.14) and (3.15) define the relationships between the BESS charging and discharging power and its SOC considering charging and discharging efficiencies. The SOC of BESS at the end of the optimization horizon is constrained by (3.16) to be equal to the initial SOC. Equations (3.17) and (3.18) define the power and energy capacity constraints respectively, which are determined based on BESS characteristics in terms of its type and size. Equations (3.19)-(3.21) are coordination constraints for BESS charging/discharging status using the big M method [56].

In order to improve the optimization programs computational performance, equations (3.14) and (3.15) can be replaced by a set of linearized equations formulated using the big M method. This will result in two equations for the charging state and another two equations for the discharging state, as follows:

Charging state:

$$MZdch_t + Pb_t \Delta t \lambda_{ch} \geq SOC_{t-1} - SOC_t \qquad \forall t \qquad (3.22)$$

$$MZdch_t - Pb_t \Delta t \lambda_{ch} \geq SOC_t - SOC_{t-1} \qquad \forall t \qquad (3.23)$$

Discharging state:

$$M(Zch_t - Zdch_{t+1}) + \frac{Pb_t \Delta t}{\lambda_{dch}} \geq SOC_{t-1} - SOC_t \qquad \forall t \qquad (3.24)$$

$$M(Zch_t - Zdch_{t+1}) - \frac{Pb_t \Delta t}{\lambda_{dch}} \geq SOC_t - SOC_{t-1} \qquad \forall t \qquad (3.25)$$

3.4.6 Model Predictive Control

The WPS is subject to several uncertainties over its daily operation cycle. Such uncertainties may jeopardize the expected benefits of the EMS as the actual inputs deviates from the forecasted profiles used in the optimization problem. In this work, the MPC technique is used to deal with energy price, water demand, and wind generation uncertainties. The receding horizon MPC is applied in order to meet the operational requirement of maintaining a certain water volume in the WPS storage at the end of the optimization horizon. Using MPC, the EMS problem is reformulated as follows:

$$Min. \quad Z_i = \sum_{t=i}^{T} \rho_t \, P_{LDC_t} \, \Delta t + \lambda_p \, P_{max} \qquad \forall i \qquad (3.26)$$

$$s.t. \quad Equations\,(3.4) - (3.24) \qquad \forall i, t = i, ..., T \qquad (3.27)$$

$$\rho_t = \rho_t^{updated} \qquad \forall i, t = i, ..., T \qquad (3.28)$$

$$D_t = D_t^{updated} \qquad \forall i, t = i, ..., T \qquad (3.29)$$

$$P_{RE_t} = P_{RE_t}^{updated} \qquad \forall i, t = i, ..., T \qquad (3.30)$$

At each time interval (iteration), (3.26)-(3.30) are solved over an optimization horizon but the solution is implemented for the first time interval only. The forecasted energy price (ρ_t), water demand (D_t), and RES generation (P_{RE_t}) are updated at each iteration and (3.28)-(3.30) are updated with recent forecasted data.

3.5 Case Studies and Discussions

The WPS used in the case studies is based on the facility shown in Figure 2.5 [10]. The power and water flow ratings of the pumps are given in Table 3.2. The minimum, maximum, and initial capacities of the storage are $L_{min} = 2,400\,m^3$,$L_{max} = 18,200\,m^3$, and $L_0 = 7,800\,m^3$.

The load models of the five pumps are estimated by executing PSCAD simulations of 4.16 kV VSD driven induction machines, where the mechanical torque is assumed to be equal to N^2 according to a centrifugal pump's torque characteristic [57]. The reference frequency (f) for VSD inverter control loop is varied between 0.5 and 1 p.u. in steps of $0.01\,p.u.$, to generate 51 readings of power demand. The pump flow rate (q) is proportional to N, with rated flow rate occurring at rated N.

The generated data set of power demand and flow rate of each pump is used to train a NN with one hidden layer comprising 10 neurons. A single layer NN model was selected to ensure an acceptable level of accuracy while also considering the model computational aspects. In the process of developing the NN load models of the five pumps of the WPS, the accuracy of the NN was examined with different number of neurons (K) in the hidden layer. Using a trial-and-error approach, the best accuracy was noted at $K = 10$ for three of the five pumps, and at $K = 11$ for the other two pumps. Therefore $K = 10$ was selected for all the pumps in order to avoid higher complexity.

The data set is divided into training set (60%), validation set (20%), and testing set (20%) using *Dividerand* function of MATLAB NN toolbox which divides the data set using random indicies. The MSE criterion is considered as the performance function for NN training and the resulting errors for the five pumps are shown in Table 3.3.

Figure 3.5 shows the schematic of the proposed CLE for the WPS where power demand and pump output rate datasets are generated using PSCAD simulations and used for NN training. Then the power demand model acquired from NN training is used in the EMS optimization problem to find the optimal pump flow rate schedules. These optimal

schedules are used to regenerate NN training datasets resulting in improved power demand estimation model. The stopping criterion used in this work for CLE convergence is a difference in EMS objective function value of less than 1% for two successive iterations.

Table 3.2: Power and Flow Ratings of Pumps

j	1	2	3	4	5
Power (kW)	595	445	260	260	595
Flow (m^3/h)	1,800	1,440	828	828	1,800

Table 3.3: Neural Network Training Performance

j	1	2	3	4	5
MSE	2.06E-07	8.30E-07	3.25E-05	3.25E-05	2.06E-07

The EMS optimization problem is formulated as a mixed integer nonlinear programming (MINLP) problem and solved using the DICOPT solver [38] in GAMS with a 0.01 MIP optimality tolerance. Three case studies are presented; Case 1 corresponds to the optimal scheduling of the WPS without DER, Case 2 corresponds to the optimal scheduling of the WPS with the wind energy source, and Case 3 corresponds to the optimal scheduling of the WPS equipped with a wind energy source and a BESS. Three scenarios are constructed for each case study as follows:

- Scenario-1: EMS without the proposed CLE
- Scenario-2: CLE based EMS

- Scenario-3: MPC technique applied to CLE based EMS under demand, price, and RES generation uncertainties.

The energy price in the case studies is assumed to follow the Hourly Ontario Energy Price (HOEP) of October 26, 2015, shown in Figure 3.6 [58] and the demand charge is assumed to be 7.0 $/kW. Figure 3.6 also shows the forecasted energy price profile considered for MPC analysis. Figure 3.7 and Figure 3.8 present the actual and forecasted water demand and wind generation profiles respectively. The actual water demand profile is taken from [10] while the actual wind generation profile is based on wind speed data extracted from [59] for a typical day in Toronto area. The forecasted profiles in Figure 3.6-Figure 3.8 are generated by adding an increasing random error to the actual profiles assuming a normal distribution for the error with the mean equal to the actual value and the standard deviation increasing with time.

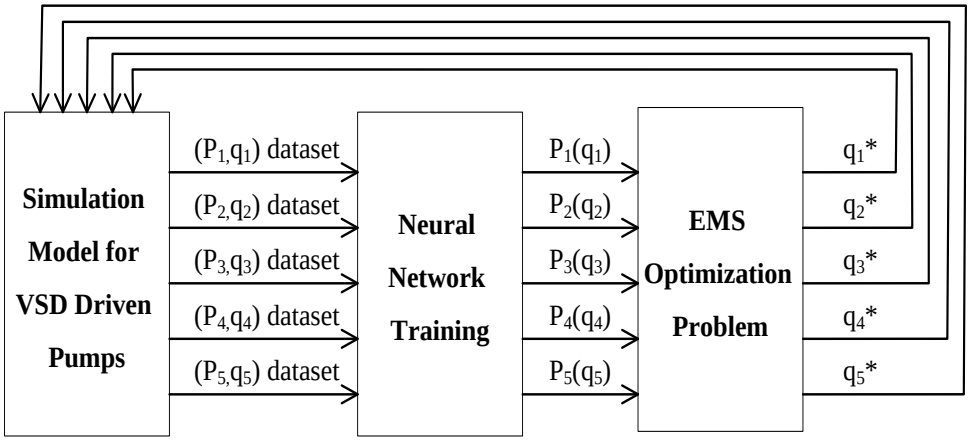

Figure 3.5: CLE schematic of the WPS.

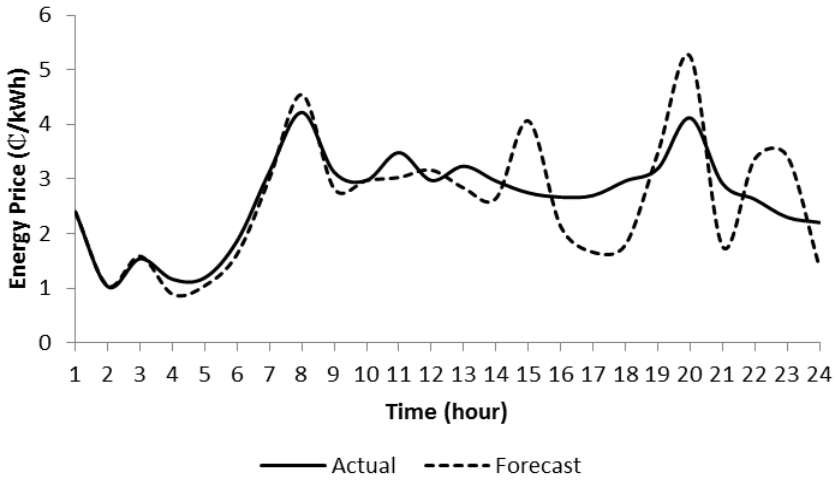

Figure 3.6: Actual and forecasted energy price profiles.

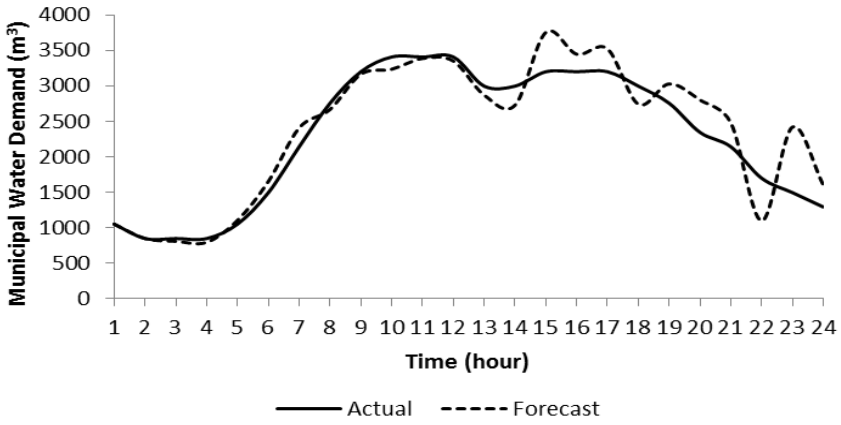

Figure 3.7: Actual and forecasted water demand profiles.

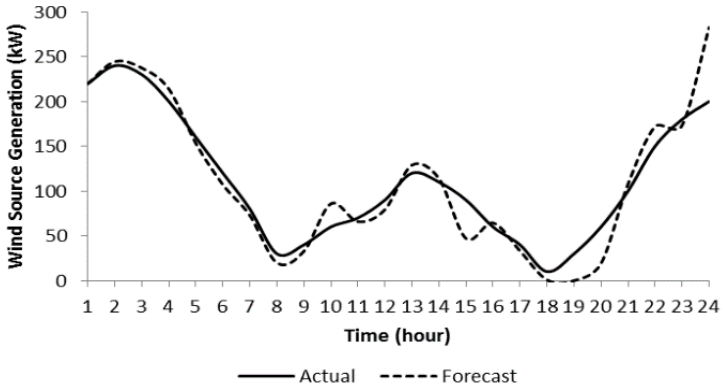

Figure 3.8: Actual and forecasted wind generation profiles.

3.5.1 Case 1: WPS without DER

In this case study the WPS buys the needed energy from the LDC. Therefore, the hourly power demand need be optimized to minimize its energy costs and demand charges while meeting the demand and the WPS operational constraints. Two sources of uncertainty are considered in this case which are, energy price and municipal water demand. Summary results are presented in Table 3.4 and hourly power exchanges of the WPS with the LDC are shown in Figure 3.9.

It is noted from the results that neither Scenario-1 nor Scenario-2 is able to maintain the final water volume in the storage facility at the desired volume of L_0 (Figure 3.10). There is a deviation of 2,178 m^3 from the desired volume of $L_0 = 7,800\,m^3$ for both Scenarios 1 and 2. This is because the actual water demand deviates from the forecasted demand, which is used in the EMS optimization model. On the other hand, it is noted that with the application of the MPC technique in the CLE based EMS, the final water volume is precisely maintained at L_0. Non-maintenance of final water volume in storage gives rise to many indirect costs to the WPS, which are not captured through the energy cost and demand charge only. Therefore, a final water volume penalty is assumed, of $0.005\,\$/m^3$ of deviation from L_0 in order to account for the effective cost to the WPS, which is different from the energy related costs.

It is noted from Table 3.4 that the CLE based EMS resulted in 2% reduction in total costs, while when MPC technique is applied on the CLE based EMS, the cost savings increased to 5.2%; when final water volume penalty charge is considered, this savings in Scenario-3 increases to 10.5%. The main contributors to this saving are the reductions in demand charges and in final water volume penalty charges. As shown in Figure 3.9, the power demand profile in Scenario-3 is more flattened than Scenarios 1 and 2 resulting in 12.9% reduction in demand charges (Table 3.4).

Table 3.4: Case 1 Results

	Scenario-1 (Base)	Scenario-2 (CLE)	Scenario-3 (CLE + MPC)
Net Energy Drawn from LDC (kWh/day)	5,038	4,833 (-4.1%)	4,754 (-5.6%)
Peak Power Drawn from LDC (kW)	254	251.6 (-0.9%)	221.2 (-12.9%)
Energy Costs ($/day)	124.4	121.4 (-2.4%)	122.5 (-1.5%)
Demand Charges ($/day)	59.3	58.7 (-0.9%)	51.6 (-12.9%)
Total Cost to WPS ($/day)	183.7	180.1 (-2%)	174.1 (-5.2%)
Final Water Volume Penalty Charges ($/day)	10.9	10.9	0
Total Effective Costs ($/day)	194.6	191 (-1.9%)	174.1 (-10.5%)

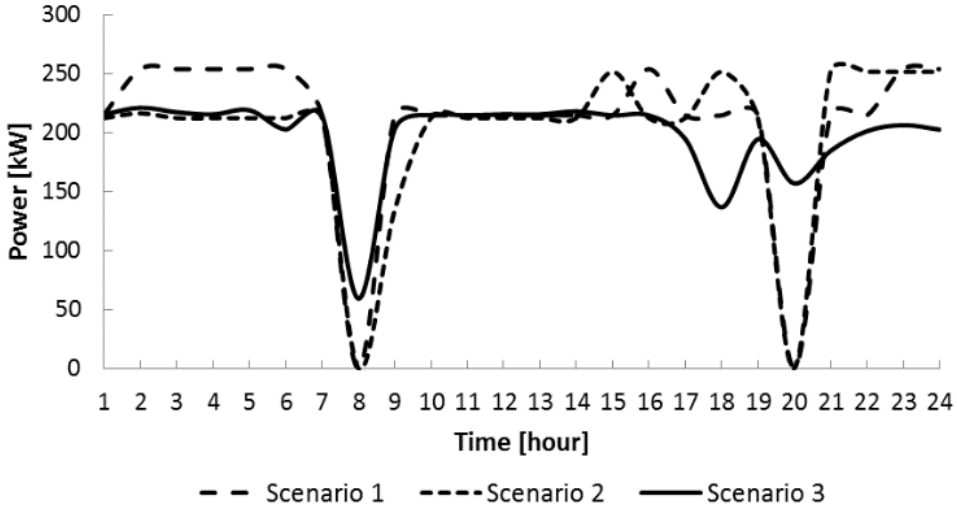

Figure 3.9: Power exchange by the WPS with LDC for Case 1.

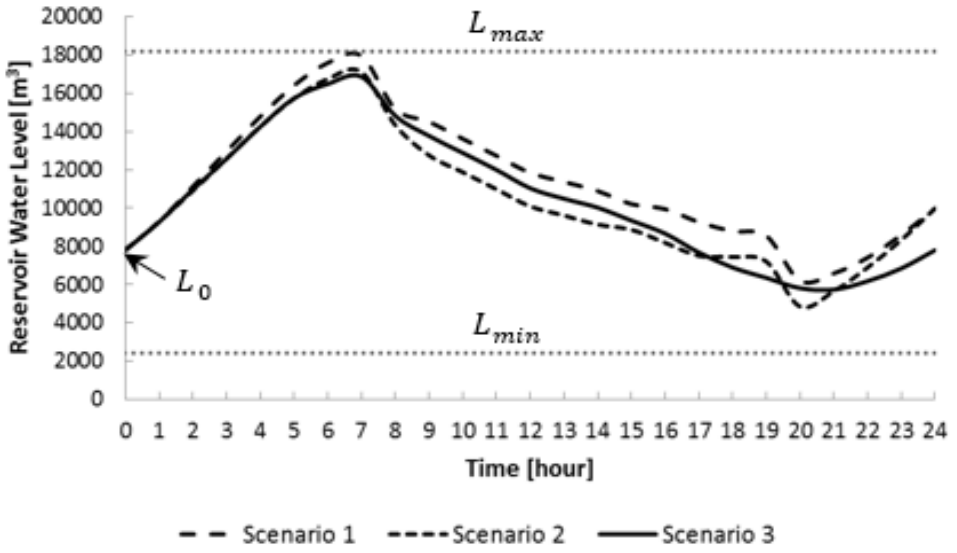

Figure 3.10: Storage water volume for Case 1.

3.5.2 Case 2: WPS with Wind Energy Source

In this case, the WPS is considered to be equipped with a wind energy source, where the actual and forecast wind generation profiles are shown in Figure 3.8, with actual total wind generation of 2,690 kWh and a forecasted total generation of 2,675 kWh over the 24-hour horizon. Therefore, wind generation is considered as a third source of uncertainty in addition to energy price and water demand. Summary results are presented in Table 3.5 and hourly power exchanges between the WPS and the LDC are shown in Figure 3.11.

It is noted that the WPS sells power during the first hour in all the three scenarios as a result of high wind generation and low water demand at this hour. Scenario-3 resulted in the lowest peak demand of 158.8 kW at hour 24 (Figure 3.11). Notice also that peaks occurred in Scenarios 1 and 2 between hours 16 and 19 because of low energy price forecast during this period with a very high deviation from the actual price profile, while in Scenario-3 the peak did not occur during this period because of the continuous updates of forecasted prices.

The 3.8% reduction in total costs, resulting from the use of CLE in Scenario-2, is mainly from the 6.3% reduction in energy costs. Scenario-3 resulted in 17.8% reduction in total effective costs due to 9.4% decrease in energy costs, 9.9% decrease in demand charges, and eliminating the final water volume penalty charges. Comparing the results of Case 2 with Case 1, it is noted that there is a large reduction in energy cost because of the presence of the wind energy source. An economic study to assess the feasibility of integrating wind generation with the WPS should include the capital and running cost of the wind source. In addition to the energy cost savings, social cost of emission reduction should be included in the analysis. However, such analysis is beyond the scope of this work, and it is simply assumed that the WPS has already gone through such studies to equip itself with the wind resource.

Table 3.5: Case 2 Results

	Scenario-1 (Base)	Scenario-2 (CLE)	Scenario-3 (CLE + MPC)
Net Energy Drawn from LDC (kWh/day)	2,410	2,334 (-3.2%)	2,242 (-7%)
Wind Generation (kWh/day)	2,675	2,675	2,690
Total Energy Consumption by WPS (kWh/day)	5,085	5,009 (-1.5%)	4,932 (-3%)
Peak Power drawn from LDC (kW)	176.3	175.2 (-0.6%)	158.8 (-9.9%)
Energy Costs ($/day)	67.8	63.5 (-6.3%)	61.4 (-9.4%)
Demand Charges ($/day)	41.1	40.9 (-0.6%)	37.1 (-9.9%)
Total Cost to WPS ($/day)	108.9	104.4 (-4.1%)	98.5 (-5.7%)
Final Water Volume Penalty Charges ($/day)	10.9	10.9	0
Total Effective Costs ($/day)	119.8	115.3 (-3.8%)	98.5 (-17.8%)

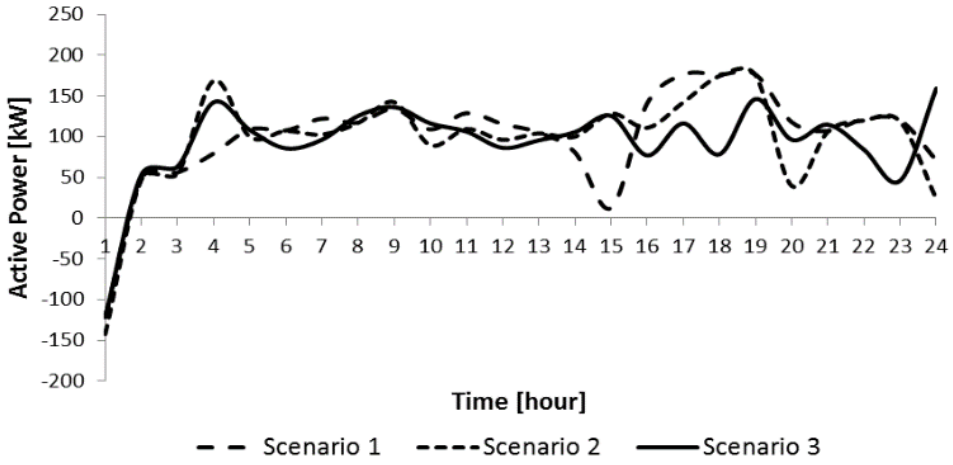

Figure 3.11: Power exchange by the WPS with LDC for Case 2.

3.5.3 Case 3: WPS with Wind Energy Source and BESS

In addition to the wind energy source, the WPS is considered to be equipped with a BESS (Table 3.6) in this case. Summary results are presented in Table 3.7 and hourly power exchange profiles are shown in Figure 3.12 and Figure 3.13. It is noted in Figure 3.12 that there is a high variability in energy consumption profiles between the three scenarios because of the flexibility provisions from the BESS. The WPS sells the maximum amount of energy to the LDC in Scenario-1 but this scenario results in the highest peak of 191.1 kW and a low level of power exchange with the BESS (Figure 3.13).

Scenarios-2 and 3 resulted in much lower peak demands because of the high level of power exchange with BESS. However, it is noted from Table 3.7 that the charging/discharging losses in BESS in Scenario-2 contributed to a 0.5% increase in the energy cost. Scenario-2 resulted in 5% reduction in total effective cost, accounted for by 14% decrease in demand charge despite the 0.5% increase in energy cost. Scenario-3 resulted in a 20.7% reduction in total effective cost due to 8% decrease in energy cost, 18.9% decrease in demand charge, and eliminating the final water volume penalty charge.

Table 3.6: BESS Characteristics

Type	PbA
Capacity	500 kWh
Maximum Charging/Discharging Rate	100 kW
Charging/Discharging Efficiency	95%
Depth of Discharge (DoD)	0.8
Initial SOC	0.6

Table 3.7: Case 3 Results

	Scenario-1 (Base)	Scenario-2 (CLE)	Scenario-3 (CLE + MPC)
Net Energy Drawn from LDC (kWh/day)	2,330	2,323 (-0.3%)	2,175 (-6.7%)
Wind Generation (kWh/day)	2,675	2,675	2,690
Total Energy Consumption by WPS (kWh/day)	4,995	4,979 (-0.3%)	4,838 (-3.1%)
Peak Power drawn from LDC (kW)	191.1	164.4 (-14%)	154.9 (-18.9%)
Energy Costs ($/day)	61.2	62.5 (+0.5%)	57.2 (-8%)
Demand Charges ($/day)	44.6	38.4 (-14%)	36.2 (-18.9%)
Total Cost to WPS ($/day)	105.8	100.9 (-4.6%)	93.4 (-11.7%)
Final Water Volume Penalty Charges ($/day)	10.9	10.9	0
Total Effective Costs ($/day)	116.7	111.8 (-5.0%)	93.3 (-20.7%)

There is no significant difference in energy cost savings between Case 3 and Case 2; therefore, integrating the BESS with the WPS may not be feasible, considering the high capital and running costs of such an installation. Although a storage system generally provides flexibility in buying and selling energy at optimal time periods, this flexibility did not result in large energy savings for the WPS under study. This can be attributed to the high controllability of the load which resulted in shifting the load to high wind generation time periods rendering the flexibility provided by BESS not very useful.

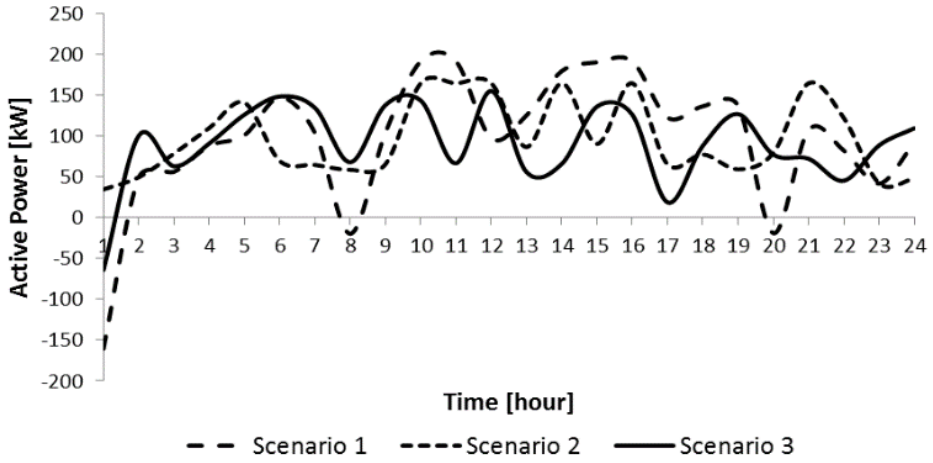

Figure 3.12: Power exchange by the WPS with LDC for Case 3

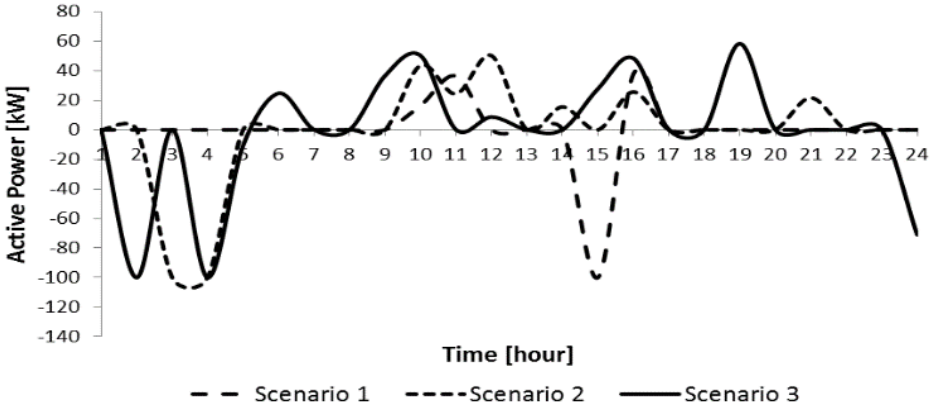

Figure 3.13: BESS power output for Case 3

3.5.4 Computational Efficiency

The base scenario (Scenario-1) for the three case studies involves solving the EMS problem once for the entire optimization horizon. The solution times along with the number of variables for the three cases are shown in Table 3.8. The computational efficiency of Scenario-2 depends on the number of iterations needed the CLE algorithm to reach convergence. Assuming that NN re-training time is negligible compared to the EMS problem solution time, the solution time for Scenario-2 can be calculated as the number of iterations needed, multiplied by the solution time of Scenario-1, shown in Table 3.9. In Scenario-3, the MPC technique involves solving the EMS problem at each time interval (one hour) in the optimization horizon (24 hours). Table 3.10 presents the total solution time for the whole day and the maximum solution time for a single MPC iteration.

The NN training time is not considered in the evaluation of the computational efficiency of the proposed EMS framework because the NN training completes in just few seconds which is negligible compared to the EMS solution times shown in Table 3.8 - Table 3.10. The NN training time is not long in this work due to the small size of training data used to develop the power demand models of the pumps.

Table 3.8: Scenario-1 Solution Time

Case	Number of Variables	Number of Binary Variables	Solution Time
1	1874	120	2 min
2	1898	120	2.5 min
3	1994	168	6.3 min

Table 3.9: Scenario-2 Solution Time

Case	Number of CLE Iterations	Solution Time
1	4	8 min
2	7	17.5 min
3	4	25.2 min

Table 3.10: Scenario-3 Solution Time

Case	Maximum Solution Time for One MPC Iteration	Total Solution Time
1	10.2 min	53.3 min
2	20.6 min	75.4 min
3	31.8 min	157.3 min

3.6 Summary

This chapter presented an EMS application through the optimum load control of a WPS. The optimization of energy utilization was achieved through the development of power demand models for variable speed driven pumps. Simulation results showed potential for daily savings on energy costs and demand charges as pumps' operational schedules and flow rates are optimized. The proposed CLE improved the load estimation accuracy yielding better optimal solutions when the NN-based load model is incorporated into the optimization problem. On the other hand, the receding horizon MPC technique improved the forecasting accuracy of energy price, RES generation, and demand, resulting in notable savings as the EMS problem uses more accurate data. Also the MPC approach allowed for continuous adjustment of the operational schedules in order to maintain a certain water volume in the storage of the WPS at the end of the optimization horizon.

Chapter 4

Retail Pricing Controlled Demand Response for Industrial Loads Considering Distribution Feeder Operations[‡]

4.1 Nomenclature

Indices

b	Bus, $b = 1, 2, ..., B$
l	Line, $l = 1, 2,..., N.$
p	Phase, $p = a, b, c$
t	Time interval, hours, $t = 1, 2, ..., T$

[‡]Parts of this chapter have been submitted as a paper for review in: O. Alarfaj and K. Bhattacharya, Retail pricing controlled demand response for industrial loads considering distribution feeder operations, IEEE Transactions on Smart Grid, 2018.

Parameters

D_{IC}^{DA}	Day-ahead industrial customer's production demand
D_{IC}^{RT}	Real-time industrial customer's production demand
$P_1, ..., P_n$	Retail pricing power demand thresholds, $[kW]$
P_{IC}^{max}	Industrial customer's maximum load, $[kW]$
pf	Power factor of industrial load
P_{RE}^{DA}	Day-ahead renewable generation by industrial customer, $[kW]$
P_{RE}^{RT}	Real-time renewable generation by industrial customer, $[kW]$
V^{sp}	Specified nominal phase voltage, $[V]$
ρ_m^{DA}	Day-ahead market price, $[\$/kWh]$
ρ_m^{RT}	Real-time market price, $[\$/kWh]$
$\lambda_1, ..., \lambda_4$	Retail pricing coefficients
λ_d	Peak demand coefficient, $[\$/kW]$

Variables

d	Industrial customer's power demand deviation from P_{IC}^*, $[kW]$
I	Phase current, $[A]$
I_s	Sending-end phase current, $[A]$
I_r	Receiving-end phase current, $[A]$
J_{IC}^{DA}	Objective function of industrial customer in day-ahead operation, [$]
J_{IC}^{RT}	Objective function of industrial customer in real-time operation, [$]
J_{LDC}^{DA}	LDC's day-ahead objective, $[kWh]$
J_{LDC}^{RT}	LDC's real-time objective, $[kWh]$
P_{gap}^{DA}	Day-ahead retail pricing power gap, $[kW]$
P_{gap}^{RT}	Real-time retail pricing power gap, $[kW]$
P_{IC}^{DA}	Day-ahead industrial customer's active power demand, $[kW]$
P_{IC}^{RT}	Real-time industrial customer's active power demand, $[kW]$
$\overline{P_{IC}^{DA}}$	Day-ahead industrial customer's peak demand, $[kW]$
$\overline{P_{IC}^{RT}}$	Real-time industrial customer's peak demand, $[kW]$

P_{IC}^{*}	Desired demand profile signal, $[kW]$
P_{IC}^{max}	Industrial customer's total connected load, $[kW]$
P_{LDC}^{DA}	Day-ahead LDC's power demand, $[kW]$
P_{LDC}^{RT}	Real-time LDC's power demand, $[kW]$
$\overline{P_{LDC}^{DA}}$	Day-ahead LDC's peak demand, $[kW]$
$\overline{P_{LDC}^{RT}}$	Real-time LDC's peak demand, $[kW]$
Q_{IC}	Reactive power demand of industrial load, $[kVAR]$
V	Bus phase voltage, $[V]$
Z_{IC}	Industrial customer load's impedance, $[\Omega]$
ρ_{LDC}^{DA}	Day-ahead retail price, $[\$/kWh]$
ρ_{LDC}^{RT}	Real-time retail price, $[\$/kWh]$
$\overline{\rho_{LDC}^{DA}}$	Maximum day-ahead retail price, $[\$/kWh]$
$\overline{\rho_{LDC}^{RT}}$	Maximum real-time retail price, $[\$/kWh]$
λ_t	Hourly retail pricing coefficient, $[p.u.]$

4.2 Introduction

DSM is an important concept in electric utilities that helps defer some capacity addition requirements in the long-term, which is very significant in power systems with continuously growing demand for energy. However, there is a need to develop new DSM strategies for efficient energy usage by existing and new loads, and encourage the participation of customers in DR programs. Industrial loads are important targets for DR programs because of their high energy density, availability of automated controls at the equipment switching level, and the presence of supervisory control centers. While automated controls facilitate the implementation of load control strategies, the supervisory control centers allow for two-way interaction with the energy provider and hence provides efficient energy management for the benefit of both parties. When equipped with an EMS, an industrial facility can use DR signals to optimize its energy utilization and communicate the EMS decisions to the energy provider to achieve its DR targets in a collaborative manner.

A novel framework is proposed in this chapter for industrial loads participating in DR provisions, from the LDC's and customer's perspectives, simultaneously. In the context of this work, the LDC is an entity that owns and operates the local distribution network and also engages in the sale of retail electricity to customers. Optimization models are developed for the LDC and the industrial customer, which are solved independently and sequentially, using locally obtained data and data communicated by the other party. For LDC's operation, a distribution optimal power flow (DOPF) model is developed while for the industrial facility, an appropriate EMS model is used. Also a retail pricing model (RPM) is developed, using the customer's historical load profiles, which produces a dynamic price signal that is included in the customer's EMS program to determine the optimal DR decisions. The proposed framework also considers the uncertainty in energy prices, RES generation, and industrial facility's demand by applying the model predictive control (MPC) technique in real-time operation of the industrial customer's EMS model. The main contributions of this work are:

- A novel and interactive DR framework is proposed for industrial customers, to be implemented by the LDC in day-ahead and real-time operations. The main purpose of the day-ahead DR strategy is to reach an agreement on the load shift to be carried out by the industrial customer, while minimizing the peak demand of the distribution system. At the real-time stage, the DR strategy seeks to minimize the deviations in DR decisions from the day-ahead schedules, taking into account the uncertainties of energy prices and energy demand of the customer.

- Two DR signals are proposed to influence the customer's demand as part of the day-ahead DR strategy, the first signal is based on a "desired demand profile" and the second is based on a retail pricing scheme. The performance of the DR strategy with the two proposed DR signals is compared with a TOU based pricing scheme.

- The retail pricing based DR signal is derived from a novel RPM, designed to influence the customer's demand profile in order to achieve a desired load shifting and hence

reducing the peak demand of the distribution system. Customers historical load data and demand schedules are used by the LDC to determine this price signal.

- Uncertainties arising at the customers end during real-time operations are mitigated by the application of the MPC technique within its EMS, while those at the LDCs end are mitigated through effective communication with the customer on updated energy demand schedules and by revising the retail prices at the real-time stage using the RPM.

The rest of the chapter is organized as follows: Section 4.3 describes the proposed DR framework for industrial loads. The mathematical models of the DOPF are described in Section 4.4. Case study results are presented and discussed in Section 4.5. Finally, Section 4.6 presents the conclusions of this work.

4.3 Proposed Demand Response Framework

The proposed DR framework for industrial loads considers both day-ahead and real-time operations. At the day-ahead stage, the LDC seeks to minimize its peak demand while the industrial customer seeks to minimize its energy cost and peak demand. At the real-time stage, the decisions are adjusted so as to account for uncertainties arising from various factors. In the proposed DR schemes, it is assumed that the industrial customer has entered into a contractual agreement with the LDC to respond to its DR signal by incorporating the DR signal within its EMS program in an appropriate manner and hence adjusting its demand.

The proposed DR scheme is designed to be generic, for application to an industrial facility, which accounts for a significant share of the local distribution system load. Different industrial loads will have differing degrees of flexibility, in response to the DR signals, and hence the magnitude of benefits realized from the DR programs will be different based on the application.

4.3.1 Day-Ahead Operations

At the day-ahead stage, an interactive process (Figure 4.1) is proposed where the industrial customer executes its EMS model using day-ahead market price ρ_m^{DA}, production demand D_{IC}^{DA}, and RES generation P_{RE}^{DA} forecast data. The initial objective for the customer's EMS is to minimize its energy cost and peak demand charge, given as follows:

$$J_{IC}^{DA} = \sum_t \rho_{mt}^{DA} P_{IC_t}^{DA} \Delta t + \lambda_d \overline{P_{IC}^{DA}} \tag{4.1}$$

where peak demand is capped using the following constraint:

$$P_{IC_t}^{DA} \leq \overline{P_{IC}^{DA}} \qquad \forall t \tag{4.2}$$

The optimized load profile P_{IC}^{DA} is communicated to the LDC. After receiving information from the customer's EMS, the LDC executes either DOPF1 or DOPF2 (see Figure 4.1) with the objective of minimizing the LDC's peak demand and feeder losses, given as follows:

$$J_{LDC}^{DA} = \overline{P_{LDC}^{DA}} + \sum_t P_{Loss_t} \tag{4.3}$$

The loss minimization component is included so as to achieve improved system operation, such as reduced reactive power flows in the feeders and improved voltage profiles. From the DOPF and RPM, the LDC obtains an appropriate DR signal which is communicated to the customer in order to shift some of its load to off-peak periods. Two types of DR signals are proposed in this work:

- DR1: Desired demand profile signal. (Figure 4.1a)
- DR2: Retail price signal. (Figure 4.1b)

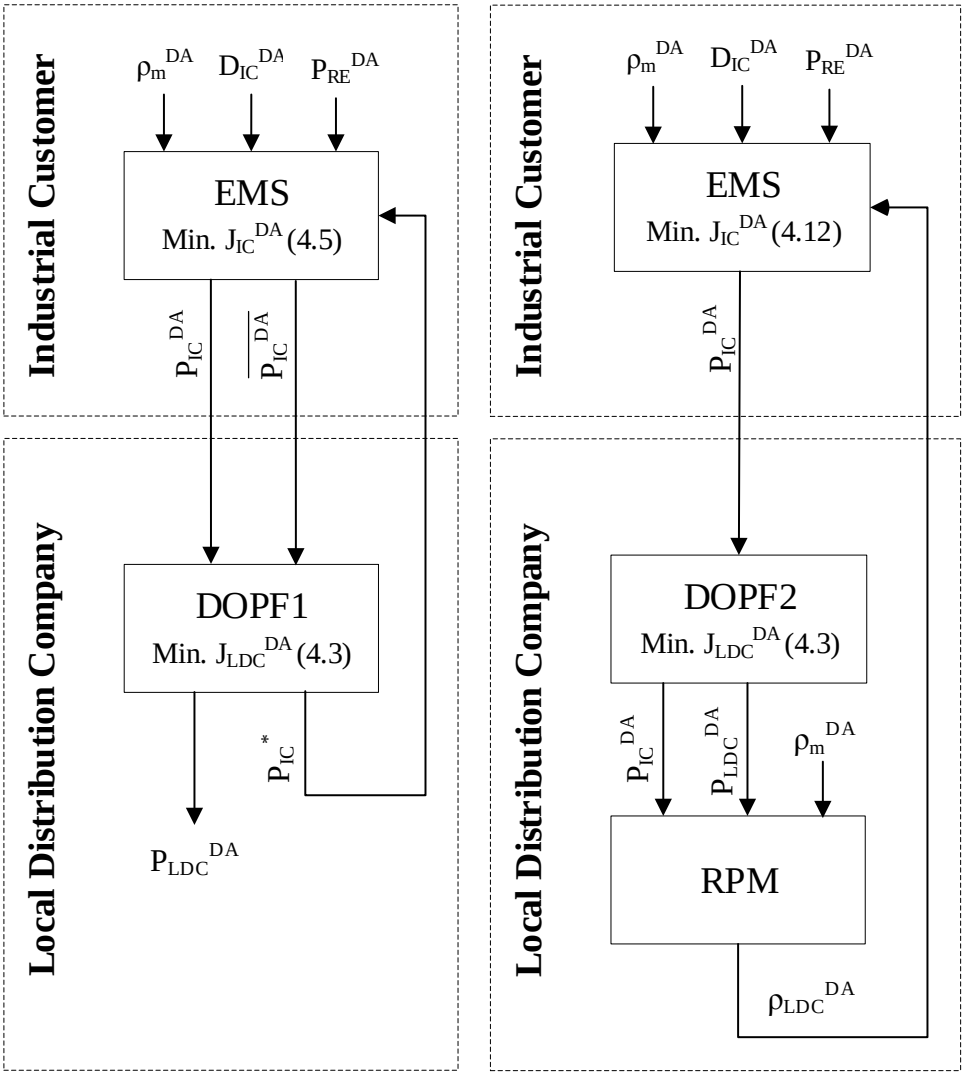

a) DR1 Signal b) DR2 Signal

Figure 4.1: DR in day-ahead operations.

4.3.1.1 DR1: Desired Demand Profile Signal

In this approach, the LDC controls the industrial customer's demand by sending a *desired demand profile* signal P^{*}_{IC} which is determined from DOPF1 model to be included by the customer in its EMS program as an upper bound for its demand. To this effect, a new constraint is included in the customer's EMS for subsequent solutions in the day-ahead interactive process, given as follows:

$$P^{DA}_{IC_t} \leq P^{*}_{IC_t} + d_t \qquad \forall t \tag{4.4}$$

Note that, while a peak demand constraint (4.2) is considered in the initial execution of the customer's EMS, constraint (4.4) is used instead, for all subsequent executions. While (4.1) is used as the objective function in the first execution of the EMS model, it is appropriately modified in all subsequent runs for the DR1 case, by replacing $\overline{P^{DA}_{IC}}$ by the sum of d_t. The sum of d_t is minimized to ensure that customer's load profile is close to that desired by the LDC. The modified objective function of the customer's EMS is given as follows:

$$J^{DA}_{IC} = \sum_t \rho^{DA}_{m_t} P^{DA}_{IC_t} \Delta t + \lambda_d \sum_t d_t \tag{4.5}$$

In the proposed DR1 interactive process (Fig. 1a), the LDC executes DOPF1 model after receiving the scheduled demand profile from the customer P^{DA}_{IC} to determine the desired demand profile signal P^{*}_{IC} which is communicated to the customer. The customer includes this signal as an upper bound for its demand and re-executes its EMS program using the objective function in (4.5) and submits a revised day-ahead demand schedule to the LDC. Depending on how close is the customer's revised load profile to the LDC's desired load profile, the LDC may re-execute DOPF1 and send a revised DR1 signal to the customer. This process continues until there is no further reduction in peak demand of the distribution system. Note that in the DR1 scheme the customers energy tariff is solely based on the day-ahead wholesale market price, ρ^{DA}_{m}, that is included in (4.5).

4.3.1.2 DR2: Retail Price Signal

In this approach, the LDC influences the customer's load profile using a suitable retail price signal, ρ_{LDC}^{DA}, to achieve a desired load shifting. To determine this price signal, a novel RPM is proposed herein, which is based on the analysis of the scheduled demand profile of the industrial customer P_{IC}^{DA}, and other loads connected to the distribution feeder. It uses the peak demand of the feeder $\overline{P_{LDC}^{DA}}$, as a reference point for determining the retail price signals.

Since the LDC seeks to minimize its peak demand, the retail price at each hour is determined based on the expected feeder load proximity to $\overline{P_{LDC}^{DA}}$; therefore hourly power gaps P_{gap}^{DA} are calculated using the following equation:

$$P_{gap_t}^{DA} = \overline{P_{LDC}^{DA}} - (P_{LDC_t}^{DA} - P_{IC_t}^{DA}) \qquad \forall t \tag{4.6}$$

In order to minimize the LDC's peak demand, high retail prices should be selected for hours with low power gap, and vice versa. This is achieved by comparing the power gap with a certain number of threshold values $(P_1, P_2, ..., P_n)$ of the industrial customer demand to determine pricing coefficients, λ_t^{DA}, for each hour using the following piece-wise function:

$$\lambda_t^{DA} = \begin{cases} \lambda_1 & P_{gap}^{DA} > P_1 \\ \lambda_2 & P_2 < P_{gap}^{DA} \leq P_1 \\ \lambda_3 & P_3 < P_{gap}^{DA} \leq P_2 \\ \bullet & \bullet \\ \bullet & \bullet \\ \lambda_n & P_n < P_{gap}^{DA} \leq P_{n-1} \\ 1 & P_{gap}^{DA} \leq P_n \end{cases} \qquad \forall t \tag{4.7}$$

where

$$0 < \lambda_1 < \lambda_2 < ... < \lambda_n < 1 \tag{4.8}$$

$$P_n < P_{n-1} < ... < P_1 \leq P_{IC}^{max} \tag{4.9}$$

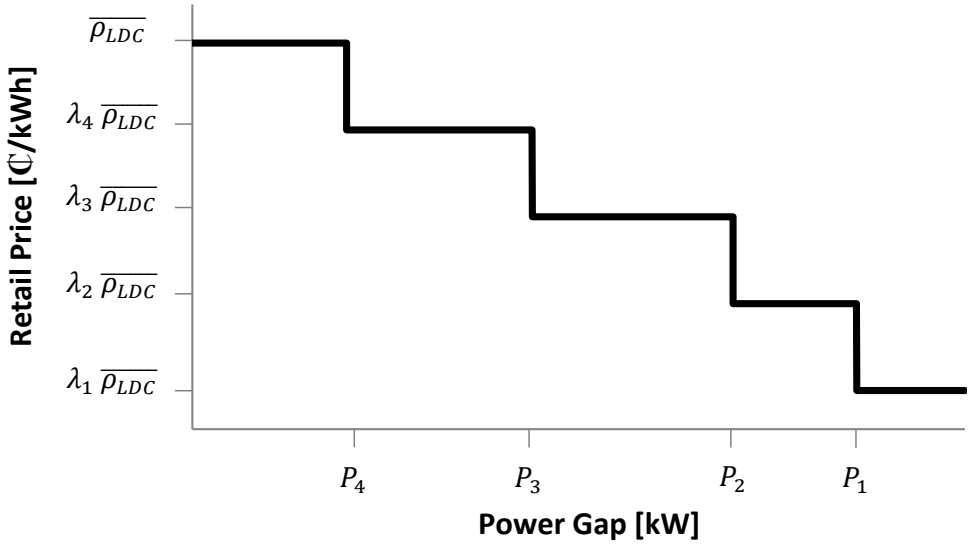

Figure 4.2: Retail pricing structure.

Figure 4.2 illustrates the proposed retail pricing structure considering $n = 4$ as the number of levels in the staircase function (4.7). The hourly pricing coefficients, λ_t^{DA}, are used to determine retail prices $\rho_{LDC_t}^{DA}$ as given below:

$$\rho_{LDC_t}^{DA} = \lambda_t^{DA}\ \overline{\rho_{LDC}^{DA}} \qquad \forall t \tag{4.10}$$

where $\overline{\rho_{LDC}^{DA}}$ is determined to maintain the energy costs for the customer under retail prices, equal to the costs associated with initially submitted demand profile under market prices using the following equation:

$$\overline{\rho_{LDC}^{DA}} = \frac{\sum_t \rho_{m_t}^{DA} P_{IC_t}^{DA}}{\sum_t \lambda_t^{DA} P_{IC_t}^{DA}} \tag{4.11}$$

The number of levels, n, in the staircase function (4.7), the threshold values, $P_1, P_2, ..., P_n$, and the retail pricing coefficients, λ_1,$\lambda_2, ..., \lambda_n$, are selected by analyzing the historical demand profile of the industrial customer to determine the most probable power demand levels. These parameters are determined in advance and are kept fixed during the execution of the interactive DR2 scheme.

In the proposed DR2 interactive process (Fig. 4.1b), the LDC executes DOPF2 model after receiving scheduled demand profile from the customer P_{IC}^{DA} to determine the corresponding distribution system demand profile P_{LDC}^{DA} and its associated peak demand $\overline{P_{LDC}^{DA}}$. Hourly power gaps P_{gap}^{DA} are then calculated using (4.6) and used to determine a retail price signal ρ_{LDC}^{DA} using equations (4.7), (4.10), and (4.11) of the RPM model. After that, the retail pricing signal, $\rho_{LDC_t}^{DA}$, is communicated to the customer to be included in the EMS objective function in place of ρ_m^{DA} as given below:

$$J_{IC}^{DA} = \sum_t \rho_{LDC_t}^{DA} P_{IC_t}^{DA} \Delta t + \lambda_d \overline{P_{IC}^{DA}} \tag{4.12}$$

The customer re-executes its EMS to obtain a revised day-ahead demand schedule using the modified EMS objective function (4.12), in place of (4.1), which considers that the customer will be charged based on the retail price, and not the market price. When the revised demand profile of the customer ρ_{LDC}^{DA} is communicated back to the LDC, it is incorporated into the DOPF2 model to ensure that the distribution system's peak demand has reduced. This process continues until the retail price signal from the LDC and the 'responsive' load profile of the customer reach steady-states, and there is no further reduction in distribution system's peak demand.

The convergence of the interactive strategy is guaranteed because of the design of the RPM where a power gap is calculated as a function of the peak demand and used to determine the retail price; the retail price inversely varies with the magnitude of the power gap. So with a small change in the peak demand indicating reduced flexibility in customer's response, the change in power gap will be very small and therefore the retail price will not change as a result of the staircase function design used in the RPM. When the retail price remains unchanged, the resulting demand profile of the customer will also not change and as a result the peak demand of the distribution system will stop changing, indicating a convergence of the interactive scheme.

4.3.2 Real-Time Operations

As the proposed DR scheme is implemented in the day-ahead operations, the attainable benefits in real-time operations is also examined considering the impact of uncertainties in energy prices and industrial costumer operations on real-time decisions. As a proof of concept, only real-time operations associated with DR2 day-ahead scheme are considered. After convergence of the day-ahead operations in DR2 scheme, the LDC and the customer reaches a settlement on the desired load profile, which is considered to be the contracted (or scheduled) load, and the final day-ahead retail price signal.

In real-time, the following objective function is used by the customer in its EMS, which seeks to minimize the penalty for deviations in its real-time load from the scheduled day-ahead load profile and also minimizing its real-time peak demand charge, as given below:

$$J_{IC}^{RT} = \sum_{t} \rho_{LDC_t}^{RT} (P_{IC_t}^{RT} - P_{IC_t}^{DA}) \Delta t + \lambda_d \overline{P_{IC}^{RT}} \tag{4.13}$$

The real-time operations are affected by uncertainties such as deviations in energy market prices from forecast, and process power demand from their day-ahead schedules. The MPC technique is used to deal with these uncertainties and hence reduce the deviations in the real-time load profile of the customer from the communicated (contracted) day-ahead

profile. The MPC formulation is included as part of the industrial customer's EMS model to update the various uncertain parameters. At each time instant, $i \epsilon \{1, T\}$, the following receding-horizon MPC optimization problem is solved over the optimization horizon $\{i, .., T\}$, but the solution is implemented for time interval, i, only:

$$Min. \quad J^{RT}_{IC_i} = \sum_{t=i}^{T} \rho^{RT}_{LDC_t} (P^{RT}_{IC_t} - P^{DA}_{IC_t}) \Delta t + \lambda_d \overline{P^{RT}_{IC}} \tag{4.14}$$

$$s.t. \quad \rho^{RT}_{LDC} = \rho^{RT^{updated}}_{LDC} \qquad For \quad t = i, ..., T \tag{4.15}$$

$$D^{RT}_{IC} = D^{RT^{updated}}_{IC} \qquad For \quad t = i, ..., T \tag{4.16}$$

$$P^{RT}_{RE} = P^{RT^{updated}}_{RE} \qquad For \quad t = i, ..., T \tag{4.17}$$

The real-time retail prices ρ^{RT}_{LDC}, production demand D^{RT}_{IC}, and renewable generation P^{RT}_{RE} are updated at each time interval with recently obtained data using (4.15)-(4.17). In addition to updating its own parameters, the industrial customer communicates with the LDC in real-time with updated demand profiles, as shown in Figure 4.3, which reduces the uncertainty in its load demand, to the benefit of LDC's real-time operation. Using the updated load profile of the customer, the LDC executes the DOPF2 model on an hourly basis using the following objective function:

$$J^{RT}_{LDC} = \overline{P^{RT}_{LDC}} + \sum_{t} P_{Loss_t} \tag{4.18}$$

As the LDC's demand profile is updated using the customer's communicated demand data, the RPM is used to revise the real-time retail price signal ρ^{RT}_{LDC} on an hourly basis to influence the customer's demand in order to reduce the peak demand of the distribution system. Similar to the day-ahead retail price signal, the real-time retail price signal ρ^{RT}_{LDC} is determined using the following equations:

$$P^{RT}_{gap_t} = \overline{P^{RT}_{LDC}} - (P^{RT}_{LDC_t} - P^{RT}_{IC_t}) \qquad \forall t \tag{4.19}$$

$$\lambda_t^{RT} = \begin{cases} \lambda_1 & P_{gap}^{RT} > P_1 \\ \lambda_2 & P_2 < P_{gap}^{RT} \leq P_1 \\ \lambda_3 & P_3 < P_{gap}^{RT} \leq P_2 \\ \bullet & \bullet \\ \bullet & \bullet \\ \lambda_n & P_n < P_{gap}^{RT} \leq P_{n-1} \\ 1 & P_{gap}^{RT} \leq P_n \end{cases} \quad \forall t \tag{4.20}$$

$$\rho_{LDC_t}^{RT} = \lambda_t^{RT} \overline{\rho_{LDC}^{RT}} \quad \forall t \tag{4.21}$$

$$\overline{\rho_{LDC}^{RT}} = \frac{\sum_t \rho_{m_t}^{RT} P_{IC_t}^{RT}}{\sum_t \lambda_t^{RT} P_{IC_t}^{RT}} \tag{4.22}$$

4.4 DOPF Models of the LDC

This section presents the mathematical models developed for the LDC's feeder operations; the DOPF1 and DOPF2, which determine the optimal operations for the LDC distribution network supplying the industrial load and other connected loads. An appropriate EMS model is to be used for the optimal operation of the industrial customer's facility assuming the existence of a two-way communication facility between the LDC and the industrial customer for proper coordination of the models.

4.4.1 Distribution System Equations:

These include the total power drawn by the distribution system from substation bus ($b = 1$), and peak demand constraints for the distribution system.

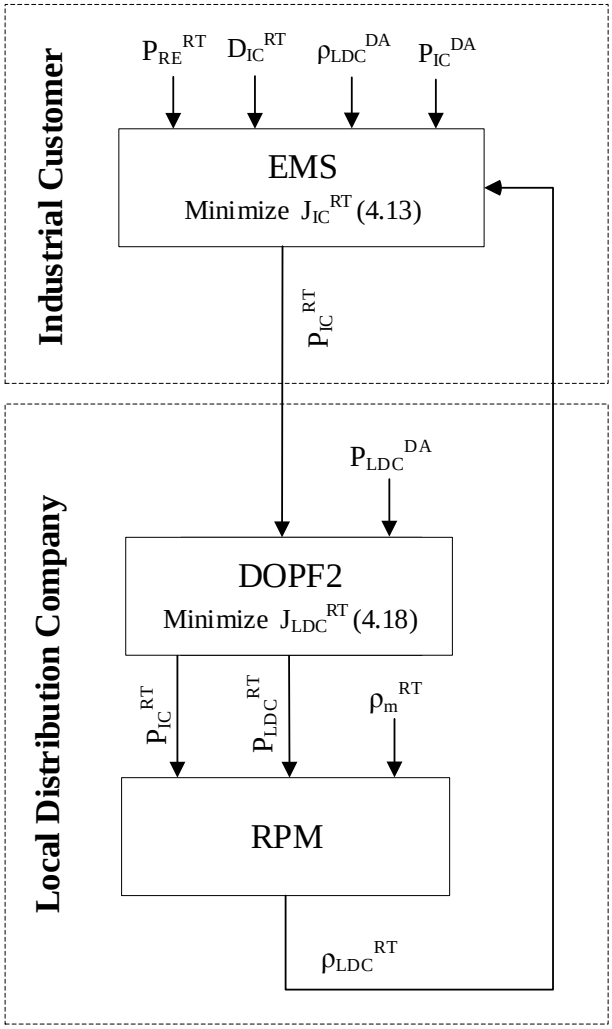

Figure 4.3: DR in real-time operations.

$$P_{LDC_t} = \sum_p Real(V_{b,p,t} I_{s_{l,p,t}}) \qquad For\, b = 1 \tag{4.23}$$

$$P^{DA}_{LDC_t} \leq \overline{P^{DA}_{LDC}} \qquad \forall t \tag{4.24}$$

$$P^{RT}_{LDC_t} \leq \overline{P^{RT}_{LDC}} \qquad \forall t \tag{4.25}$$

4.4.2 Industrial Load Related Constraints:

The industrial load is included in the DOPF models, as a balanced load, at distribution feeder bus i, using the following equations:

$$V_{b,p,t} = Z_{IC_{b,p,t}} I_{IC_{b,p,t}} \qquad b = i, \forall p, \forall t \tag{4.26}$$

$$Z_{IC_{b,p,t}} = \frac{3\, V^{sp^2}_{b,p}}{P_{IC_t} + jQ_{IC_t}} \qquad b = i, \forall p, \forall t \tag{4.27}$$

Additional constraints for industrial load are included in the DOPF1 model only, to determine the desired optimal load profile of the customer taking into account the LDC's contracts with the customer for energy and DR. These additional constraints are not included in DOPF2 since it is solved with a fixed industrial load profile as an input to the model.

$$P^*_{IC_t} \leq \overline{P^{DA}_{IC}} \qquad \forall t \tag{4.28}$$

$$\sum_t P^*_{IC_t} \geq \sum_t P^{DA}_{IC_t} \tag{4.29}$$

$$Q_{IC_t} = P^*_{IC_t} \sqrt{\tfrac{1}{pf^2} - 1} \qquad \forall t \tag{4.30}$$

Constraint (4.28) ensures that the desired load profile does not result in an increased peak demand for the industrial customer which would increase its demand charges. Constraint (4.29) defines the load shifting relationship in the DR. The reactive power demand

of the customer is calculated as a function of the active power demand using (4.30) based on an agreed operating power factor of the industrial facility.

4.5 Case Studies and Discussions

The distribution feeder used in this work is a 41 bus practical test feeder reported in [28], and shown in Figure 4.4. The non-industrial loads are modeled as constant impedance loads with random 24-hour profiles generated using the procedure described in [28]. The three-phase transformers at nodes 7, 15, and 40 are modeled with LTCs for regulating the voltage at their secondary terminals.

The proposed DR framework is applied to a water pumping system (WPS) facility reported in [10]; the power ratings of the pumps are scaled up to match the LDC's connected load ratings. The EMS model used in this work for the WPS facility is based on the model proposed in Chapter 3. The EMS model is appropriately modified for implementing the DR strategies discussed earlier. The WPS is assumed to be connected to node 3 of the feeder, as shown in Figure 4.4. The total connected load of the WPS is 4.3 MW, while the total connected non-industrial load is 15.2 MW. The WPS facility is assumed to maintain a power factor of 0.9 lagging.

The Hourly Ontario Energy Prices (HOEP) of July 18, 2017 are used as day-ahead market prices, and the demand charge λ_d is assumed to be 6.0 \$/kW. The real-time market prices are generated by adding an increasing random error to the day-ahead market prices assuming a normal distribution for the error with a standard deviation that is increasing with time.

The structure and parameters of the RPM are selected based on the historical demand profiles of the WPS facility. These historical profiles are generated by executing the EMS model of the WPS over many scenarios. HOEP data for 90 days, from January 1 to March 31, 2017 [58], are used to obtain the various scenario simulations of the EMS. Also, wind speed profiles are acquired for the same period, and are used to produce the

generation profiles of the wind resource of the WPS facility. Furthermore, 90 randomized water demand profiles of the WPS are produced, assuming a normal distribution of water demand over the days ($\sigma = 50\,m^3$).

By analyzing the WPS demand profiles, the number of levels in the staircase function (4.7) is selected to be, $n = 4$, and the power demand thresholds and the pricing coefficients are selected as shown in Table 4.1. The most probable power demand levels for customer's load are selected as the power demand thresholds since these levels are expected to represent cost effective operating points for the WPS facility. The price coefficients are selected in such a way that a large enough variation is attained between different price levels of the RPM to influence the customer's demand (either increasing or decreasing).

Table 4.1: Retail Pricing Model Parameters

P_1	P_2	P_3	P_4
4,310 kW	3,500 kW	2,204 kW	980 kW
λ_1	λ_2	λ_3	λ_4
0.1	0.325	0.55	0.775

4.5.1 Day Ahead Operations

The day-ahead operations involve solving the EMS, DOPF1 or DOPF2, and RPM models as per the framework proposed in Figure 4.1. Solving the EMS model for the WPS facility using the assumed day-ahead market prices resulted in an initial demand profile as shown in Figure 4.5 with a total energy consumption of 39 MWh, peak demand of 2.2 MW, and total energy cost of 617 \$/day. Solving the DOPF model of the LDC with this WPS profile, results in an initial feeder load profile shown in Figure 4.6, with a total energy demand of 308.8 MWh and peak demand of 15.13 MW.

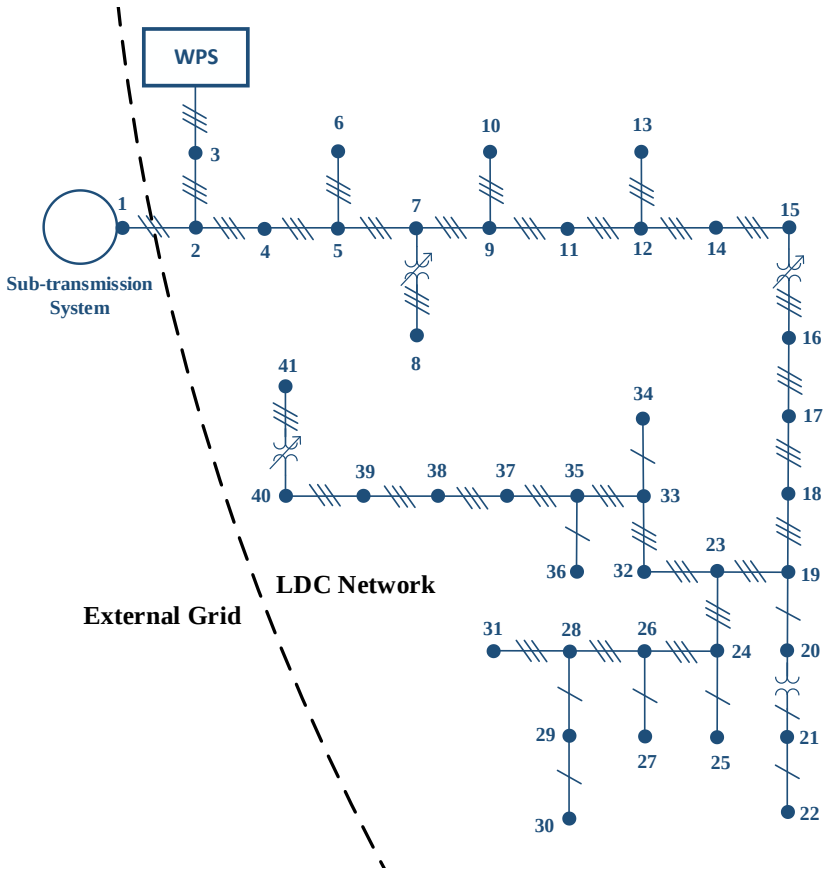

Figure 4.4: 41-Bus practical test feeder.

Three cases are considered for the DR strategy; in the first case TOU pricing scheme is considered, where Ontario IESO's TOU structure is used with some scaling by multiplying the TOU price for all hours by a single factor that makes the cost for the customer initial demand schedule equivalent to the cost associated with applying market prices. The other two cases are considered as discussed earlier- DR1 and DR2; in DR1 the desired demand profile is used, while in DR2 the retail price signal is used. The final results of the three cases are tabulated in Table 4.2, and the final scheduled day-ahead load profiles for the WPS facility and the distribution system for the three cases are shown in Figure 4.5 and Figure 4.6, respectively.

The solution of TOU case did not result in reduction in peak demand for the distribution network which actually increased slightly by 0.5% compared to the initial schedule. Also the energy cost to the WPS increased by 2.1%. However, peak demand has decreased for the WPS by 23.8%. The solution of DR1 is attained in three interaction cycles (Figure 4.7) and the distribution system's peak demand is 14.2 MW, and total energy cost of the WPS is \$694.6. There is a 6.1% reduction in feeder peak demand with DR1 as shown in Table 4.2. The solution of DR2 is attained in five interaction cycles (Figure 4.7) and results in distribution system's peak demand of 14.35 MW and total energy cost of the WPS of \$554.3. There is a 5.2% reduction in feeder peak demand as shown in Table 4.2, the final day-ahead retail prices are shown in Figure 4.8.

DR1 resulted in a lower peak load for the distribution system as compared to DR2. However, the energy cost for the WPS increased in DR1 while it slightly decreased in DR2 with the retail prices instead of market prices. In both DR1 and DR2 cases, some of WPS demand is shifted from hours 10-15 to hours 18-21 where feeder demand is low. No WPS demand is shifted to hours 1-7 because it would increase the peak demand, while the EMS seeks to minimize the peak load of the WPS facility.

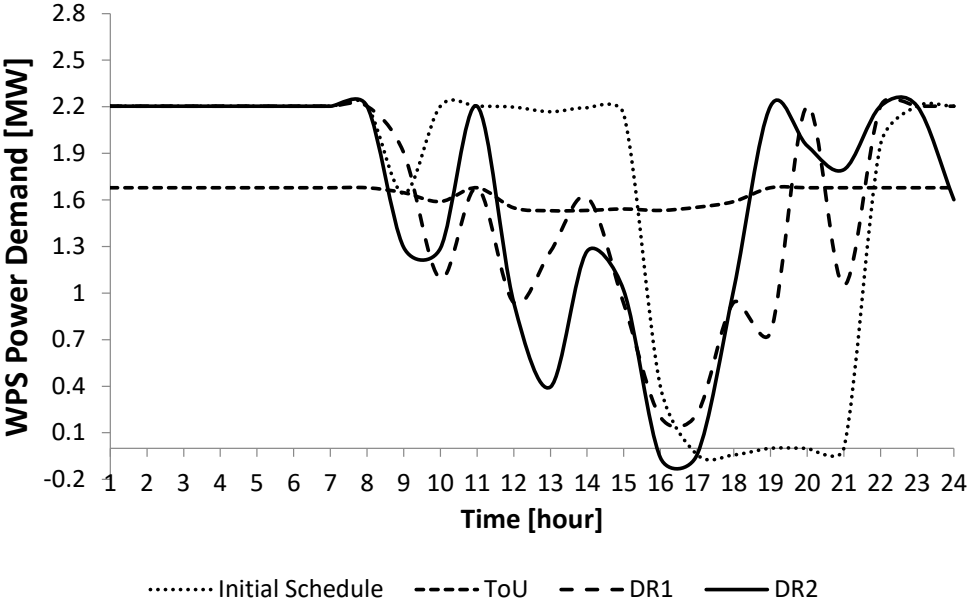

Figure 4.5: Scheduled power demand profiles of WPS facility.

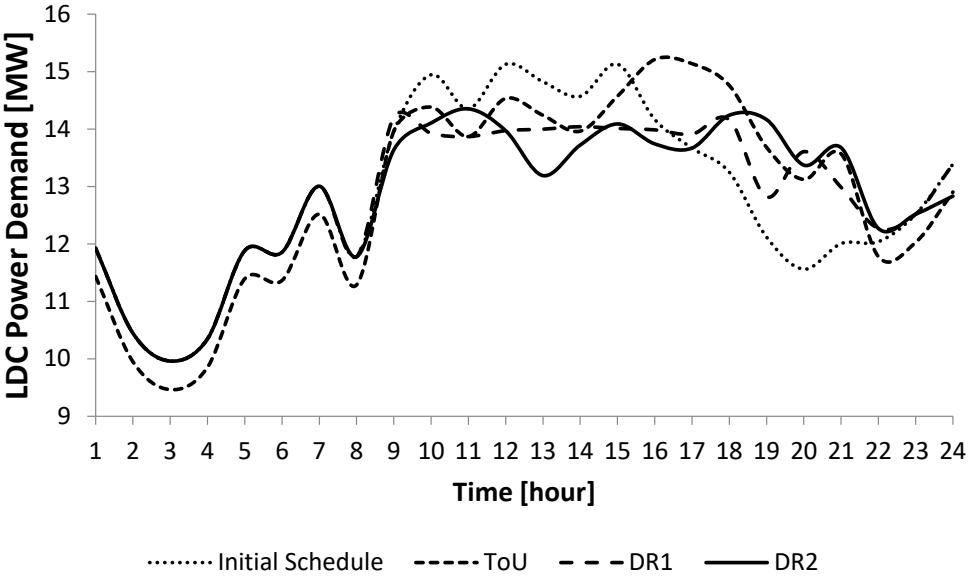

Figure 4.6: Scheduled power demand profiles of distribution system.

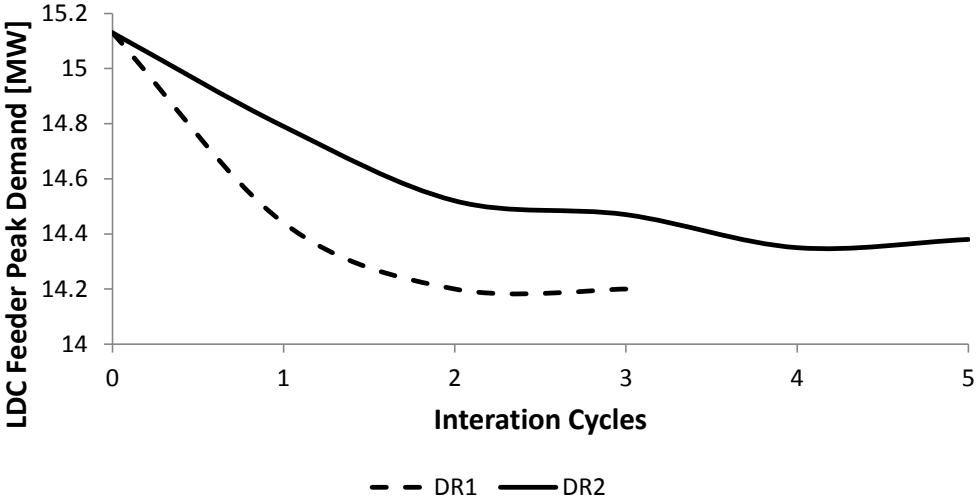

Figure 4.7: Convergence of day-ahead DR controls.

Table 4.2: Day-ahead Operations Results

	Initial Schedule	Final Schedule		
		ToU	DR1	DR2
Total Energy Consumption for WPS [MWh/day]	39.0	39.1 (+0.3%)	39.0 (0%)	38.9 (-0.3%)
Energy Costs for WPS [$/day]	617	629.9 (+2.1%)	694.6 (+12.6%)	554.3 (-10.2%)
Peak Demand for WPS [kW]	2203.8	1678.5 (-23.8%)	2203.8 (0%)	2203.8 (0%)
Total Energy Consumption for LDC [MWh/day]	308.8	308.9 (+0.03%)	308.8 (0%)	308.7 (-0.03%)
Peak Demand for LDC [MW]	15.13	15.21 (+0.5%)	14.20 (-6.1%)	14.35 (-5.2%)

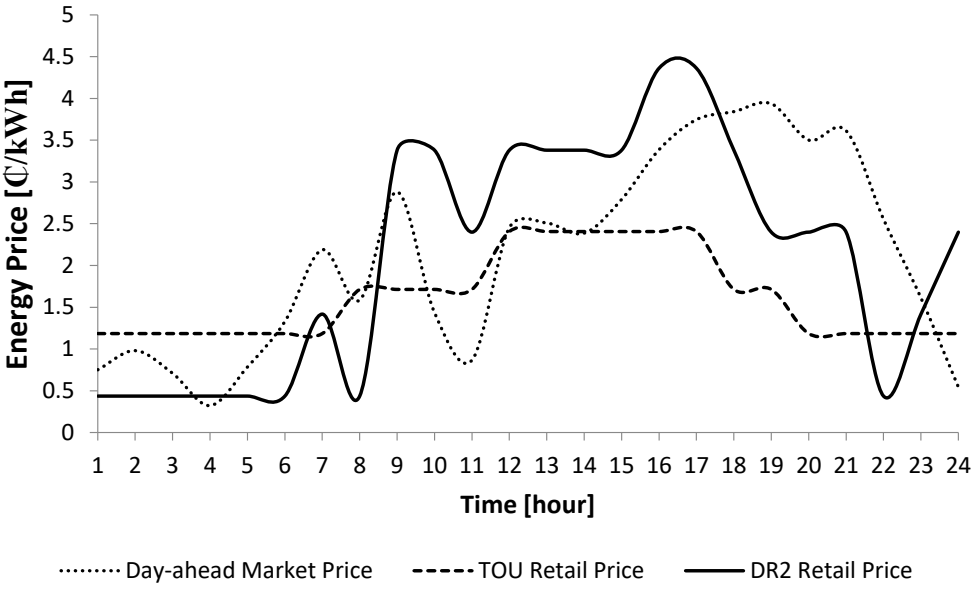

Figure 4.8: Day-ahead market and retail prices.

4.5.2 Real-Time Operations

The real-time operations involve solving the customer's EMS and the LDC's DOPF models on an hourly basis. As the WPS operations deviate from the day-ahead schedules (Figure 4.5), its operating schedules are updated each hour and the EMS is re-executed to minimize the impact of uncertainties on EMS decisions. Also, as the WPS updates its load demand schedule in the MPC approach, the updated profile is sent to the LDC every hour, which helps in its real-time operations.

Using the updated WPS power demand schedules, the LDC revises its real-time retail price signal, which is sent to the WPS on an hourly basis. Two scenarios are considered for the real-time problem; in Scenario 1 the customer does not send hourly updates to the LDC and the retail price signal is not updated in real-time; while in Scenario 2 the operation is carried out as proposed in Section 4.3.2. The results of both scenarios are compared with final day-ahead results in Table 4.3. The power demand profiles of the WPS facility and the distribution system are shown in Figure 4.9 and Figure 4.10 respectively.

Implementing the proposed strategy in Scenario 2 resulted in lower peak demand for the distribution system and the WPS facility compared to Scenario 1. Also Scenario 2 resulted in lower energy cost for the WPS with the application of the MPC technique. The increased cost and energy consumption of the WPS facility in real-time, as compared to the day-ahead schedule, is attributed to its increased total water demand as it deviates from the day-ahead schedule (Table 4.3).

The increase in distribution system's peak demand in Scenario 1 results from the increased pumping requirement in the WPS at hour 18, due to depletion of stored water in reservoir, as compared to day-ahead schedule. Although, this is prevented in Scenario 2 by additional water pumping at hour 9, it creates another peak, but lower than that in Scenario 1.

Table 4.3: Real-time Operations Results

	Day-ahead Schedule	Scenario 1	Scenario 2
Total Energy Consumption of WPS [MWh/day]	38.9	39.7 (+2%)	39.4 (+1.3%)
Energy Cost of WPS [$/day]	554.3	574.8 (+3.7%)	560.53 (+1.1%)
Peak Demand of WPS [kW]	2203.8	2405.9 (+9.2%)	2203.8 (0%)
Total Water Demand for WPS $[m^3]$	191,470	192,821 (+0.7%)	192,821 (+0.7%)
Total Energy Consumption for LDC [MWh/day]	308.7	309.5 (+0.26%)	309.2 (+0.16%)
Peak Demand for LDC [MW]	14.35	14.53 (+1.3%)	14.44 (+0.6%)

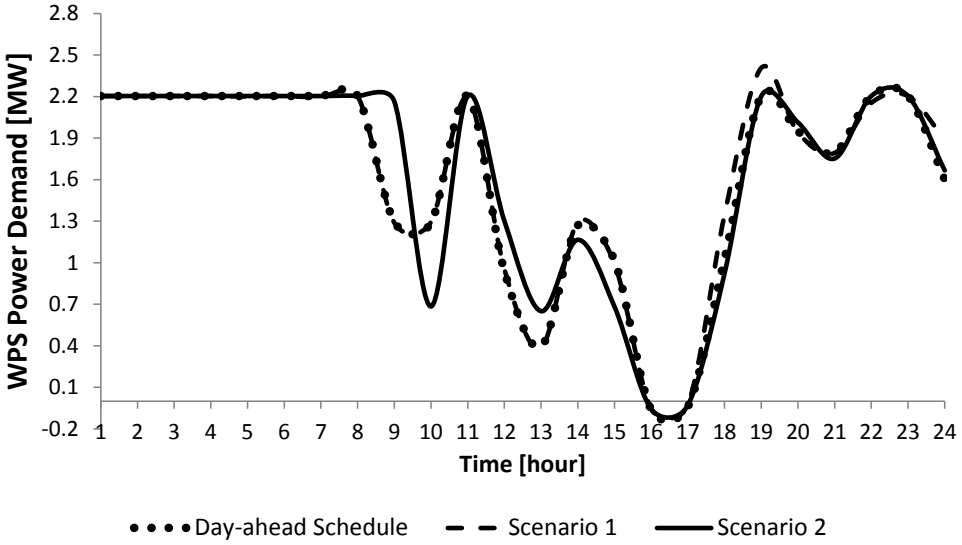

Figure 4.9: Real-time power demand profiles of WPS facility.

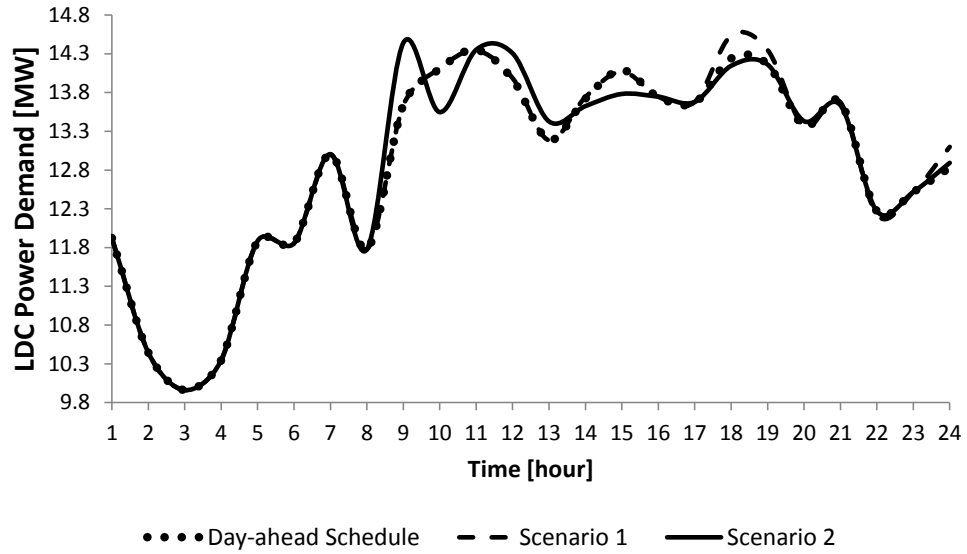

Figure 4.10: Real-time demand profiles of distribution system.

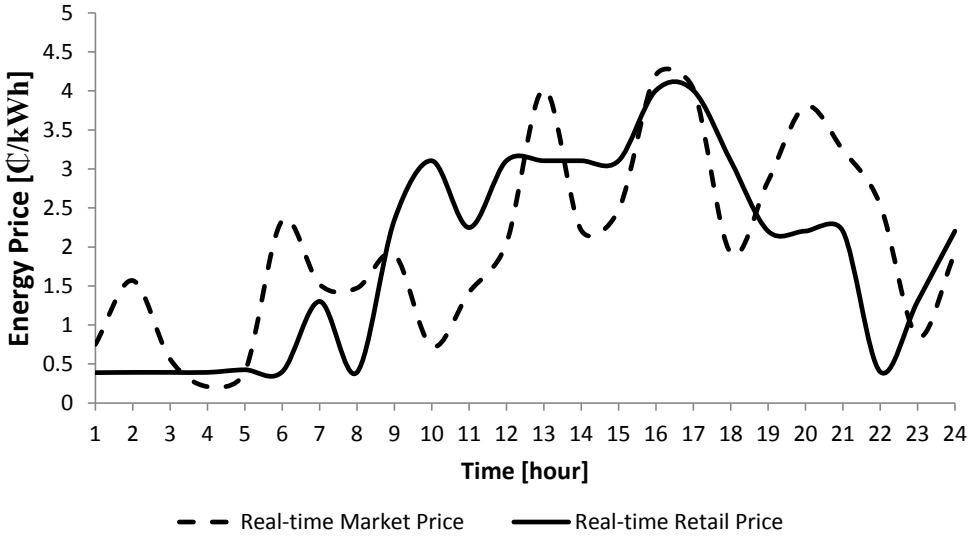

Figure 4.11: Real-time market and retail prices.

4.5.3 Solution Method and Computational Efficiency

The DOPF1 and DOPF2 models are formulated as nonlinear programming (NLP) problems and solved using the IPOPT solver in GAMS environment [37]. The switching states of LTCs are rounded to the nearest integers after the NLP solution is obtained. This approach is adopted from [53] which showed that the differences in solutions are minimal when integer variables are considered in the formulation compared to the solutions obtained by rounding. The EMS model of the WPS facility is solved as a mixed integer nonlinear programming (MINLP) problem using the DICOPT solver of GAMS. The computational times for the DOPF and EMS models are detailed in Table 5.7.

The average computational times for one interaction cycle in DR1 and DR2 schemes are 224 seconds and 180 seconds, respectively. In the presented case study, the number of interaction cycles needed for DR1 and DR2 schemes were 3 and 5, respectively. Therefore, the proposed schemes are easily implementable in the day-ahead stage. The real-time scheme using the MPC approach works on an hourly basis in this work, and the average time for one interaction cycle is 117 seconds, which can also be met within the considered

time-frame, or even for small time granularities. Therefore, the proposed schemes can be considered computationally efficient.

Table 4.4: Computational property of the mathematical models

Model	Average Solution Time
Initial EMS	148 sec
DR1 modified EMS	163 sec
DR2 modified EMS	148 sec
Real-time EMS	85 sec
DOPF1	29 sec
DOPF2	32 sec

4.6 Summary

This chapter presented a novel DR framework for industrial customers considering LDC's operations. The framework proposed two types of DR signals; a desired demand profile signal and a retail price signal, which were sent to the customer to achieve the desired DR in a collaborative manner. In the retail price based control approach, the signal was produced by an RPM which was designed based on customer's historical data. The results showed the capability of the proposed framework to reduce the peak demand of the distribution system, without increasing the day-ahead scheduled energy costs for the customer. The impact of uncertainties on DR was studied in the real-time operations stage, and it was noted that hourly updates between the LDC and the customer enhanced the capability of the DR strategy to achieve its targets.

Chapter 5

Material Flow Based Power Demand Modeling of an Oil Refinery Process for Optimal Energy Management[‡]

5.1 Nomenclature

Indices

f	Refinery feedstock or product, $f = 1,2,...,F.$
i	Processing unit, $i = CDU,VDU,...,GRU.$
j	Cogeneration unit, $j = 1,2,...,J.$
t	Time interval, hours, $t = 1,2,...,T.$

Parameters

$a_{0_j}, ..., a_{3_j}$	Cogeneration unit electrical output constants

[‡]Parts of this chapter have been submitted as a paper for review in: O. Alarfaj and K. Bhattacharya, Material flow based power demand modeling of an oil refinery process for optimal energy management, IEEE Transactions on Power Systems, 2018.

$b_{0_j}, ..., b_{3_j}$	Cogeneration unit thermal output constants
d_i	Production time of processing unit, $[hours]$
F_{hv}	Fuel heat value, $[kWh/m^3]$
$M_{i,f_m,t}^{in^0}$	Processing unit's main feed initial mass rate, $[kg/h]$
M_{cr}^{min}	Minimum crude mass flow rate, $[kg/h]$
M_{cr}^{max}	Maximum crude mass flow rate, $[kg/h]$
M_{cr}^{total}	Total daily processed crude mass, $[kg/day]$
$P_{cg_j}^{el^{min}}$	Minimum cogeneration unit electrical power output, $[kW]$
$P_{cg_j}^{el^{max}}$	Maximum cogeneration unit electrical power output, $[kW]$
$P_{cg_j}^{el^0}$	Initial cogeneration unit electrical power output, $[kW]$
P_{RES_t}	Renewable energy source output power, $[kW]$
$R_{cg_j}^{UP}$	Cogeneration unit maximum ramp up rate, $[kW/h]$
$R_{cg_j}^{DN}$	Cogeneration unit maximum ramp down rate, $[kW/h]$
R_{cr}^{UP}	Crude feed maximum ramp up rate, $[kg/h/h]$
R_{cr}^{DN}	Crude feed maximum ramp down rate, $[kg/h/h]$
S_{PV}	PV panels surface area, $[m^2]$
$st_{cg_j}^0$	Initial cogeneration unit operating status, (1: ON, 0: OFF)
T_{PV}^R	PV panels temperature rating, $[^\circ C]$
T_t^a	Ambient temperature, $[^\circ C]$
$\alpha_{i,f}$	Mass flow coefficient
α_{S_i}	Steam demand coefficient
α_{PV}	PV panels temperature coefficient, $[^\circ C^{-1}]$
λ_{P_i}	Electrical demand coefficient, $[kWh/kg]$
λ_S	Steam thermal demand coefficient, $[kWh/kg]$
Φ_t	Solar irradiance, $[kW/m^2]$
ρ_{m_t}	Electricity market price, $[\$/kWh]$
$\rho_{cg_{fuel}}$	Cogeneration fuel price, $[\$/m^3]$
$\rho_{b_{fuel}}$	Boiler fuel price, $[\$/m^3]$
η_b	Boiler overall efficiency, $[\%]$

$\eta^{fc}_{cg_j}$	Cogeneration fuel combustion efficiency, [%]
η_{PV}	PV panels efficiency, [%]

Variables

$FC_{cg_{j,t}}$	Cogeneration unit's fuel consumption, $[m^3/h]$
FC_{b_t}	Boiler's fuel consumption, $[m^3/h]$
$M^{in}_{i,f,t}$	Processing unit's input mass rate, $[kg/h]$
$M^{out}_{i,f,t}$	Processing unit's output mass rate, $[kg/h]$
$M^{in}_{i,f_m,t}$	Processing unit's main feed mass rate, $[kg/h]$
$M^{out}_{i_p,f,t}$	Preceding processing unit's output mass rate, $[kg/h]$
$P_{i,t}$	Processing unit electrical demand, $[kW]$
$P^{th}_{b_t}$	Boiler's thermal power demand, $[kW]$
$P^{in}_{cg_{j,t}}$	Cogeneration unit's input power, $[kW]$
$P^{el}_{cg_{j,t}}$	Cogeneration unit's electrical power output, $[kW]$
$P^{th}_{cg_{j,t}}$	Cogeneration unit's thermal power output, $[kW]$
P_D	Power exchanged by the refinery with the local distribution company (LDC), $[kW]$
$P^{th}_{S_t}$	Thermal power demand for steam production, $[kW]$
Q_D	Refinery's reactive power demand, $[kVAR]$
S_{d_t}	Refinery's total steam demand, $[kg/h]$
$S_{i,t}$	Processing unit steam demand, $[kg/h]$
$W_{cg_{j,t}}$	Binary decision variable for cogeneration unit status (1: ON, 0: OFF)
$TP_{f,t}$	Total production rate of feedstock or product, $[kg/h]$
ρ_{LDC}	Retail price, $[\$/kWh]$
ρ^{max}_{LDC}	Maximum retail price, $[\$/kWh]$

5.2 Introduction

Oil refining is an energy intensive industry, often equipped with distributed generation (DG) resources for the supply of base load or emergency power; a significant share of on-site generation is from cogeneration facilities which produce both electricity and heat for refining processes. Optimal energy management of the refinery's load and its DG resources, under a dynamic electricity pricing scheme, improves the facility's electricity consumption behavior and reduces energy costs.

An EMS model is proposed in this work for load management of an oil refinery considering an on-site cogeneration facility. The EMS includes a model for the electrical demand considering the mass flow of processed materials and processing steam demand. The objective of the EMS is to minimize the cost of electrical and thermal energy consumption of the refinery. The steam production cost is minimized as it is coupled with electricity generation by the cogeneration units, which were represented by a joint electrical-thermal model to account for the electricity and steam production. Also with the increasing regulations for reducing the carbon footprint of industrial facilities, it is assumed in this work the the Oil Refinery is equipped with a PV-based solar energy source to supplement or substitute its energy needs from conventional sources.

The participation of refinery in DR provisions is examined by applying a DR strategy that is based on effective communication between the refinery's EMS and the operations of the local distribution company (LDC). The main contributions of this work are:

- A comprehensive EMS framework is proposed for minimizing electricity consumption costs of an oil refinery facility based on power demand modeling of the refinery process.
- A cogeneration facility operation optimization is proposed using a joint electrical-thermal model, considering both electricity and steam production costs associated with its operation.

- The developed EMS model is used as part of a DR strategy to illustrate the impact of EMS decisions on distribution system operations.

The rest of the chapter is organized as follows: Section 5.3 describes the developed model for power demand and the mass flow of the oil refinery process. The proposed EMS model for the refinery is described in Section 5.4. The applied DR strategy is presented in Section 5.5. Case study results are reported and discussed in Section 5.6. Finally, Section 5.7 presents the conclusions of this work.

5.3 Oil Refinery Model

5.3.1 Material Flow and Energy Demand Modeling

The material flow and energy demand in a processing unit of the refinery can be represented by a schematic flow diagram as shown in Figure 5.1 [60]. Each unit processes the input streams (X_1 and X_2) to produce the output streams (Y_1, Y_2, and Y_3) which could be inputs to another process or be the final products. The processing unit consumes E_p amount of energy which could be in the form of fuel, steam, or electricity. An example schematic flow diagram is shown in Figure 5.2 for the CDU processing unit.

As stated in [60], the energy consumption of processing units is usually proportional to the amount of processed mass; hence the energy consumption and mass flow can be modeled as a function of the amount of processed material for all processing units in the refinery. The output mass stream $M^{out}_{i,f,t}$, electric power demand $P_{i,t}$, and steam demand $S_{i,t}$ are modeled as functions of the main input stream $M^{in}_{i,f_m,t}$ of the unit, as given below:

$$M^{out}_{i,f,t} = \alpha_{i,f} M^{in}_{i,f_m,t-d_i} \qquad \forall i, \forall f, \forall t \tag{5.1}$$

$$P_{i,t} = \lambda_{P_i} M^{in}_{i,f_m,t} \qquad \forall i, \forall t \tag{5.2}$$

$$S_{i,t} = \alpha_{S_i} M^{in}_{i,f_m,t} \qquad \forall i, \forall t \tag{5.3}$$

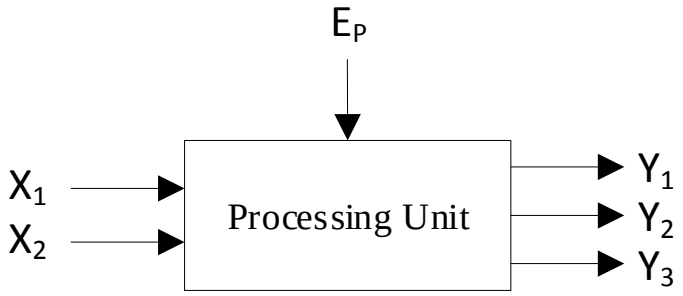

Figure 5.1: Processing unit schematic flow diagram [60].

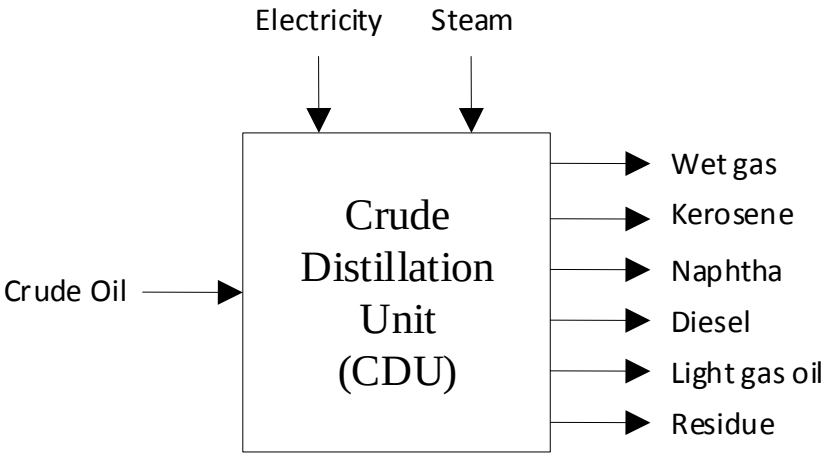

Figure 5.2: Schematic flow diagram of CDU processing unit.

The parameter $\alpha_{i,f}$ in (5.1) is a mass flow coefficient that relates the processing units' output stream mass flow with the main input stream mass flow, while parameter d_i represents the production time of the processing unit. In case of multiple input streams for a processing unit, the higher mass flow rate stream is considered to be the main input stream $M_{i,f_m,t}$. The multiple input streams are designed to arrive simultaneously to the processing unit. The parameters λ_{P_i} and α_{S_i}, in (5.2) and (5.3), are electrical and steam demand coefficients, respectively, relating the electricity and steam consumption of the processing unit with the main input stream mass flow.

In this work, the refinery is considered to be maintaining a certain production mode over the entire EMS optimization horizon, which is a 24-hour time window. When the operating mode of the refinery is changed after several days of operation, the material flow model would still be applicable to the new operations provided that mass flow coefficients, $\alpha_{i,f}$, in (5.1) are adjusted for all processing units to match the new production schedules.

5.3.2 Cogeneration Facility Model

An on-site, gas-turbine based cogeneration facility, supplies the refinery processes with electricity and steam. A joint electrical-thermal model is used for the facility to account for the production of electricity and steam, where the steam is utilized locally in the refinery while the electricity can either be consumed by the facility or exported to the grid. The electrical and thermal outputs, $P^{el}_{cg_{j,t}}$ and $P^{th}_{cg_{j,t}}$ respectively, along with the associated power input from fuel combustion, $P^{in}_{cg_{j,t}}$, are modeled using the following equations [61]:

$$P^{in}_{cg_{j,t}} = a_{3_j} P^{el^3}_{cg_{j,t}} + a_{2_j} P^{el^2}_{cg_{j,t}} + a_{1_j} P^{el}_{cg_{j,t}} + a_{0_j} W_{cg_{j,t}} \qquad \forall j, \forall t \qquad (5.4)$$

$$P^{th}_{cg_{j,t}} = b_{3_j} P^{in^3}_{cg_{j,t}} + b_{2_j} P^{in^2}_{cg_{j,t}} + b_{1_j} P^{in}_{cg_{j,t}} + b_{0_j} W_{cg_{j,t}} \qquad \forall j, \forall t \qquad (5.5)$$

The fuel consumption, $FC_{cg_{j,t}}$, of a cogeneration unit is calculated as a function of its input power as follows:

$$FC_{cg_{j,t}} = \frac{P^{in}_{cg_{j,t}}}{\eta^{fc}_{cg_j} F_{hv}} \qquad \forall j, \forall t \tag{5.6}$$

5.4 Energy Management System of Oil Refinery

5.4.1 Objective Function

The optimization objectives of the EMS is to minimize the refinery's electricity consumption cost, which includes the purchased energy from the external grid and that generated within the facility from the cogeneration units. The cost of steam production is also minimized because it is correlated with electricity production costs from the cogeneration facility. The objective function is given as follows:

$$J = \sum_t \rho_{m_t} P_{D_t} \Delta t + \rho_{cg_{fuel}} \sum_t FC_{cg_t} \Delta t + \rho_{b_{fuel}} \sum_t FC_{b_t} \Delta t \tag{5.7}$$

The first term in (5.7) represents the cost associated with energy exchanged with the LDC, the second term represents the fuel consumption cost incurred by the cogeneration facility, and the third term represents fuel consumption cost incurred by the refinery boiler.

5.4.2 Material Flow Constraints

The mass flow inside each processing unit of the refinery is determined using (5.1), while the mass flow between the processing units is modeled using the following equations:

$$M^{in}_{i,f,t} = M^{out}_{i_p,f,t} \qquad \forall i, \forall f, \forall t \tag{5.8}$$

$$TP_{f,t} = \sum_i M_{i,f,t} \qquad \forall f, \forall t \tag{5.9}$$

$$M^{min}_{cr} \leq M^{in}_{i,f_m,t} \leq M^{max}_{cr} \qquad i = 1, \forall t \tag{5.10}$$

$$\sum_t M^{in}_{i,f_m,t} \Delta t = M^{total}_{cr} \qquad i = 1 \tag{5.11}$$

$$M^{in}_{i,f_m,t+1} - M^{in}_{i,f_m,t} \leq R^{UP}_{cr} \Delta t \qquad i = 1, \forall t \tag{5.12}$$

$$M^{in}_{i,f_m,t} - M^{in}_{i,f_m,t+1} \leq R^{DN}_{cr} \Delta t \qquad i = 1, \forall t \tag{5.13}$$

$$M^{in}_{i,f_m,t} = M^{in^0}_{i,f_m,t} \qquad i = 1, t = 1 \tag{5.14}$$

Equation (5.8) relates the intermediate stream mass flows while (5.9) represents the final product streams. Equation (5.10) represents the maximum and minimum crude feed limits for the CDU, while (5.11) ensures that the entire scheduled amount of crude oil is processed. Equations (5.12) and (5.13) are the ramping constraints limiting the rate of change in crude feed to CDU, while (5.14) specifies the initial crude feed to the unit. While (5.10) to (5.14) impose the limits on the crude feed to the CDU, no limits were imposed on the inputs to the other processing units assuming that these are appropriately designed to continuously process the feeds arriving at their inlets during normal operation.

5.4.3 Steam Demand Balance

The steam demand of each processing unit of the refinery is determined using (5.3), and the total refinery steam demand is given by:

$$S_{d_t} = \sum_i S_{i,t} \qquad \forall t \tag{5.15}$$

The total thermal energy needed for steam production is a function of the total steam mass S_{d_t}, as given below:

$$P_{S_t}^{th} = \lambda_S S_{d_t} \qquad \forall t \tag{5.16}$$

The total thermal demand $P_{S_t}^{th}$ is produced by two sources- the cogeneration facility, and refinery boiler, as given below:

$$P_{S_t}^{th} = \sum_j P_{cg_{j,t}}^{th} + P_{b_t}^{th} \qquad \forall t \tag{5.17}$$

The thermal energy output $P_{cg_{j,t}}^{th}$ from the cogeneration unit is determined using the cogeneration model described earlier, while the boiler thermal energy output $P_{b_t}^{th}$ is determined to satisfy the total energy need for steam production $P_{S_t}^{th}$ considering fuel consumption of the boiler, given by:

$$FC_{b_t} = \frac{P_{b_t}^{th}}{\eta_b \, F_{hv}} \qquad \forall t \tag{5.18}$$

5.4.4 Electrical Demand Balance

The electrical power demand of each processing unit is determined using (5.2). The total electrical power demand is supplied by the cogeneration facility, $P_{cg_{j,t}}^{el}$, the on-site renewable energy resource P_{RE_t}, and power from the LDC network P_{D_t}, as given below:

$$\sum_i P_{i,t} = P_{D_t} + \sum_j P_{cg_{j,t}}^{el} + P_{RES_t} \qquad \forall t \tag{5.19}$$

5.4.5 Cogeneration Constraints

Cogeneration constraints include limit on electrical output, ramping constraints, and the initial value of electrical power output.

$$P_{cg_j}^{el^{min}} W_{cg_{j,t}} \leq P_{cg_{j,t}}^{el} \leq P_{cg_j}^{el^{max}} W_{cg_{j,t}} \qquad \forall j, \forall t \qquad (5.20)$$

$$P_{cg_{j,t+1}}^{el} - P_{cg_{j,t}}^{el} \leq R_{cg_j}^{UP} \Delta t \qquad \forall j, \forall t \qquad (5.21)$$

$$P_{cg_{j,t}}^{el} - P_{cg_{j,t+1}}^{el} \leq R_{cg_j}^{DN} \Delta t \qquad \forall j, \forall t \qquad (5.22)$$

$$P_{cg_{j,t}}^{el} = P_{cg_j}^{el^0} \qquad \forall j, t = 1 \qquad (5.23)$$

5.4.6 Renewable Energy Resource

The refinery is assumed to be equipped with an on-site PV facility that supplies solar power P_{RES_t}, which can be expressed in terms of solar irradiance Φ_t and ambient temperature T_t^a, given by [62]:

$$P_{RES_t} = \eta_{PV} S_{PV} \Phi_t (1 - \alpha_{PV}(T_t^a - T_{PV}^R)) \qquad \forall t \qquad (5.24)$$

5.5 Case Study and Discussion

The oil refinery process used as a case study is based on the benchmark process described in [42]. The tabulated results of the energy analysis of the process in [42], are used to determine the energy consumption (λ_{P_i},α_{S_i}) and products' mass flow ($\alpha_{i,f}$) coefficients for each processing unit of the refinery with appropriate conversions of units. The processing times for the units are assumed based on the production time delays given in [19]. The crude processing capacity of the CDU is assumed as 33,000 ton/day, with a scheduled processing amount of 29,700 ton/day.

The on-site cogeneration facility is considered to be equipped with three identical 5.47 MW generation units with the characteristics shown in Table 5.1. The cogeneration model parameters in (5.4) and (5.5), shown in Table 5.3, are taken from [63] which are based on manufacturer's data fitting. The characteristics of the PV-based solar source are shown in

Table 5.2, while the hourly data for the solar irradiance and ambient temperature of the PV site are taken from [64]; the resulting output power forecast for the solar source is shown in Figure 5.3. The natural gas price of 9.2346 ¢/m^3 prevailing in Ontario since April 1, 2018 [65] is used to calculate the fuel cost of the cogeneration units. This rate doesn't include fuel transportation cost, assuming that the fuel is produced in the refinery. The HOEP of March 21, 2018, shown in Figure 5.4 [58] is considered for the studies. The refinery EMS optimization problem is formulated in GAMS as a MINLP problem and solved using the DICOPT solver [38]. The simulations are carried out for one day of refinery operation with equal time intervals of 15 minutes.

Table 5.1: Cogeneneration Unit Characteristics

Electrical Output	5,470 kW
Thermal Output	10,132 kW
Electrical Efficiency	28.16%
Thermal Efficiency	52.16%
Overall Efficiency	80.32%

Table 5.2: Solar Source Characteristics

Rated Power	5 MW
Total PV surface area	31,850 m^2
PV panel efficiency	15.7%
PV temperature coefficient	0.005
PV temperature rating	25 °C
PV solar irradiance rating	1000 W/m^2

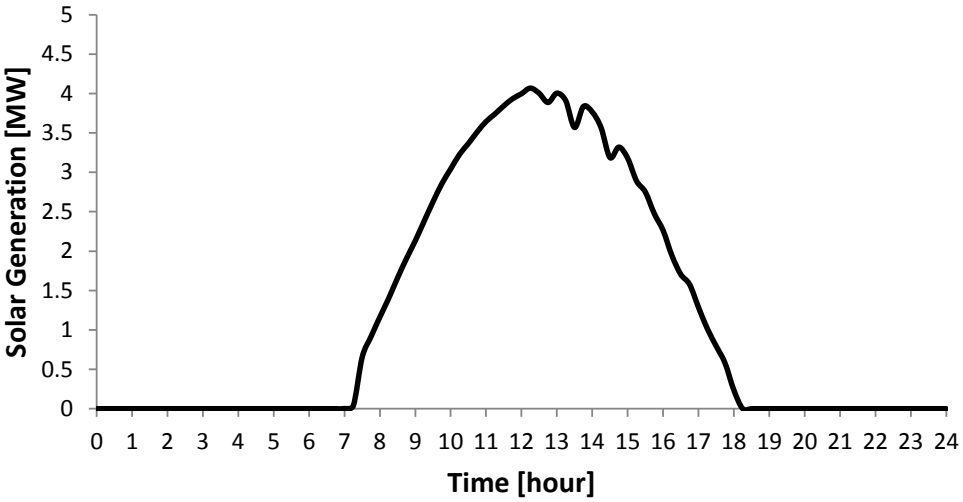

Figure 5.3: Solar power generation profile.

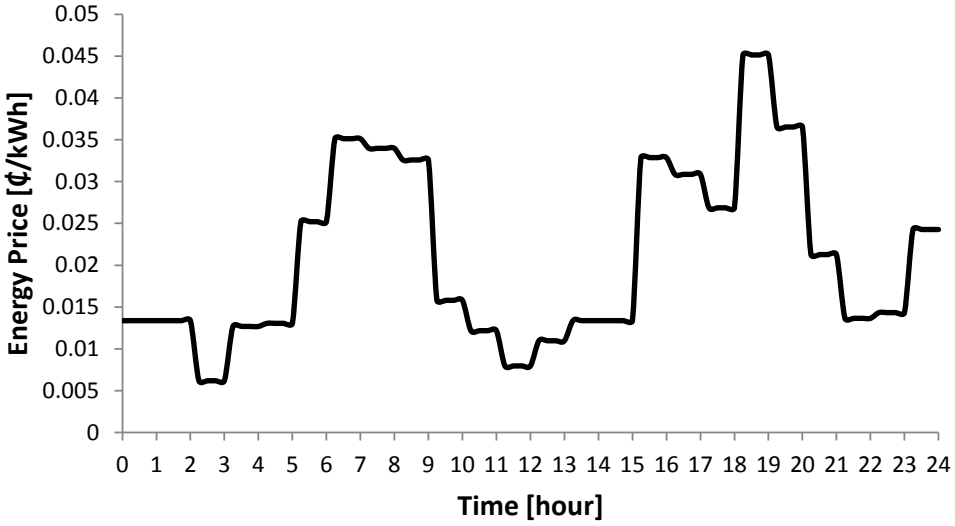

Figure 5.4: Electricity price profile.

Table 5.3: Cogeneration model parameters [59]

a_0	a_1	a_2	a_3
7.24103	2.33050	-0.08663	0.01239
b_0	b_1	b_2	b_3
1.41195	0.13609	0.02124	-0.00026

5.5.1 Refinery EMS Studies

To illustrate the benefits of the proposed EMS model, three scenarios are constructed as follows:

- Scenario 1 (Base): Crude feed rate of the refinery is considered fixed over time, and the electrical output of the cogeneration units is considered fixed at the rated value.
- Scenario 2: Crude feed rate is fixed while electrical output of cogeneration units is variable.
- Scenario 3: Crude feed rate is considered variable, which enables the refinery's load shifting capability.

The resulting costs associated with 24-hour operation of the refinery, for the three scenarios, are detailed in Table 5.4. The total cost in Scenario 2 reduced by 1.0% as a result of optimizing the cogeneration units' electrical output while considering the impact of changes in thermal output on boiler fuel costs. An additional 1.4% reduction in total cost resulted in Scenario 3 from the refinery load management executed by optimizing the crude feed rate to the refinery over time. It is noted that the boiler fuel cost accounted for more than 55% of the total costs in all scenarios. This is due to the fact that the thermal energy demand for steam production in the refinery is much greater than the electrical energy demand.

The hourly crude feed rates for the three scenarios are shown in Figure 5.5 and the associated refinery total electrical demand is shown in Figure 5.6. It is noted that the total demand in Scenario 3 follows the changes in crude feed with some time shift caused by the propagation time of the processed material in the refinery process flow. Also it is noted that the high crude feed rate periods coincide with low electricity price periods, and vise versa. The reduction in crude feed rate occurring between hours 22 and 23, reduces the power drawn from the LDC between hours 23 and 24 (Figure 5.7) when electricity price is relatively high.

The total cogeneration electrical output for the three scenarios is shown in (Figure 5.8). Scenarios 2 and 3 exhibited similar cogeneration schedule where the electrical output is kept at minimum during low electricity price periods, and is at maximum during high price periods. The opposite is noticed for the power drawn from LDC (Figure 5.7), more power is drawn at hours with low electricity prices, and vise versa. Figure 5.9 shows the steam thermal demand balance for refinery in Scenario 3, where 10% of the thermal demand is supplied by the cogeneration facility while the remaining 90% is supplied by the boiler.

It is to be noted that the electricity cost is not a very significant component of the total cost of operation of an oil refinery. Consequently, the number of available controls, which can be used to bring about energy cost minimization, are not too many. In such a situation, it is evident that the proposed EMS results in only a limited amount of electricity cost savings, which does not vary much across the scenarios. Nevertheless, as can be noted from Table 5.4, there is a 1% and 2.4% savings in Scenarios 2 and Scenario 3, respectively, as compared to Scenario 1; which effectively means an actual annual cost savings to the order of $189,435 and $447,125 respectively, which is reasonable. The annual cost savings are calculated assuming an average daily cost savings of $519 and $1,225 for Scenario 2 and Scenario 3 respectively as per the obtained results in Table 5.4.

5.5.2 Refinery DR Studies

The industrial customer's demand response strategy described in Chapter 4 is applied to the oil refinery facility used in the case study. The 41 bus distribution feeder reported in [28] is used, assuming that the refinery load is connected at bus 3 with a total connected load of 35 MW. The feeders connecting buses 1, 2, and 3 are re-sized in order to obtain acceptable voltage drops considering the high electrical demand of the refinery. The non-industrial loads are modeled as constant impedance loads with random 24-hour profiles generated using the procedure described in [28], with a total connected load of 15.2 MW.

It was noted in the retail price based approach (DR2) that the proposed strategy works well only when the refinery does not have dispatchable generators as it results in periods

Table 5.4:
Energy Management Results

	Scenario 1	Scenario 2	Scenario 3
Total refinery electrical demand [MWh/day]	755.5	755.5 (0%)	753.2 (-0.3%)
Total cogeneration electrical energy output [MWh/day]	393.8	164.1 (-58.3%)	168.2 (-57.3%)
Total energy drawn from LDC [MWh/day]	333.2	563 (+68.9%)	556.6 (+67%)
Cost for energy drawn from LDC [$/day]	7,121	10,352 (+45%)	9,610 (+35%)
Cogeneration units fuel cost [$/day]	15,907	7,472 (-53%)	7,638 (-52%)
Boiler fuel cost [$/day]	28,945	33,630 (+16.2%)	33,501 (+15.7%)
Total costs [$/day]	51,973	51,454 (-1.0%)	50,748 (-2.4%)
Per-year cost savings [$/year]		189,435	447,125

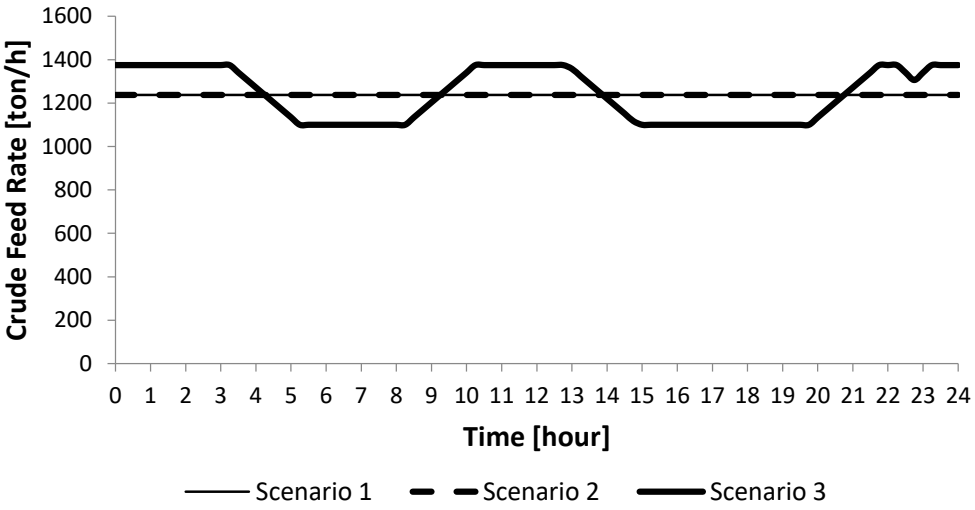

Figure 5.5: Crude feed rate profile.

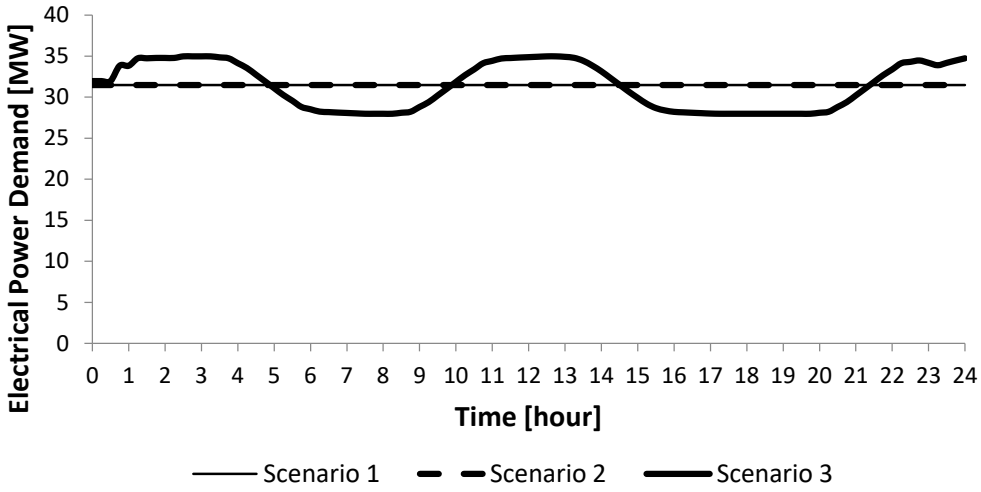

Figure 5.6: Refinery total electrical demand profile.

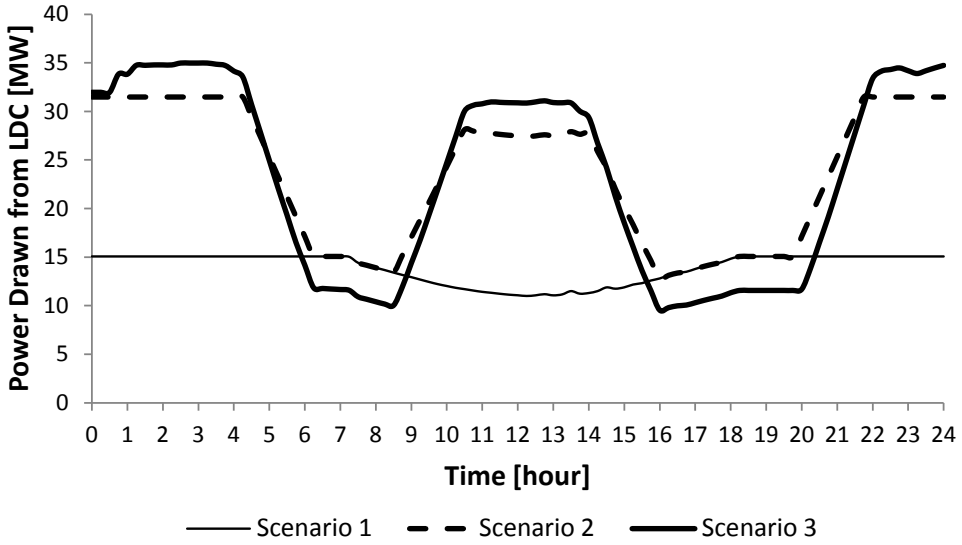

Figure 5.7: Power drawn from LDC profile.

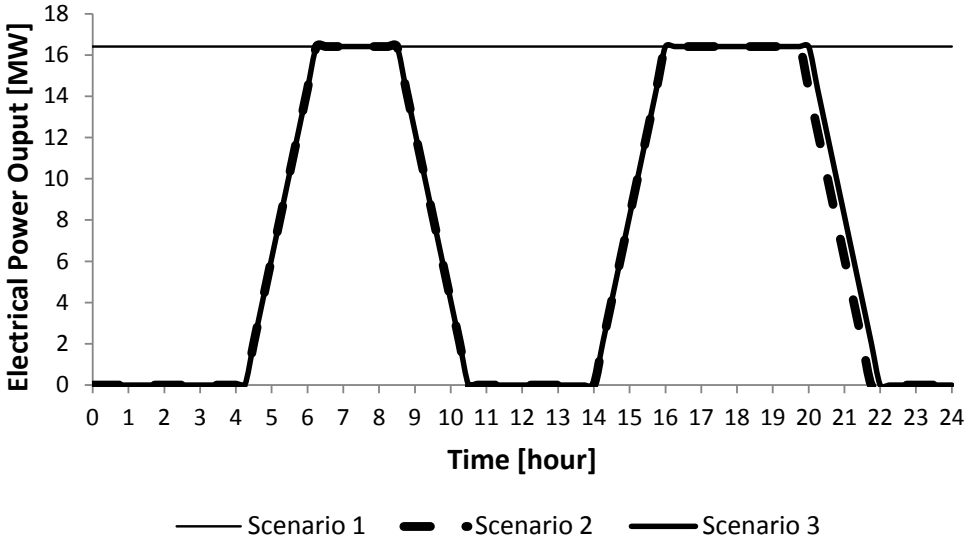

Figure 5.8: Total cogeneration electrical output profile.

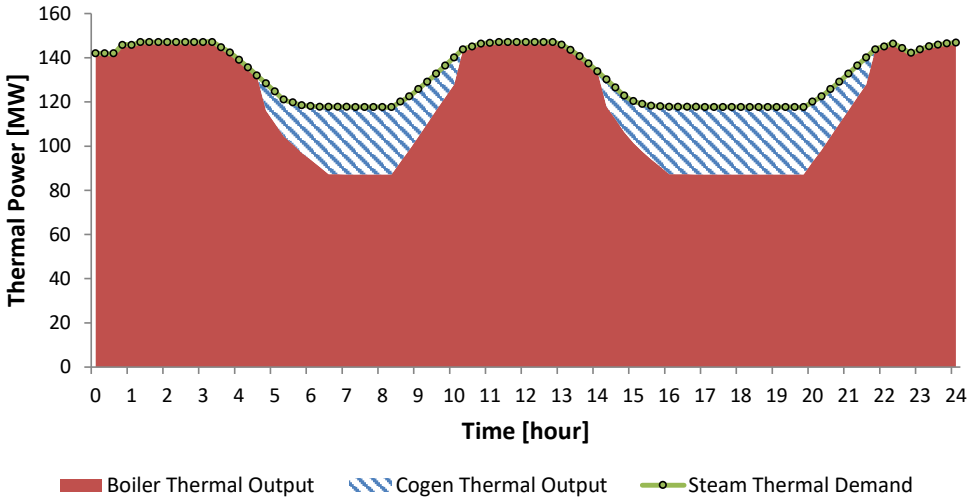

Figure 5.9: Steam thermal demand balance for Scenario 3.

with low prices that cause generators' shutdown decision by EMS, rendering the DR2 based strategy unable to achieve peak demand reduction similar to that achieved by DR1 based strategy. Therefore, it is assumed that the cogeneration units are at continuous maximum output in DR2. In practice, this can be negotiated by the LDC with the refinery since maximizing the on-site generation will reduce the LDC's peak demand. The parameters of the RPM are selected based on generated load profiles of the refinery under different price signals. The power thresholds and pricing coefficients resulting from load profiles analysis are shown in Table 5.5.

Two cases are considered, Case 1: DR1- which uses a desired demand profile signal, and Case 2: DR2- which uses a retail price signal. The solution of Case 1 is attained in four iterations and the distribution system peak demand is 25.9 MW, and day's total energy cost of the refinery is \$51,683. There is a 41% reduction in peak demand with DR1 as shown in Table 5.6, which resulted mainly from operating the cogeneration units at maximum output as shown in Figure 5.10. The final scheduled day-ahead load profiles for the refinery facility and the distribution system are shown in Figure 5.11 and Figure 5.12, respectively.

The solution of Case 2 is attained in six iterations and results in a distribution system peak demand of 27.9 MW and day's total energy cost of the refinery of $51,220. There is a 36.5% reduction in feeder peak demand as shown in Table 5.6. The final day-ahead retail prices are shown in Figure 5.13, and the final scheduled day-ahead load profiles for the refinery and the LDC are shown in Figure 5.11 and Figure 5.12, respectively. DR1 (Case 1) resulted in a lower peak load for the LDC as compared to DR2 (Case 2). However, the increase in energy cost for the refinery is lower for Case 2, as compared to Case 1, as a result of applying the retail prices instead of market prices.

The increase in total refinery cost needs to be compensated by the LDC as part of an incentive program that encourages customer's participation in DR provisions. Incentive-based DR programs are widely used by power utilities to encourage customers' participation in DR. In Ontario, DR incentives include monthly "availability payments" which are paid to customers who agree to curtail power during peak power events. Also, there is a "utilization payment" which is paid only if the customer responded to a DR event by curtailing its load according to the agreement. [66]

The fluctuating load schedules in Figure 5.11 and Figure 5.12 are those based on the initial schedule of the oil refinery, obtained using the proposed EMS, without DR. From the LDC's perspective, this creates periods of very high demand on the distribution system. In order to circumvent such demand fluctuations, the novel DR scheme is proposed in this work. As seen in Figure 5.11 and Figure 5.12, implementation of the proposed DR strategies by the LDC, influences the EMS decisions and hence results in significant reduction in the peak power drawn by the refinery from the LDC and consequently reduction in the LDC's peak demand, for both Case 1 and Case 2. However, by inclusion of DR signals in the refinery EMS, the refinery's operating cost would increase. It has been suggested in this work that the LDC should cover this cost increase through an incentive for the refinery's participation in DR provisions. Therefore, the proposed DR would benefit both the LDC and the refinery- the LDC will benefit through reduction of its peak demand and the customer through the incentives received for participation in the DR program.

Table 5.5:
Retail Pricing Model Parameters

P_1	P_2	P_3	P_4
19 MW	18 MW	15 MW	12 MW
λ_1	λ_2	λ_3	λ_4
0.1	0.325	0.55	0.775

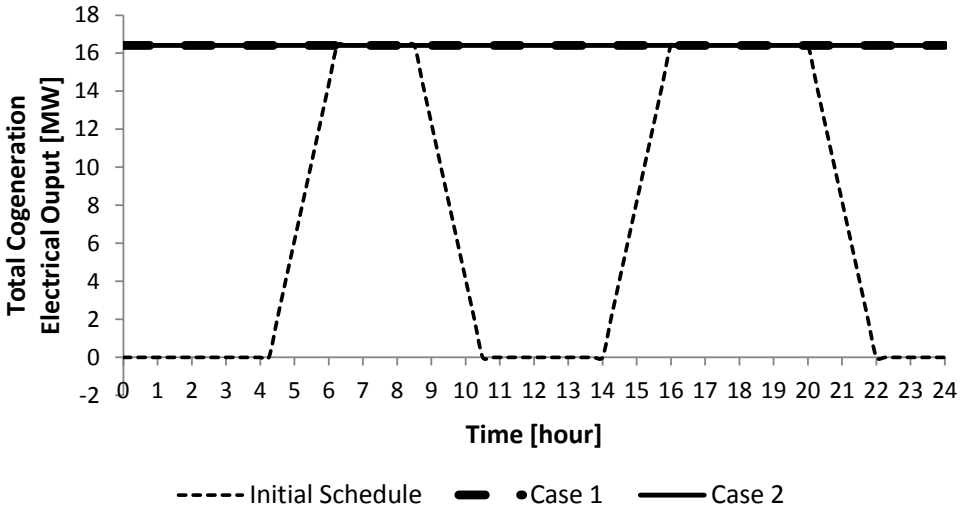

Figure 5.10: Total cogeneration electrical output profiles.

Table 5.6:
Demand Response Results

	Initial Schedule	Final Schedule	
		Case 1	Case 2
Total Energy Consumption for the Refinery [MWh/day]	753.2	755.1 (+0.2%)	754.5 (+0.2%)
Total Cogeneration Electrical Energy Output [MWh/day]	168.2	393.8 (+134%)	393.8 (+134%)
Total Energy Drawn from LDC [MWh/day]	556.6	332.8 (-40.2%)	332.2 (-40.3%)
Total Costs for the refinery [$/day]	50,748	51,683 (+1.8%)	51,220 (+0.9%)
Total Energy Consumption for LDC [MWh/day]	802.8	599.2 (-25.4%)	598.5 (-25.5%)
Peak Demand for LDC [MW]	43.9	25.9 (-41%)	27.9 (-36.5%)

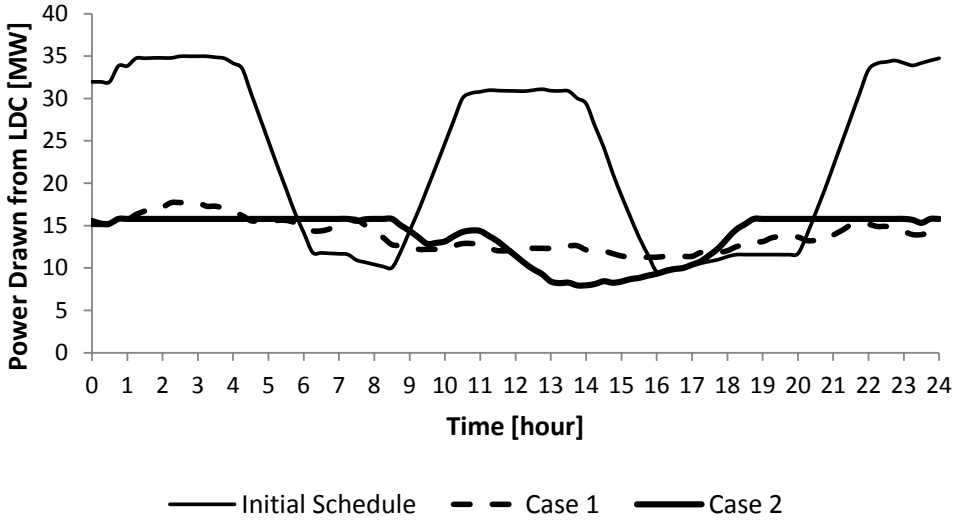

Figure 5.11: Refinery facility scheduled power demand profiles.

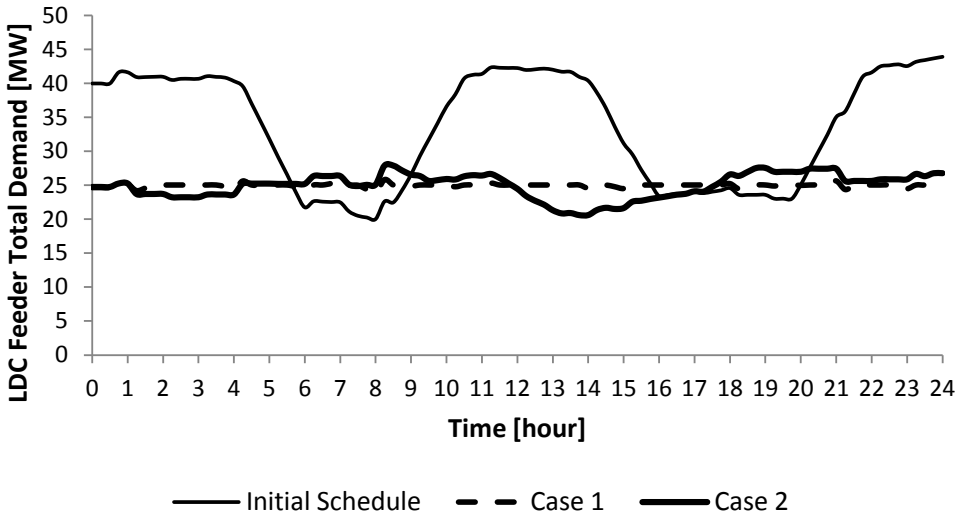

Figure 5.12: LDC scheduled power demand profiles.

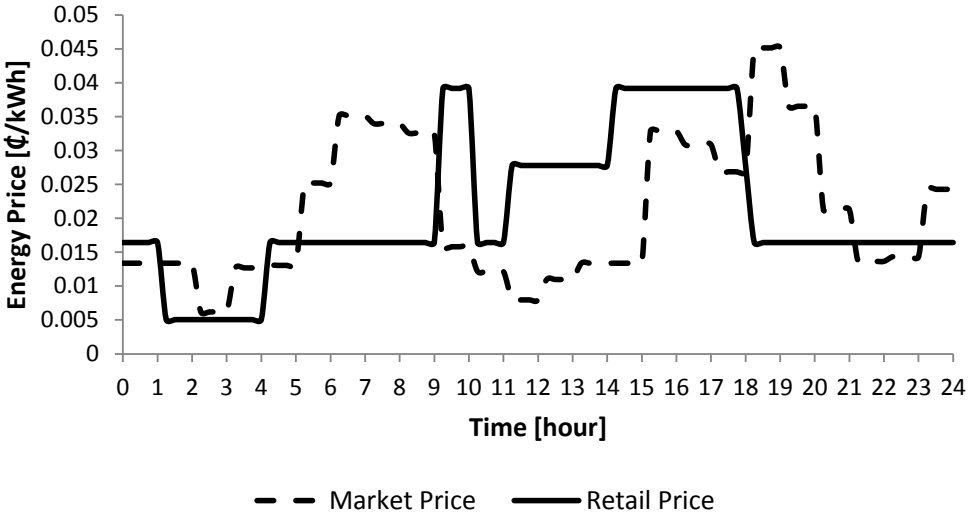

Figure 5.13: Day-ahead market and retail prices.

5.5.3 Solution Method and Computational Efficiency

The refinery EMS optimization problem is formulated as a mixed integer nonlinear programming (MINLP) problem and solved using the DICOPT solver [38] in GAMS environment, while the The DOPF model of the LDC is formulated as a nonlinear programming (NLP) problem and solved using the IPOPT solver [37] in GAMS. The simulation in the case study is carried out for 24-hours of refinery operation with equal time intervals of 15 minutes resulting in a total time slots of 96 slots. The computational times of the EMS and DOPF models are detailed in Table 5.7. The proposed models are computationally efficient as they can be solved within the considered time-frame, 15 minutes, or even for smaller time granularities.

Table 5.7: Computational Property of The Mathematical Models

Model	Solution Time
EMS Scenario 1	52.4 sec
EMS Scenario 2	58.6 sec
EMS Scenario 3	81.3 sec
DR1 DOPF	114.8 sec
DR2 DOPF	167.9 sec

5.6 Summary

This chapter presented a novel EMS application through the optimum load control of an oil refining process. The optimization of energy utilization was achieved through the development of an energy-based material flow model for the refinery. Also a joint electrical-thermal model was developed for the on-site cogeneration system. The cost associated with electrical generation was minimized along with the cost of buying electricity from the grid. Simulation results showed potential for daily savings for the refinery on energy costs as crude feed and cogeneration dispatch schedules were optimized. Also when participating in DR provisions, the distribution system benefited from significant peak demand reduction as the refinery responded to DR signals by revising its EMS decisions.

Chapter 6

Conclusions

6.1 Summary

The research presented in this thesis focused on energy management and demand response of industrial loads. Chapter 1 presented the motivation of this research, emphasising the need for the development of smart tools for energy management and conservation in the industrial sector, and the potential of industrial loads participating in DSM programs. A literature review of related works, particulary on industrial load management and industrial DR, was presented. This chapter also presented an overview of the research and the expected contributions.

Chapter 2 presented a brief background to the topics related to this research including; EMS, load modeling, MPC, WPS and oil refinery processes, and DSM. EMS functions and architecture were discussed with emphasis on power system optimization and OPF as important functions of the EMS. This chapter also discussed load modeling techniques such as polynomial and NN-based models. MPC was discussed as an uncertainty management technique. Also DSM and DR were discussed by outlining different types of DR programs.

Chapter 3 presented the development of an EMS model for a WPS facility. A controlled load estimator (CLE) was developed for the WPS using the data generated from

a PSCAD simulation model. A NN was trained, using the generated data, to estimate the power demand of the WPS as a function of the control variables. This NN-based load model was then incorporated into the EMS to determine the optimal operational schedules of the pumps with the objective of minimizing the energy consumption costs and charges associated with peak power demand. Modeling related uncertainties were captured through a novel recursive mechanism for NN retraining, while operational uncertainties were accounted for, by applying a receding horizon MPC technique.

Chapter 4 presented a DR strategy for industrial customers, to be implemented by the LDC in day-ahead and real-time operations. The day-ahead problem involved peak demand minimization for the LDC and the customer, while energy cost minimization was considered for the customer only. The real-time problem minimized the deviations in DR strategies from the day-ahead schedules, taking into account the uncertainties of energy prices and energy demand of the customer. The strategy was based on a day-ahead contractual mechanism between the two parties for a desired load profile, and a real-time operational scheme to mitigate the uncertainties through improved forecast of energy price and power demand, using the MPC technique.

Chapter 5 presented an EMS model for minimizing electricity consumption costs of an oil refinery facility considering an on-site cogeneration capability. The energy management is based on power demand modeling of the oil refinery process. A joint electrical-thermal model is used for the cogeneration units to account for the electricity and steam production. The potential for participating in DR was also studied by applying the DR framework proposed in Chapter 4 to the refinery load which showed the impact of refinery's EMS decisions on distribution system operations.

6.2 Contributions

The main contributions of this research are as follows:

- A comprehensive EMS framework was proposed for a WPS considering various operational aspects including load management, water flow management, process control technology, equipment operational limits, uncertainty mitigation, and carbon footprint alleviation. The proposed framework comprised a module for simulation of the WPS load which considered variable speed pumping as a means to control the water flow output of the pumps. This energy efficient control was not considered in the previous works discussed in the literature review section of this thesis.

- A novel iterative CLE approach was proposed which comprised a feedback of the EMS optimal decisions to the WPS load simulation module, followed by NN retraining, and re-solving the EMS model. This approach improved the accuracy of load estimation at optimal operating points, and enabled the EMS model to re-examine the optimality of the reached solution considering other potential schedules.

- A DR strategy was proposed for industrial loads, wherein the LDC used a retail price signal to control the load energy consumption in a manner to reduce the distribution system peak demand. The proposed DR strategy was based on effective communication between the customer's EMS and the LDC's operations which considered unbalanced representation of the distribution feeder, supplying the industrial facility.

- A novel retail pricing model was proposed, which used customer's historical load data and day-ahead demand schedules to determine a price signal that influences customer's EMS decisions, seeking to shift some of the industrial load from peak to off-peak periods.

- An EMS framework was proposed for optimal load management of an oil refining process considering an on-site cogeneration facility. A load estimation model was de-

veloped for the oil refinery process at the processing units' level, and a joint electrical-thermal model was developed for the cogeneration facility to account for electricity and steam supplied to the refinery.

The main contents and contributions of Chapter 3 have been published in IEEE Transactions on Smart Grid [67] and IEEE Power and Energy Society General Meeting [68]. The main contents of Chapter 4 is submitted to IEEE Transactions on Smart Grid [69], and the main contents of Chapter 5 is submitted to IEEE Transactions on Power Systems [70].

6.3 Future Work

Based on the work presented in this thesis, further research may be pursued in the following topics:

- Investigate the impact of changing the industrial load connection node at the distribution feeder on the performance of the proposed DR strategy.
- Develop a retail pricing based DR strategy for industrial customers that is less dependent on the other loads connected to the distribution feeder, and more dependent on industrial load's characteristics.
- Study the current DR programs for candidate DR incentives to be considered by LDC to encourage industrial customers participation in proposed DR strategy.
- Test the performance of the developed industrial loads DR strategy with other types of industrial facilities such as chemical plants and data centers.
- Validate the developed material flow based power demand model of the oil refinery using measurement data acquired from an actual facility. The acquired data can also be used to develop a measurement-based demand model by regression or NN training.

- Study the performance of the EMS model for the oil refinery when an objective function of minimizing peak demand is used instead of minimizing energy costs.
- Investigate the possibility of considering electrical energy consumption costs in the oil refinery long-term production planning problem.

References

[1] Provincial and territorial energy profiles canada. [Online]. Available: https://www.neb-one.gc.ca/nrg/ntgrtd/mrkt/nrgsstmprfls/cda-eng.html?=undefined&wbdisable=true

[2] Y. M. Ding, S. H. Hong, and X. H. Li, "A demand response energy management scheme for industrial facilities in smart grid," *IEEE Transactions on Industrial Informatics*, vol. 10, no. 4, pp. 2257–2269, 2014.

[3] S. Paudyal, C. A. Cañizares, and K. Bhattacharya, "Optimal operation of industrial energy hubs in smart grids," *IEEE Transactions on Smart Grid*, vol. 6, no. 2, pp. 684–694, 2015.

[4] A. Madhavan, "An integrated voltage optimization approach for industrial loads," Master's thesis, University of Waterloo, 2013. [Online]. Available: http://hdl.handle.net/10012/7554

[5] S. Ashok and R. Banerjee, "Load-management applications for the industrial sector," *Applied energy*, vol. 66, no. 2, pp. 105–111, 2000.

[6] ——, "An optimization mode for industrial load management," *IEEE Transactions on Power Systems*, vol. 16, no. 4, pp. 879–884, 2001.

[7] C. Babu and S. Ashok, "Peak load management in electrolytic process industries," *IEEE Transactions on Power Systems*, vol. 23, no. 2, pp. 399–405, 2008.

[8] A. Gholian, H. Mohsenian-Rad, and Y. Hua, "Optimal industrial load control in smart grid," 2014.

[9] J. F. Ordonez Giron, "Optimal load management application for industrial customers," Master's thesis, University of Waterloo, 2015. [Online]. Available: http://hdl.handle.net/10012/9564

[10] B. Barán, C. von Lücken, and A. Sotelo, "Multi-objective pump scheduling optimisation using evolutionary strategies," *Advances in Engineering Software*, vol. 36, no. 1, pp. 39–47, 2005.

[11] M. Neufeld, O. Ramirez, and A. Ustinovich, "A comparative study of fixed speed vs. variable speed control of a series configured pipeline pumping application," in *2014 IEEE Petroleum and Chemical Industry Technical Conference (PCIC)*. IEEE, 2014, pp. 491–500.

[12] *Variable Speed Pumping: A Guide to Successful Applications*. Elsevier, 2004.

[13] G. M. Jones, B. E. Bosserman, R. L. Sanks, and G. Tchobanoglous, *Pumping station design*. Gulf Professional Publishing, 2006.

[14] N. Wu, Y. Qian, M. Zhou, and F. Chu, "Issues on short-term scheduling of oil refinery," in *2006 IEEE International Conference on Systems, Man and Cybernetics*, vol. 4. IEEE, 2006, pp. 2920–2925.

[15] N. Wu, L. Bai, M. Zhou, F. Chu, and S. Mammar, "A novel approach to optimization of refining schedules for crude oil operations in refinery," *IEEE Transactions on Systems, Man, and Cybernetics, Part C (Applications and Reviews)*, vol. 42, no. 6, pp. 1042–1053, 2012.

[16] Y. Hou, N. Wu, and M. Zhou, "Scheduling crude oil operations in refineries with genetic algorithm," in *2016 IEEE 13th International Conference on Networking, Sensing, and Control (ICNSC)*. IEEE, 2016, pp. 1–6.

[17] Y. Hou, N. Wu, M. Zhou, and Z. Li, "Pareto-optimization for scheduling of crude oil operations in refinery via genetic algorithm," *IEEE Transactions on Systems, Man, and Cybernetics: Systems*, vol. 47, no. 3, pp. 517–530, 2017.

[18] S. Ashok and R. Banerjee, "Optimal operation of industrial cogeneration for load management," *IEEE Transactions on power systems*, vol. 18, no. 2, pp. 931–937, 2003.

[19] A. Gholian, H. Mohsenian-Rad, Y. Hua, and J. Qin, "Optimal industrial load control in smart grid: A case study for oil refineries," in *Proc. of IEEE PES General Meeting, Vancouver, Canada*. Citeseer, 2013.

[20] "An introduction to petroleum refining and the production of ultra low sulfur gasoline and diesel fuel," International Council on Clean Transportion (ICCT), Tech. Rep., 2011.

[21] T. Remani, E. Jasmin, and T. I. Ahamed, "Load scheduling problems under demand response schemes: A survey," in *Signal Processing, Informatics, Communication and Energy Systems (SPICES), 2015 IEEE International Conference on*. IEEE, 2015, pp. 1–5.

[22] J. Leithon, T. J. Lim, and S. Sun, "Battery-aided demand response strategy under continuous-time block pricing," *IEEE Transactions on Signal Processing*, vol. 64, no. 2, pp. 395–405, 2016.

[23] F. Y. Xu and L. L. Lai, "Novel active time-based demand response for industrial consumers in smart grid," *IEEE Transactions on Industrial Informatics*, vol. 11, no. 6, pp. 1564–1573, 2015.

[24] K. Ma, G. Hu, and C. J. Spanos, "A cooperative demand response scheme using punishment mechanism and application to industrial refrigerated warehouses," *IEEE Transactions on Industrial Informatics*, vol. 11, no. 6, pp. 1520–1531, 2015.

[25] A. Mnatsakanyan and S. W. Kennedy, "A novel demand response model with an application for a virtual power plant," *IEEE Transactions on Smart Grid*, vol. 6, no. 1, pp. 230–237, 2015.

[26] I. Sharma, K. Bhattacharya, and C. Cañizares, "Smart distribution system operations with price-responsive and controllable loads," *IEEE Transactions on Smart Grid*, vol. 6, no. 2, pp. 795–807, 2015.

[27] E. Vaahedi, *Practical power system operation*. John Wiley & Sons, 2014.

[28] S. Paudyal, C. A. Cañizares, and K. Bhattacharya, "Optimal operation of distribution feeders in smart grids," *IEEE Transactions on Industrial Electronics*, vol. 58, no. 10, pp. 4495–4503, 2011.

[29] B.-K. Choi, H. D. Chiang, Y. Li, Y. T. Chen, D. H. Huang, and M. G. Lauby, "Development of composite load models of power systems using on-line measurement data," *Journal of Electrical Engineering and Technology*, vol. 1, no. 2, pp. 161–169, 2006.

[30] O. Nelles, "Nonlinear system identification," *Springser, Berlin, Germany*, 2001.

[31] D. Chen and R. R. Mohler, "Neural-network-based load modeling and its use in voltage stability analysis," *IEEE Transactions on Control Systems Technology*, vol. 11, no. 4, pp. 460–470, 2003.

[32] *MATLAB Documentation*. Mathworks.

[33] Paudyal, Sumit, "Optimal energy management of distribution systems and industrial energy hubs in smart grids," Ph.D. dissertation, 2012. [Online]. Available: http://hdl.handle.net/10012/6884

[34] W. L. Winston, M. Venkataramanan, and J. B. Goldberg, *Introduction to mathematical programming*. Thomson/Brooks/Cole Duxbury; Pacific Grove, CA, 2003.

[35] S. S. Rao, *Engineering optimization: theory and practice*. John Wiley & Sons, 1996.

[36] E. Castillo, A. J. Conejo, P. Pedregal, R. Garcia, and N. Alguacil, *Building and solving mathematical programming models in engineering and science*. John Wiley & Sons, 2002.

[37] Ipopt. [Online]. Available: https://www.gams.com/latest/docs/S_IPOPT.html

[38] Dicopt. [Online]. Available: https://www.gams.com/help/index.jsp?topic=/gams.doc/userguides/mccarl/dicopt.htm

[39] C. Chen, J. Wang, Y. Heo, and S. Kishore, "Mpc-based appliance scheduling for residential building energy management controller," *IEEE Transactions on Smart Grid*, vol. 4, no. 3, pp. 1401–1410, 2013.

[40] D. E. Olivares, J. D. Lara, C. A. Cañizares, and M. Kazerani, "Stochastic-predictive energy management system for isolated microgrids," *IEEE Transactions on Smart Grid*, vol. 6, no. 6, pp. 2681–2693, 2015.

[41] T. Walski, K. Zimmerman, M. Dudinyak, and P. Dileepkumar, "Some surprises in estimating the efficiency of variable speed pumps with the pump affinity laws," in *ASCE World Water Congress, Philadelphia*, 2003.

[42] H. L. Brown, *Energy analysis of 108 industrial processes*. The Fairmont Press, Inc., 1996.

[43] M. Kancijan, M. Ivanjko, P. Ilak, and S. Krajcar, "An oil refinery production optimization," in *Energy (IYCE), 2015 5th International Youth Conference on*. IEEE, 2015, pp. 1–11.

[44] K. Malmedal, P. Sen, and J. Candelaria, "Electrical energy and the petro-chemical industry: Where are we going?" in *2011 Record of Conference Papers Industry Applications Society 58th Annual IEEE Petroleum and Chemical Industry Conference (PCIC)*. IEEE, 2011, pp. 1–8.

[45] P. Jazayeri, A. Schellenberg, W. Rosehart, J. Doudna, S. Widergren, D. Lawrence, J. Mickey, and S. Jones, "A survey of load control programs for price and system stability," *IEEE Transactions on Power Systems*, vol. 20, no. 3, pp. 1504–1509, 2005.

[46] T. Logenthiran, D. Srinivasan, and T. Z. Shun, "Demand side management in smart grid using heuristic optimization," *IEEE Transactions on Smart Grid*, vol. 3, no. 3, pp. 1244–1252, 2012.

[47] S. F. Bush, "Demand-response and the advanced metering infrastructure."

[48] R. Deng, Z. Yang, M.-Y. Chow, and J. Chen, "A survey on demand response in smart grids: Mathematical models and approaches," *IEEE Transactions on Industrial Informatics*, vol. 11, no. 3, pp. 570–582, 2015.

[49] P. Palensky and D. Dietrich, "Demand side management: Demand response, intelligent energy systems, and smart loads," *IEEE transactions on industrial informatics*, vol. 7, no. 3, pp. 381–388, 2011.

[50] A. P. Sanghvi, "Flexible strategies for load/demand management using dynamic pricing," *IEEE Transactions on Power Systems*, vol. 4, no. 1, pp. 83–93, 1989.

[51] Managing costs with time-of-use rates. [Online]. Available: https://www.oeb.ca/rates-and-your-bill/electricity-rates/managing-costs-time-use-rates

[52] V. J. Gutierrez-Martinez, C. A. Cañizares, C. R. Fuerte-Esquivel, A. Pizano-Martinez, and X. Gu, "Neural-network security-boundary constrained optimal power flow," *IEEE Transactions on Power Systems*, vol. 26, no. 1, pp. 63–72, 2011.

[53] I. Sharma, C. Cañizares, and K. Bhattacharya, "Residential micro-hub load model using neural network," in *North American Power Symposium (NAPS), 2015*. IEEE, 2015, pp. 1–6.

[54] B. V. Solanki, A. Raghurajan, K. Bhattacharya, and C. A. Canizares, "Including smart loads for optimal demand response in integrated energy management systems

for isolated microgrids," *IEEE Transactions on Smart Grid*, vol. 8, no. 4, pp. 1739–1748, 2017.

[55] A. Parisio, E. Rikos, and L. Glielmo, "A model predictive control approach to microgrid operation optimization," *IEEE Transactions on Control Systems Technology*, vol. 22, no. 5, pp. 1813–1827, 2014.

[56] H. Alharbi and K. Bhattacharya, "Optimal sizing of battery energy storage systems for microgrids," in *Electrical Power and Energy Conference (EPEC), 2014 IEEE*. IEEE, 2014, pp. 275–280.

[57] R. Halfpap. (2000) Tutorial: Selecting an appropriate pump motor. [Online]. Available: http://machinedesign.com/motorsdrives/tutorial-selecting-appropriate-pump-motor

[58] Power data. [Online]. Available: http://www.ieso.ca/Pages/Power-Data/default.aspx

[59] Canada weather stats. [Online]. Available: http://toronto.weatherstats.ca/charts/wind_speed-24hrs.html

[60] M. Wang, H. Lee, and J. Molburg, "Allocation of energy use in petroleum refineries to petroleum products," *The International Journal of Life Cycle Assessment*, vol. 9, no. 1, pp. 34–44, 2004.

[61] A. H. Azit and K. M. Nor, "Optimal sizing for a gas-fired grid-connected cogeneration system planning," *IEEE Transactions on Energy Conversion*, vol. 24, no. 4, pp. 950–958, 2009.

[62] D. T. Nguyen and L. B. Le, "Optimal bidding strategy for microgrids considering renewable energy and building thermal dynamics," *IEEE Transactions on Smart Grid*, vol. 5, no. 4, pp. 1608–1620, 2014.

[63] M. Shaaban, A. Azit, and K. Nor, "Grid integration policies of gas-fired cogeneration in peninsular malaysia: Fallacies and counterexamples," *Energy policy*, vol. 39, no. 9, pp. 5063–5075, 2011.

[64] Photovoltaic data. [Online]. Available: http://www.ieso.ca/Pages/Power-Data/default.aspx

[65] Natural gas rates. [Online]. Available: https://www.oeb.ca/rates-and-your-bill/natural-gas-rates

[66] Capacity-based demand response. [Online]. Available: http://www.ieso.ca/en/Sector-Participants/Market-Operations/Markets-and-Related-Programs/Capacity-Based-Demand-Response

[67] O. Alarfaj and K. Bhattacharya, "A controlled load estimator-based energy management system for water pumping systems," *IEEE Transactions on Smart Grid*, vol. 9, no. 6, pp. 6307–6317, 2018.

[68] ——, "Power consumption modeling of water pumping system for optimal energy management," in *Power and Energy Society General Meeting (PESGM), 2016.* IEEE, 2016, pp. 1–5.

[69] ——, "Retail pricing controlled demand response for industrial loads considering distribution feeder operations," *IEEE Transactions on Smart Grid*, 2018, in revision.

[70] ——, "Material flow based power demand modeling of an oil refinery process for optimal energy management," *IEEE Transactions on Power Systems*, 2018, in revision.

Glossary of Terms

AGC	Automatic Generation Control
BESS	Battery Energy Storage System
CDU	Crude Distillation Unit
CLE	Controlled Load Estimator
CPP	Critical Peak Pricing
CVR	Controlled Voltage Reduction
DER	Distributed Energy Resource
DG	Distributed Generation
DOPF	Distribution Optimal Power Flow
DR	Demand Response
DSM	Demand Side Management
ELD	Economic Load Dispatch
EMS	Energy Management System
ESS	Energy Storage System
FCC	Fluid Catalyst Cracking
GAMS	General Algebraic Modeling System
HEMS	Home Energy Management System
HOEP	Hourly Ontario Energy Price
IBR	Inclined Block Rate
IEEE	Institute of Electrical and Electronic Engineers
ILM	Industrial Load Management

LDC	Local Distribution Company
LTC	Load Tap Changer
LPG	Liquefied Petroleum Gas
MCS	Monte Carlo Simulation
MILP	Mixed Integer Linear Programming
MINLP	Mixed Integer Non-linear Programming
MPC	Model Predictive Control
MSE	Mean Squared Error
NLP	Non-linear Programing
NN	Neural Network
OPF	Optimal Power Flow
PSCAD	Power System Computer Aided Design
PV	Photovoltaic
PWM	Pulse Width Modulation
RES	Renewable Energy Source
RPM	Retail Pricing Model
RTP	Real-time Pricing
RTU	Remote Terminal Unit
SCADA	Supervisory Control and Data Acquisition
SOC	State of Charge
TOU	Time of Use
VDU	Vacuum Distillation Unit
VPP	Virtual Power Plant
VSD	Variable Speed Drive
WPS	Water Pumping System